



Remarks on the Sachdev-Ye-Kitaev model

Juan Maldacena and Douglas Stanford

Institute for Advanced Study, Princeton, New Jersey 08540, USA

(Received 8 September 2016; published 4 November 2016)

We study a quantum-mechanical model proposed by Sachdev, Ye and Kitaev. The model consists of N Majorana fermions with random interactions of a few fermions at a time. It is tractable in the large- N limit, where the classical variable is a bilocal fermion bilinear. The model becomes strongly interacting at low energies where it develops an emergent conformal symmetry. We study two- and four-point functions of the fundamental fermions. This provides the spectrum of physical excitations for the bilocal field. The emergent conformal symmetry is a reparametrization symmetry, which is spontaneously broken to $SL(2, R)$, leading to zero modes. These zero modes are lifted by a small residual explicit breaking, which produces an enhanced contribution to the four-point function. This contribution displays a maximal Lyapunov exponent in the chaos region (out-of-time-ordered correlator). We expect these features to be universal properties of large- N quantum mechanics systems with emergent reparametrization symmetry. This article is largely based on talks given by Kitaev, which motivated us to work out the details of the ideas described there.

DOI: 10.1103/PhysRevD.94.106002

I. INTRODUCTION

Studies of holography have been hampered by the lack of a simple solvable model that can capture features of Einstein gravity. The simplest model, which is a single matrix quantum mechanics, does not appear to lead to black holes [1] (see Ref. [2] for a review). $\mathcal{N} = 4$ super Yang-Mills at strong 't Hooft coupling certainly leads to black holes, and exact results are known at large N for many anomalous dimensions and some vacuum correlation functions, but at finite temperature the theory is difficult to study.

A system that reproduces some of the dynamics of black holes should be interacting, but we might hope for a model with interactions that are simple enough that it is still reasonably solvable.

Kitaev has proposed to study a quantum-mechanical model of N Majorana fermions interacting with random interactions [3]. It is a simple variant of a model introduced by Sachdev and Ye [4], which was first discussed in relation to holography in Ref. [5]. The Hamiltonian of Ref. [3] is simply

$$H = \sum_{iklm} j_{iklm} \psi_i \psi_k \psi_l \psi_m \quad (1.1)$$

where the couplings j_{iklm} are taken randomly from a Gaussian distribution with zero mean and a width of order $\mathcal{J}/N^{3/2}$.

One interesting feature of this model is that it develops an approximate conformal symmetry in the infrared. Understanding how to deal with quantum-mechanical

theories that develop such a conformal symmetry seems very important for both condensed matter physics and gravity. One naively expects a full Virasoro symmetry. However, in the model, the symmetry is both explicitly as well as spontaneously broken, so we end up with “nearly conformal quantum mechanics,” or $NCFT_1$. [We propose to use the term $NCFT_1$ to denote systems that have one time dimension which are nearly invariant under a full reparametrization (or Virasoro) symmetry.¹] The same situation arises in gravity, when we consider very near extremal black holes. These are black holes that develop a nearly AdS_2 region, which we can call $NAdS_2$; see Ref. [7] for a recent discussion. It is well known that purely AdS_2 gravity is not consistent, except for the ground states. So the right setting in which to study holography for near extremal black holes is $NAdS_2/NCFT_1$.

Besides this structural similarity, it was noted in Refs. [3,8] that the out-of-time-order correlators of the Sachdev-Ye-Kitaev (SYK) model (1.1) grow in a manner that reflects an underlying chaotic dynamics. At relatively low energies this growth matches the one expected in a theory of gravity [9–11], which saturates the chaos bound [12].

In this paper we study this model a bit further. We start by summarizing the computation of the two-point functions [4,13] in the large- N limit, following Sachdev, Ye, Parcollet, and Georges. We will discuss this in a variant of the model where the interaction involves q fermions at a

¹This should be contrasted to what is usually called “conformal quantum mechanics,” such as in Ref. [6], which are only invariant under $SL(2, R)$.

time [3]. We will further show that the equations simplify considerably in the large- q limit. This allows us to connect analytically the free UV theory to the interacting and nearly conformal IR theory. Further recent work in this or similar models includes Refs. [7,14–19]. See also Refs. [20,21] for a string-motivated model with disorder.

We then derive an explicit integral expression for the four-point function in the infrared limit. This problem was also considered in Ref. [19]. The four-point function is actually infinite in the strict conformal limit, due to Nambu-Goldstone bosons associated to the spontaneously broken reparametrization invariance. To remove the infinity we have to take into account the explicit breaking of this symmetry, which lifts these modes by a small amount. We expect that this should be a universal feature of large, but finite, entropy NCFT₁ systems. Namely, the systems cannot realize the conformal symmetry exactly,² and the small explicit breaking leads to a universal contribution that dominates the four-point function and saturates the chaos bound.³ In particular, AdS₂ dilaton gravity is an example with the same explicit breaking [26], leading to the same dominant term in the four-point function.

In addition to this term, the SYK four-point function contains subleading pieces that are finite in the low-temperature limit. These contain information about the composite operators that appear in the operator product expansion (OPE) of $\sum_i \psi_i(\tau) \psi_i(0)$. These get anomalous dimensions at leading order in N and seem analogous to the single trace operators of the usual gauge theory examples of holography. One finds a tower of states with an approximately integer spacing. This tower of states is reminiscent of the one appearing in large- N O(N) models, where we have one state for each spin. Here we get a similar structure, but with dimensions which have $O(1)$ corrections relative to the dimensions in the free theory. This suggests that the bulk theory contains low-tension strings. These extra states do not compete with the dilaton gravity piece, even though the strings are light, simply because of the enhancement of gravity in N AdS₂.

Much of the analysis in this paper, including the ladder diagrams, the spectrum of the kernel $k_c(h)$, and the effective theory of reparametrizations, is simply what

²The argument in Ref. [22] shows that an exact $SL(2, R)$ symmetry is incompatible with a thermofield interpretation with a finite number of states. Of course, in gravity the exact $SL(2, R)$ symmetry is broken by the presence of a dilaton field; see Ref. [7] for a recent discussion.

³In 1 +1-dimensional conformal field theory the conformal symmetry is also spontaneously broken (recall that $L_{-2}|0\rangle \neq 0$), but it is not explicitly broken. In that case we also have a universal (stress tensor) contribution to the four-point function. By itself this piece saturates the chaos bound [23–25], but only in special theories does it dominate.

Kitaev presented in his talks [3], and we are thankful to him for several further explanations.

A. Organization of the paper and summary of results

The article might seem a bit technical in some parts, so we will summarize below what is done in various sections. The reader might want to jump directly to the sections that look most interesting to him/her.

In Sec. II we review the large- N structure of the theory. The model has one dimensionful parameter \mathcal{J} , with dimensions of energy, which characterizes the size of the interaction terms in the Hamiltonian. This implies that the interaction is relevant and becomes strong at low energies. For large N the diagrams have a simple structure that is reminiscent of the one for large- N O(N) theories (see also the discussion in Ref. [18]). There is a bilocal field $\tilde{G}(\tau_1, \tau_2)$ depending on two times which becomes classical in the large- N limit. On the classical solution, G , this field is equal to the two-point function of the fermions $G(\tau_1, \tau_2) = \frac{1}{N} \sum_{i=1}^N \langle \psi_i(\tau_1) \psi_i(\tau_2) \rangle$. The classical equation for G is nonlocal in time but it can be solved numerically. G can be inserted in the action to compute the partition function. We also show that in the variant of the model where q fermions interact at a time, the large- q limit becomes analytically tractable and one can solve the classical equations for any value of the coupling. Another simple solvable limit is the case $q = 2$. In that case, the Hamiltonian has the form $H = i \sum_{kl} j_{kl} \psi_k \psi_l$ which is a random mass-like term. This can be diagonalized and we get a spectrum of masses, or energies, given by the usual semicircle law distribution for random matrices. This particular example is integrable and some properties are different than the one for the generic q case. In particular, we find that there is no exponentially growing contribution to the out-of-time-order four-point function.

At low energies the model simplifies further due to the emergence of a conformal symmetry. In one dimension the conformal group is the same as the group of all reparametrizations. One can see this symmetry explicitly in both the low-energy action, and the low-energy equations for the bilocal fields. One might expect a theory that has a full reparametrization symmetry to be topological. This is not the case here because the reparametrization symmetry is spontaneously broken down to an $SL(2, R)$ subgroup. In other words, the bilocal function $G(\tau_1, \tau_2) = G(\tau_1 - \tau_2)$ becomes $G_c \propto \tau_{12}^{-2\Delta}$ for large values of $\mathcal{J} \tau_{12}$ (with $\tau_{12} = \tau_1 - \tau_2$). The partition function displays a zero-temperature entropy of order N . In addition, there is a finite-temperature entropy which is linear in the temperature, proportional to $N/(\beta \mathcal{J})$. Generically the model is expected to have a single ground state, but here we are considering temperatures that are fixed in the large- N limit. This means that we are accessing an exponentially large number of states.

In Sec. III we discuss general features of the four-point function of the fermions $\langle \psi_i \psi_j \psi_j \psi_i \rangle$. This can also be viewed as a two-point function of the bilocal fields. The final form for the leading $1/N$ piece in the four-point function is displayed in Eq. (3.112).

This computation of the four-point function is a bit technical and, for this reason, this section is rather long. The diagrams that contribute have the form of ladder diagrams. Therefore, they can be summed by defining a kernel K that corresponds to adding a rung to a ladder. Then the full ladder has a form proportional to $\frac{1}{1-K} F_0$ where F_0 is a diagram with no rungs. This is conceptually easy. However, it is tricky to invert the kernel since one has to understand in more detail the space of functions where it is acting. Fortunately the problem partially simplifies at low energies due to the unbroken $SL(2, R)$ symmetry. This symmetry can be used to diagonalize the kernel and also to describe the space of functions we should sum over. This leads to a relatively explicit expression for the four-point function in terms of a sum over intermediate states [Eqs. (3.50) and (3.52)], once we exclude the Goldstone bosons which need to be treated separately. We can read off the spectrum of operators that appear in the OPE of two fermions. The spectrum is given by the solutions h_m to the equation $k_c(h_m) = 1$, with $k_c(h)$ in Eq. (3.35). We can vaguely view this tower of operators as $\psi_i \partial^{1+2m} \psi_i$. We say ‘‘vaguely’’ because the proper dimensions we obtain from the above procedure display an order-one correction from the naively expected values (which would be $2\Delta + 1 + 2m$). This is an important clue for a possible bulk interpretation. It is saying that the fermions cannot be associated to weakly interacting particles in the bulk. Their interactions would have to be of order one rather than $1/N$.

We then give a proper treatment for the Goldstone modes that have $K_c = 1$ in the conformal limit. These arise from reparametrizations of the conformal solution, G_c . These fluctuations have zero action in the conformal limit, but get a nonzero action when we take into account the leading corrections to the conformal answers. We first take a direct approach and compute the leading correction to the classical solution G away from the conformal limit $G = G_c + \delta G$. It turns out that the leading correction involves an extra factor of $1/\mathcal{J}$. One can then proceed to compute the variation of the kernel K away from the conformal limit $K = K_c + \delta K$. We then evaluate δK on reparametrizations of the conformal solution $\delta_\epsilon G_c$, where $\epsilon(\tau)$ is an infinitesimal reparametrization. We get a nonzero answer which can then be used to compute the four-point function. Since δK ends up in the denominator in the expression for the four-point function, we get an enhanced contribution with an additional factor of $(\beta\mathcal{J})$ as compared to the conformal answer, which is independent of $\beta\mathcal{J}$. This enhanced contribution is not conformally covariant. However, it has a very simple form in the OPE limit which can be understood as follows. The OPE gives rise to an

energy operator of the model, which has quadratic fluctuations $\langle (\delta E)^2 \rangle$ in the thermal ensemble. These fluctuations are governed by the specific heat of the system, which again is nonzero once we take into account the effects of the breaking of the conformal symmetry. We also consider the contribution of these Goldstone modes in the chaos limit. There they give the dominant term $(\beta\mathcal{J}/N) e^{\frac{2c}{\beta} t}$ that saturates the bound. The reparametrization symmetry of the model is essential to obtain this pseudo-Goldstone boson. In Appendix H we discuss a model that has a low-energy $SL(2, R)$ symmetry but without the conformal symmetry, by thinking of the couplings as dynamical with an $SL(2, R)$ -invariant correlation function. In this case there is no pseudo-Goldstone mode, the low-energy physics is $SL(2, R)$ invariant and the chaos exponent is less than maximal.

In Sec. IV, we give a discussion of the four-point function from the perspective of the large- N effective action for the bilocal field \tilde{G} ; see also Ref. [18]. The intermediate states that appear can be understood from the on-shell condition for fluctuations of this field. The enhanced nonconformal part of the four-point function arises from the functional integral over \tilde{G} configurations that are reparametrizations of the infrared saddle point solution. We give a simple effective field theory argument showing that the effective action is given by the Schwarzian derivative, $\{f(\tau), \tau\}$, of the reparametrization (4.8), with a coefficient of order $(\beta\mathcal{J})^{-1}$ [3]. This action constitutes an explicit breaking of the conformal symmetry. It can be used to derive the enhanced contribution mentioned above, and also to compute the specific heat.

In Sec. V we discuss some features of the spectrum of the model. We start by presenting a numerical computation of the spectrum for the case of $N = 32$. The spectrum in this case is reminiscent of that of a random matrix and, as expected, is statistically symmetric under $H \rightarrow -H$ since the random couplings can be positive as well as negative. At low temperature one is interested in the region near the bottom end of the spectral distribution. We then look at the expression for the free energy at leading order in N , which has the low-temperature expansion $\log Z = -\beta E_0 + S_0 + \frac{c}{2\beta}$ where all terms are of order N . The first term is the ground-state energy, which is not interesting. The second is the zero-temperature entropy. The third, with the specific heat $c \propto N/\mathcal{J}$, arises from the breaking of the conformal symmetry and can be computed in terms of the Schwarzian action for the reparametrizations, after noticing that we can change the temperature by making a reparametrization of the Euclidean circle (or, equivalently, we can go from the circle to the line by a reparametrization). We further consider the N^0 correction to $\log Z$. This arises from the one-loop correction to the effective action for the bilocal fields. All the modes that have a nonvanishing action give a contribution just to E_0 and S_0 , since they are \mathcal{J} independent

(up to UV contributions to E_0). The reparametrization modes give a term that contributes a logarithm to the free energy [27], specifically $-\frac{3}{2}\log(\beta\mathcal{J})$. This additional contribution has an interesting effect. It implies that if we compute the spectral density $\rho(E)$ by inverse Laplace transforming $Z(\beta)$ we obtain that $\rho(E) \propto \mathcal{J}^{-1} e^{\mathcal{S}_0 + \sqrt{2c(E-E_0)}}$, with no prefactor powers of $(E - E_0)$, in the regime where we can trust the computation.

In Sec. VI we comment on the possible bulk interpretation. The enhanced nonconformal contribution agrees with the four-point function one expects in a theory of dilaton gravity [7,26]. This contribution is completely general in any situation with a near extremal black hole with a $N\text{AdS}_2$ region and it follows the same pattern of spontaneous plus explicit breaking of the conformal symmetry [26] (see Ref. [25] for a similar discussion in the $\text{AdS}_3/\text{CFT}_2$ context). Therefore the information about other possible bulk states comes from the contribution that is \mathcal{J} independent and finite in the conformal limit. These are the states that appeared in the OPE expansion of two fermions. This looks like a single Regge trajectory with dimensions that are linearly increasing with “spin,” though spin is hard to define in two dimensions. This implies that a dual description would involve a string with low tension, with $l_s \sim R_{\text{AdS}}$.

Part of our motivation to study this model arose from the observation that the four-point function was saturating the chaos bound, which is a necessary condition for a gravity dual. It was shown in Ref. [11] that stringy corrections to the chaos exponent involve a factor of $1 - l_s^2/R^2$ where R is a suitable distance scale. This suggested that the condition might also be sufficient to exclude models with light strings. However, examining the scale R carefully, it is possible to show that for near extremal black holes this correction has the form $\left(1 - \frac{l_s^2}{R_{\text{AdS}}^2} \frac{(S-S_0)}{S_0}\right)$, where S is the entropy and S_0 is the zero-temperature entropy. Since the ratio of entropies is much less than one, we see that stringy corrections to the Lyapunov exponent are very suppressed, suggesting that even in cases with $l_s \sim R_{\text{AdS}_2}$ we could have a Lyapunov exponent close to the gravity value. In other words, for this case a nearly saturated Lyapunov exponent is not a guarantee of a high string tension. And indeed, in the SYK model we seem to have a low string tension. A related perspective on this is the following: the four-point function saturates the bound because it is dominated by the universal “gravity” piece coming from the zero modes discussed above. This turns out to be enhanced by a factor of $S_0/(S - S_0)$. Relative to this piece, the “stringy” contributions to the four-point function are small, so they have only a mild effect on the chaos exponent.

We also comment on the bulk interpretation of the fermion fields. We speculate that we should not have N fermions in the bulk, but rather one fermion with a string attached to the boundary.

Finally, we note that the bilocal field can be viewed as a field in one more dimension. At low energies the extra dimension defined in this way has a metric characterized by the conformal group and can be viewed as a dS_2 (or AdS_2) space in accordance with recent discussions of kinematic space [28,29]. This follows simply from the structure of the conformal group. Some terms in the action can be viewed as local terms in this space, but others have a nonlocal expression.

In the appendices we give some more details on the computations.

II. TWO-POINT FUNCTIONS

A. The model

We consider a quantum-mechanical model with N Majorana fermions with random interactions involving q of these fermions at a time, where q is an even number. The Hamiltonian is

$$H = (i)^{\frac{q}{2}} \sum_{1 \leq i_1 < i_2 < \dots < i_q \leq N} j_{i_1 i_2 \dots i_q} \psi_{i_1} \psi_{i_2} \dots \psi_{i_q}, \quad (2.1)$$

$$\langle j_{i_1 \dots i_q}^2 \rangle = \frac{J^2 (q-1)!}{N^{q-1}} = \frac{2^{q-1} \mathcal{J}^2 (q-1)!}{q N^{q-1}} \text{ (no sum)}. \quad (2.2)$$

We take each coefficient to be a real variable drawn from a random Gaussian distribution. Equation (2.2) indicates the variance of the distribution. It is characterized by a dimension-one parameter J , (or \mathcal{J} , which is defined with an extra factor that makes the model more uniform in q) which we take to be the same for all coefficients. The numerical factors, and factors of N , are introduced to simplify the large- N limit. A factor of i is necessary to make the Hamiltonian Hermitian when $q = 2 \pmod{4}$. This i means that the system is not time-reversal symmetric for odd $q/2$. Thus, if we restrict to time-reversal-symmetric interactions the model with $q = 4$ represents the dominant interactions at low energy. The others involve some degree of tuning. We assume that the system does not have a spin-glass transition [30] and we work to leading order in the $1/N$ expansion. Though the model generically has a unique ground state, we work at temperatures which are fixed in the large- N expansion, implying that we access an exponentially large number of low-energy states, of order $O(e^{\alpha N})$, $\alpha > 0$.

B. Summing the leading-order diagrams

We will work first in Euclidean space. It is useful to define the Euclidean propagator as

$$G(\tau) \equiv \langle T(\psi(\tau)\psi(0)) \rangle = \langle \psi(\tau)\psi(0) \rangle \theta(\tau) - \langle \psi(0)\psi(\tau) \rangle \theta(-\tau). \quad (2.3)$$

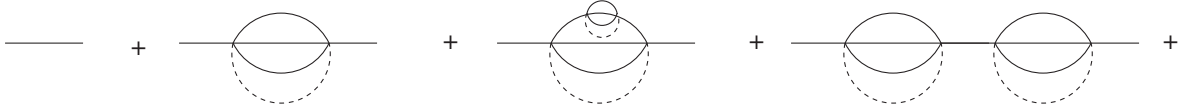


FIG. 1. Diagrams representing corrections to the two-point function, for the $q = 4$ case. The free two-point function is given by the straight line. The first correction involves also an average over disorder, which is represented by a dashed line. We have also indicated a couple more diagrams that also contribute at leading order in N .

For a free Majorana fermion this is very simple

$$\begin{aligned} G_{\text{free}}(\tau) &= \frac{1}{2} \text{sgn}(\tau), \\ G_{\text{free}}(\omega) &= -\frac{1}{i\omega} = \int dt e^{i\omega\tau} G_{\text{free}}(\tau). \end{aligned} \quad (2.4)$$

G_{free} has the same expression at finite temperature, with $\tau \sim \tau + \beta$. Notice that it is correctly antiperiodic as $\tau \rightarrow \tau + \beta$. These equations also normalize the fermion fields appearing in the interaction (2.1). Recall that the free Majorana fermions are simply described by operators that are essentially N -dimensional Dirac γ matrices; see e.g. Ref. [17]. Using this free propagator we can then compute corrections due to the interaction. Let us look at the first correction to the two-point function, shown in Fig. 1. This arises by bringing down two insertions of the interaction Hamiltonian and then averaging with respect to the disorder. The disorder average is represented by a dotted line in Fig. 1. As pointed out in Ref. [19], we can sometimes reproduce similar diagrams by considering j_{i_1, \dots, i_q} to be a dynamical field. Here we will stick to the disordered model. The disorder average links the indices appearing in the two interaction Hamiltonians and we end up with a correction that scales as J^2 relative to the free two-point function, with no additional factors of N , since we get $(q-1)$ factors of N from the sum over the indices of the intermediate lines.

Besides this first diagram, there are many more “iterated watermelon” diagrams that contribute at leading order in N . Two more are shown in Fig. 1. The set of diagrams is sufficiently simple that they can be summed by writing self-consistency equations for the sum. First, it is convenient to define a self-energy, $\Sigma(\tau, \tau')$, which includes all the one-particle-irreducible contributions to the propagator. By translation symmetry, $\Sigma(\tau, \tau') = \Sigma(\tau - \tau')$ and we can write the full two-point function, and the definition of Σ as

$$\frac{1}{G(\omega)} = -i\omega - \Sigma(\omega), \quad \Sigma(\tau) = J^2 [G(\tau)]^{q-1}. \quad (2.5)$$

Notice that the first equation is written in frequency space while the second is in the original (Euclidean) time coordinate (see Fig. 2). Here we have assumed translation symmetry. The possible values of the frequency depend on whether we are at $\beta = \infty$, where it is continuous, or at finite β where we have $\omega = \frac{2\pi}{\beta}(n + \frac{1}{2})$. When we talk about zero

temperature, we are imagining taking the large- N limit first and then the zero-temperature limit.

As a side comment, note that we could consider a model with a Hamiltonian which is a sum of terms with various q 's, and with random couplings with their own variance J_q . The large- N equations for such models would be very similar except that the right-hand side of Eq. (2.5) would be replaced by $\Sigma = \sum_q J_q^2 [G(\tau)]^{q-1}$. But we did not find any good use for this.

C. The conformal limit

At strong coupling, the first equation in Eq. (2.5) can be approximated by ignoring the first term on the right-hand side. It is convenient to write these approximate equations as

$$\begin{aligned} \int dt' G(\tau, \tau') \Sigma(\tau', \tau'') &= -\delta(\tau - \tau''), \\ \Sigma(\tau, \tau') &= J^2 [G(\tau, \tau')]^{q-1}. \end{aligned} \quad (2.6)$$

Written in this form, they are invariant under reparametrizations,

$$\begin{aligned} G(\tau, \tau') &\rightarrow [f'(\tau)f'(\tau')]^\Delta G(f(\tau), f(\tau')), \\ \Sigma(\tau, \tau') &\rightarrow [f'(\tau)f'(\tau')]^{\Delta(q-1)} \Sigma(f(\tau), f(\tau')) \end{aligned} \quad (2.7)$$

provided that $\Delta = 1/q$.

We can then use an ansatz of the form

$$\begin{aligned} G_c(\tau) &= \frac{b}{|\tau|^{2\Delta}} \text{sgn}(\tau), \quad \text{or} \\ G_c(\tau) &= b \left[\frac{\pi}{\beta \sin \frac{\pi\tau}{\beta}} \right]^{2\Delta} \text{sgn}(\tau) \end{aligned} \quad (2.8)$$

where we have given also the finite-temperature version, which follows from Eq. (2.7) with $f(\tau) = \tan \frac{\pi\tau}{\beta}$. We can determine b by inserting these expressions into the simplified equations and obtain

$$J^2 b^q \pi = \left(\frac{1}{2} - \Delta \right) \tan \pi\Delta, \quad \Delta = \frac{1}{q}. \quad (2.9)$$

We will use Δ and $1/q$ interchangeably below. To derive the first equation here, it is convenient to use the Fourier transform

$$\int_{-\infty}^{\infty} d\tau e^{i\omega\tau} \frac{\text{sgn}(\tau)}{|\tau|^{2\Delta}} = i2^{1-2\Delta} \sqrt{\pi} \frac{\Gamma(1-\Delta)}{\Gamma(\frac{1}{2}+\Delta)} |\omega|^{2\Delta-1} \text{sgn}(\omega). \quad (2.10)$$

From Eq. (2.8) it is possible also to compute the Lorentzian time versions by setting $\tau = it$. Since the correlator is not analytic at $\tau = 0$ it is important to know whether we are doing the analytic continuation of the $\tau > 0$ or the $\tau < 0$ Euclidean expressions. The two choices give different choices of ordering of the Lorentzian correlator. For example, the continuation of the $\tau > 0$ form of the Euclidean correlator gives

$$\langle \psi(t)\psi(0) \rangle = G_{c,E}(it + \epsilon) = b \frac{e^{-i\pi\Delta}}{(t - i\epsilon)^{2\Delta}} \quad (2.11)$$

where we summarized the fact that we continue from $\tau > 0$ by the $t \rightarrow t - i\epsilon$ prescription. This equation is valid for any sign of t . Of course the other ordering can be obtained by continuing from the $\tau < 0$ version. We can also get the finite-temperature version by replacing $(t - i\epsilon) \rightarrow \frac{\beta}{\pi} \sinh[\pi(t - i\epsilon)/\beta]$ in Eq. (2.11).

It is sometimes also convenient to introduce the retarded propagator defined as

$$\begin{aligned} G_{c,R}(t) &\equiv \langle \psi(t)\psi(0) + \psi(0)\psi(t) \rangle \theta(t) \\ &= 2b \cos(\pi\Delta) \left[\frac{\pi}{\beta \sinh \frac{\pi t}{\beta}} \right]^{2\Delta} \theta(t) \end{aligned} \quad (2.12)$$

where $\theta(t)$ is the step function. Of course, Eq. (2.12) also shows that the dimension Δ sets the quasinormal mode frequencies as $\omega_n = -i \frac{2\pi}{\beta} (\Delta + n)$.

Here we have given the conformal limit of the expressions. For large βJ , it is possible to solve the equations (2.5) numerically to obtain expressions that smoothly interpolate between the free UV limit and the infrared expressions given above; see Fig. 15 in Appendix G. In addition, in the next subsection we show how to do this interpolation analytically in the large- q limit.

D. Large- q limit

One convenient feature of the model in Eq. (2.1) is the fact that it simplifies considerably for large q .⁴ We can write

$$\begin{aligned} G(\tau) &= \frac{1}{2} \text{sgn}(\tau) \left[1 + \frac{1}{q} g(\tau) + \dots \right], \\ \Sigma(\tau) &= J^2 2^{1-q} \text{sgn}(\tau) e^{g(\tau)} (1 + \dots) \end{aligned} \quad (2.13)$$

where the dots involve higher-order terms in the $1/q$ expansion. We will work in the regime where $g(\tau)$ is of order one. In this regime we can approximate

⁴We are grateful to S. H. Shenker for discussions on this point.

$$\begin{aligned} \frac{1}{G(\omega)} &= \frac{1}{-\frac{1}{i\omega} + \frac{[\text{sgn} \times g](\omega)}{2q}} = -i\omega + \omega^2 \frac{[\text{sgn} \times g](\omega)}{2q} \\ &= -i\omega - \Sigma(\omega) \end{aligned} \quad (2.14)$$

where in the first equality we Fourier transformed the first equation in Eq. (2.13) and we expanded in powers of $1/q$ in the second equality, keeping only the first nontrivial term. Comparing this expression for Σ with the one in Eq. (2.13) we get the equation

$$\partial_t^2 [\text{sgn}(\tau)g(\tau)] = 2\mathcal{J}^2 \text{sgn}(\tau) e^{g(\tau)}, \quad \mathcal{J} \equiv \sqrt{q} \frac{J}{2^{\frac{q-1}{2}}}. \quad (2.15)$$

This equation determines $g(\tau)$. It is well defined in the large- q limit, when we scale J so that \mathcal{J} is kept fixed as $q \rightarrow \infty$. Of course, since J is dimensionful, we can always go to some value of τ where this equation will be valid. We are interested in a solution with $g(\tau = 0) = 0$. In other words, at short distances we should recover the free-fermion result. The derivation of this equation is valid both for zero temperature and finite temperature. The general solution is

$$e^{g(\tau)} = \frac{c^2}{\mathcal{J}^2 \sin(c(|\tau| + \tau_0))^2}. \quad (2.16)$$

We can now impose the boundary conditions $g(0) = g(\beta) = 0$ to obtain

$$e^{g(\tau)} = \left[\frac{\cos \frac{\pi v}{2}}{\cos \left[\pi v \left(\frac{1}{2} - \frac{|\tau|}{\beta} \right) \right]} \right]^2, \quad (2.17)$$

$$\beta \mathcal{J} = \frac{\pi v}{\cos \frac{\pi v}{2}}. \quad (2.18)$$

The second equation determines the parameter v , which ranges from zero to one as $\beta \mathcal{J}$ ranges from zero to infinity. It is also possible to take the $\beta = \infty$ limit of the above expressions to obtain

$$e^{g(\tau)} = \frac{1}{(|t| \mathcal{J} + 1)^2}. \quad (2.19)$$

Note that these results imply that Σ changes more rapidly than G . In fact, G is almost constant, and almost equal to $\frac{1}{2} \text{sgn}(\tau)$, when Σ is changing to its IR value.

E. $q = 2$

Another solvable example is the case of $q = 2$. In this case we can solve Eq. (2.5) as

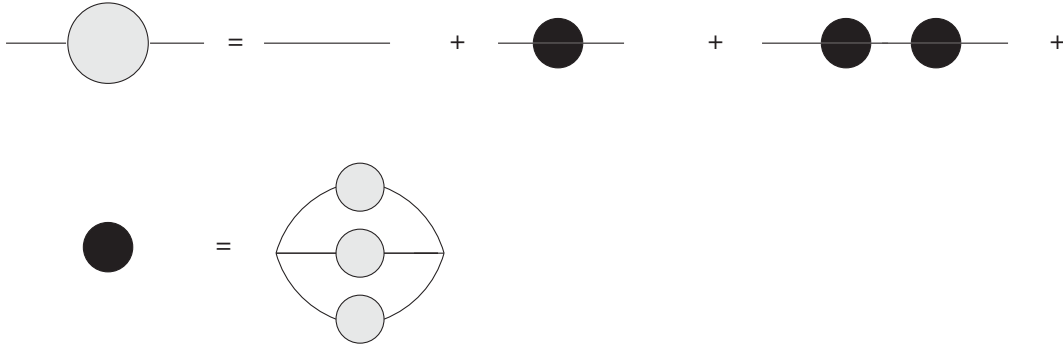


FIG. 2. Equations that define the summation of the leading large- N contributions, for the $q = 4$ case. The solid circle represents the one-particle-irreducible contributions. The dotted circle represents the full two-point function. This is a graphical representation of the equations in Eq. (2.5).

$$G(\omega) = -\frac{2}{i\omega + i\text{sgn}(\omega)\sqrt{4J^2 + \omega^2}}. \quad (2.20)$$

This is the same as the one studied in Refs. [20,31,32]. For positive Euclidean time we get

$$G(\tau) = \text{sgn}(\tau) \int_0^\pi \frac{d\theta}{\pi} \cos^2 \theta e^{-2J|\tau| \sin \theta} \quad (2.21)$$

$$= \frac{1}{\pi J \tau} - \frac{1}{4\pi(J\tau)^3} + \dots, \quad J\tau \gg 1. \quad (2.22)$$

For this particular case, we can simply diagonalize the Hamiltonian (2.1), since it is quadratic. We get a set of fermionic oscillators with some masses. The masses have a semicircle law distribution, since we are diagonalizing a random mass matrix. Near zero frequencies the distribution is constant and we get the same as what we expect for a $1+1$ -dimensional fermion field (from $\theta \sim 0, \pi$ above). The spacing between the frequencies goes like $1/N$, so this fermion is on a large circle. In this sense this example is a bit trivial since it is the same as free fermions. However, it is useful to view it as an extreme example of the more interesting models with $q > 2$. Therefore, in this model we indeed get a fermion in an extra dimension. However, note that we get a single fermion, not N fermions in the extra dimension. We can also simply obtain the finite-temperature expression for the two-point function by summing over images in the zero-temperature answer

$$\begin{aligned} G_\beta(\tau) &= \sum_{m=-\infty}^{\infty} G_{\beta=\infty}(\tau + \beta m) (-1)^m \\ &= \int_0^\pi \frac{d\theta}{\pi} \cos^2 \theta \frac{\cosh[(\frac{\tau}{\beta} - \frac{1}{2})2J\beta \sin \theta]}{\cosh(J\beta \sin \theta)}. \end{aligned} \quad (2.23)$$

F. Computing the entropy

It is possible to write the original partition function of the theory as a functional integral of the form [3,14]

$$\begin{aligned} e^{-\beta F} &= \int \mathcal{D}\tilde{G}\mathcal{D}\tilde{\Sigma} \exp \left[N \left\{ \log \text{Pf}(\partial_t - \tilde{\Sigma}) \right. \right. \\ &\quad \left. \left. - \frac{1}{2} \int d\tau_1 d\tau_2 \left[\tilde{\Sigma}(\tau_1, \tau_2) \tilde{G}(\tau_1, \tau_2) \right. \right. \right. \\ &\quad \left. \left. \left. - \frac{J^2}{q} \tilde{G}(\tau_1, \tau_2)^q \right] \right\} \right]. \end{aligned} \quad (2.24)$$

It can be checked that the classical equations obtained from this reproduce the equations in Eq. (2.5), when we vary with respect to \tilde{G} and $\tilde{\Sigma}$ independently. Here the tildes remind us that we are thinking about the integration variables, while G, Σ without tildes are the solutions of the classical equations from Eq. (2.25), obeying Eq. (2.5). Substituting those solutions into Eq. (2.24) we get the leading large- N approximation to the free energy:

$$\begin{aligned} -\beta F/N &= \log \text{Pf}(\partial_t - \Sigma) - \frac{1}{2} \int d\tau_1 d\tau_2 \\ &\quad \times \left[\Sigma(\tau_1, \tau_2) G(\tau_1, \tau_2) - \frac{J^2}{q} G(\tau_1, \tau_2)^q \right]. \end{aligned} \quad (2.25)$$

In the $q = \infty$ model we know the full solutions for G and Σ , so we can insert them into Eq. (2.25) to obtain the free energy. In order to avoid evaluating the Pfaffian term, it is convenient to take a derivative with respect to $J\partial_J$ of the free energy (2.25). Due to the fact that G and Σ obey the equations of motion, the only contributing term is the derivative of the explicit dependence on J , so that we obtain

$$\begin{aligned} J\partial_J(-\beta F/N) &= \frac{J^2\beta}{q} \int_0^\beta d\tau G(\tau)^q = -\frac{\beta}{q} \partial_\tau G \Big|_{\tau=0^+} \\ &= -\beta E \end{aligned} \quad (2.26)$$

where we have used the equations (2.5) in position space. Since the partition function only depends on the combination βJ , then $J\partial_J$ is the same as $\beta\partial_\beta$. Therefore the above expression gives us the energy.

As $q \rightarrow \infty$, we can insert the solution (2.17) into Eq. (2.26). We can also use the equation (2.15) to do the integral. Furthermore we can turn $J\partial_J \rightarrow \mathcal{J}\partial_{\mathcal{J}}$ and use Eq. (2.18) to turn it into a derivative with respect to v , always keeping q and β fixed. This gives

$$\mathcal{J}\partial_{\mathcal{J}}(-\beta F/N) = \frac{v}{1 + \frac{\pi v}{2} \tan \frac{\pi v}{2}} \partial_v(-\beta F/N) \quad (2.27)$$

$$\begin{aligned} &= \frac{\beta}{4q^2} \int_0^\beta d\tau 2\mathcal{J}^2 e^{g(\tau)} = \frac{\beta}{4q^2} 2(-g'(0)) \\ &= \frac{\pi v}{q^2} \tan \frac{\pi v}{2}, \end{aligned} \quad (2.28)$$

$$-\beta F/N = \frac{1}{2} \log 2 + \frac{1}{q^2} \pi v \left[\tan\left(\frac{\pi v}{2}\right) - \frac{\pi v}{4} \right] \quad (2.29)$$

where we fixed the integration constant using that for $\mathcal{J} \rightarrow 0$ we should recover the free value, which is simply the log of the total dimension of the Hilbert space. The expansion around weak coupling is simply an expansion in powers of v^2 , which translates into an expansion in powers of $(\beta\mathcal{J})^2$, as expected. On the other hand, at strong coupling we can use Eq. (2.18) to find

$$v = 1 - \frac{2}{\beta\mathcal{J}} + \frac{4}{(\beta\mathcal{J})^2} - \frac{(24 + \pi^2)}{3(\beta\mathcal{J})^3} + \dots \quad (2.30)$$

Then, the term of order $1/q^2$ in Eq. (2.29) behaves as

$$\begin{aligned} &\frac{1}{q^2} \left[\frac{2}{1-v} - \left(2 + \frac{\pi^2}{4}\right) + \frac{\pi^2}{3}(1-v) + \dots \right] \\ &= \frac{1}{q^2} \left[(\beta\mathcal{J}) - \frac{\pi^2}{4} + \frac{\pi^2}{2(\beta\mathcal{J})} + \dots \right]. \end{aligned} \quad (2.31)$$

Here the first term can be interpreted as a correction to the ground-state energy. The second term is a correction to the zero-temperature entropy, to which the $\frac{1}{2} \log 2$ term in Eq. (2.29) also contributes. Finally the third term is a temperature-dependent correction to the entropy, or near extremal entropy, which goes like T for low temperature.

The temperature-independent piece can be compared with the result obtained in Ref. [3] for general q (see the earlier Ref. [30] for the $q = 4$ case using the Sachdev-Ye model)

$$\begin{aligned} \frac{S_0}{N} &= \frac{1}{2} \log 2 - \int_0^\Delta dx \pi \left(\frac{1}{2} - x \right) \tan \pi x \\ &\sim \frac{1}{2} \log 2 - \frac{\pi^2}{4q^2} + \dots \end{aligned} \quad (2.32)$$

where the last expression is the approximate answer for large q , which agrees with the temperature-independent piece of Eq. (2.29) using Eq. (2.31).

It is also possible to compute the free energy at $q = 2$. Directly from the free-fermion picture, and subtracting the ground-state energy, we find

$$\begin{aligned} \log Z/N &= \int_0^\pi \frac{d\theta}{\pi} \cos^2 \theta \log [1 + e^{-2J\beta \sin \theta}] \\ &\sim \frac{\pi}{12\beta J} + \dots, \quad \text{for } \beta J \gg 1. \end{aligned} \quad (2.33)$$

We see that at small temperatures the entropy vanishes, in agreement with the first equality in Eq. (2.32) with $\Delta \rightarrow \frac{1}{2}$. We can also see that for large temperatures this reproduces the value $S/N = \frac{1}{2} \log 2$.

We will later show that for general q the expression of the free energy has the form

$$\log Z = -\beta E_0 + S_0 + \frac{c}{2\beta} \quad (2.34)$$

plus higher orders in $1/\beta$. Here E_0 is the ground-state energy, S_0 is the zero-temperature entropy and c/β is the specific heat. E_0 , S_0 and c are all of order N . The exact large- N free energy can be computed numerically for general q . Appendix G contains some discussion of this.

G. Correction to the conformal propagator

It is also interesting to consider the leading correction to the conformal two-point function. For large q the conformal answer is

$$G_c = \frac{b \operatorname{sgn}(\tau)}{|\tau|^{2/q}} = \frac{1}{2} \frac{1}{|\mathcal{J}\tau|^{2\Delta}}, \quad \mathcal{J}^2(2b)^q = 1. \quad (2.35)$$

Using Eqs. (2.13) and (2.19), we find the leading correction

$$G(\tau) = G_c(\tau) \left(1 - \frac{2}{q} \frac{1}{\mathcal{J}|\tau|} + \dots \right). \quad (2.36)$$

At finite temperature, we use Eq. (2.17) to find

$$G(\tau) = G_c(\tau) \left[1 - \frac{2}{q} \frac{1}{\beta\mathcal{J}} \left(2 + \frac{\pi - 2\pi|\tau|/\beta}{\tan \frac{\pi|\tau|}{\beta}} \right) + \dots \right]. \quad (2.37)$$

On the other hand, for $q = 2$ we see from Eq. (2.22) that the order $1/J$ correction vanishes. We will later discuss general values of q .

III. FOUR-POINT FUNCTIONS

In this section, we analyze the leading $1/N$ piece of the four-point function, at strong coupling $\beta J \gg 1$. In any correlation function, the average over disorder j_{i_1, \dots, i_q} will give zero unless the indices of the fermions are equal in

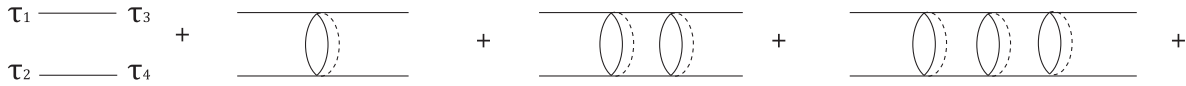


FIG. 3. Diagrams representing the $1/N$ term in the index-averaged four-point function, for the $q = 4$ case. One should also include the diagrams with $(\tau_3 \leftrightarrow \tau_4)$ and a relative minus sign. The propagators here are the dressed two-point functions discussed above.

pairs. This means that the most general nonzero four-point function is

$$\langle \psi_i(\tau_1) \psi_i(\tau_2) \psi_j(\tau_3) \psi_j(\tau_4) \rangle. \quad (3.1)$$

We will consider the case in which we average over i, j . (The pure $i = j$ and $i \neq j$ cases are related in a simple way.) The averaged correlator

$$\begin{aligned} & \frac{1}{N^2} \sum_{i,j=1}^N \langle T(\psi_i(\tau_1) \psi_i(\tau_2) \psi_j(\tau_3) \psi_j(\tau_4)) \rangle \\ & = G(\tau_{12})G(\tau_{34}) + \frac{1}{N} \mathcal{F}(\tau_1, \dots, \tau_4) + \dots \end{aligned} \quad (3.2)$$

has a disconnected piece given by a contraction with the dressed propagators, plus a power series in $1/N$. We will analyze the first term in this series, \mathcal{F} .

A. The ladder diagrams

The diagrams that one must sum to compute \mathcal{F} are ladder diagrams with any number of rungs, built from the dressed propagators discussed in the previous section. The first few diagrams for \mathcal{F} are shown in Fig. 3. We will use \mathcal{F}_n to denote the ladder with n rungs, so that $\mathcal{F} = \sum_n \mathcal{F}_n$. The first diagram, \mathcal{F}_0 , is just a product of propagators

$$\mathcal{F}_0(\tau_1 \dots \tau_4) = -G(\tau_{13})G(\tau_{24}) + G(\tau_{14})G(\tau_{23}). \quad (3.3)$$

This piece contributes at order $1/N$ because the propagators set $i = j$ in the sum of Eq. (3.2). The next diagram is a one-rung ladder, where we integrate over the locations of the ends of the rung:

$$\begin{aligned} \mathcal{F}_1 & = J^2(q-1) \int d\tau d\tau' [G(\tau_1 - \tau)G(\tau_2 - \tau') \\ & \quad \times G(\tau - \tau')^{q-2} G(\tau - \tau_3)G(\tau' - \tau_4) - (\tau_3 \leftrightarrow \tau_4)]. \end{aligned} \quad (3.4)$$

In this expression, the factor of $(q-1)$ comes from the choice of which of the lines coming out of the interaction vertex should be contracted into a rung, and which should

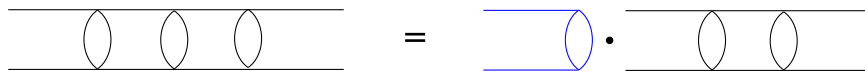


FIG. 4. The $(n+1)$ -rung ladder \mathcal{F}_{n+1} can be generated from the n -rung ladder by “multiplication” with the kernel K , shown in blue. We call the vertical propagators a “rung” and the horizontal ones a “rail.”

continue on as the side rail. This diagram also contributes at order $1/N$, because the $1/N^{q-1}$ scaling of the product of two couplings multiplies a factor of N^{q-2} from the sum over $(q-2)$ indices in the rung loops. One can check that all of the ladder diagrams (and only these!) are proportional to $1/N$.

The standard technique for summing a set of ladder diagrams is to use the fact that they are generated by multiplication by a kernel K . This is illustrated in Fig. 4. Explicitly,

$$\begin{aligned} & \mathcal{F}_{n+1}(\tau_1, \tau_2, \tau_3, \tau_4) \\ & = \int d\tau d\tau' K(\tau_1, \tau_2; \tau, \tau') \mathcal{F}_n(\tau, \tau', \tau_3, \tau_4), \end{aligned} \quad (3.5)$$

where the kernel is

$$K(\tau_1, \tau_2; \tau_3, \tau_4) \equiv -J^2(q-1)G(\tau_{13})G(\tau_{24})G(\tau_{34})^{q-2}. \quad (3.6)$$

It is convenient to think about the integral transform in Eq. (3.5) as a matrix multiplication, where the first two arguments of K form one index of the matrix, and the last two form the other index. The sum of all ladder diagrams is then a geometric series that can be summed by matrix inversion:

$$\mathcal{F} = \sum_{n=0}^{\infty} \mathcal{F}_n = \sum_{n=0}^{\infty} K^n \mathcal{F}_0 = \frac{1}{1-K} \mathcal{F}_0. \quad (3.7)$$

To carry this out, we would like to understand how to diagonalize K . The way we have defined it, K is not a symmetric operator under $(\tau_1, \tau_2) \leftrightarrow (\tau_3, \tau_4)$. However, we can conjugate by a power of the propagator to get a symmetric version

$$\tilde{K}(\tau_1, \tau_2; \tau_3, \tau_4) \equiv |G(\tau_{12})|^{\frac{q-2}{2}} K(\tau_1, \tau_2; \tau_3, \tau_4) |G(\tau_{34})|^{\frac{2-q}{2}} \quad (3.8)$$

$$= -J^2(q-1) |G(\tau_{12})|^{\frac{q-2}{2}} G(\tau_{13})G(\tau_{24}) |G(\tau_{34})|^{\frac{q-2}{2}}. \quad (3.9)$$

This is enough to show that K has a complete set of eigenvectors. We will consider this kernel as acting on the space of antisymmetric functions of two arguments, say τ_3, τ_4 . We will use both \tilde{K} and K in what follows.

B. Using conformal symmetry

So far, what we have said is true for any value of the coupling βJ . In order to proceed further, we will go to the conformal limit $\beta J \gg 1$. In this limit we can use the conformal expressions for $G_c(\tau)$ [Eq. (2.8)]. It is worth noting that the J dependence in K drops out in the conformal limit. This is due to the factors of b in the infrared expressions for G [Eqs. (2.8) and (2.9)]. In the conformal limit computations on the zero-temperature line are equivalent to computations on the finite-temperature circle, after using the map

$$\tau_{\text{line}} = f(\tau_{\text{circle}}) = \tan \frac{\pi \tau_{\text{circle}}}{\beta}. \quad (3.10)$$

This is a special case of the general reparametrization symmetry (2.7). The expressions for the propagators are simpler when we consider the theory on the line, so we will work there for most of this section. Substituting Eq. (2.8) into the kernel we get

$$K_c(\tau_1, \tau_2; \tau_3, \tau_4) = -\frac{1}{\alpha_0} \frac{\text{sgn}(\tau_{13})\text{sgn}(\tau_{24})}{|\tau_{13}|^{2\Delta} |\tau_{24}|^{2\Delta} |\tau_{34}|^{2-4\Delta}} \quad (3.11)$$

$$\alpha_0 \equiv \frac{2\pi q}{(q-1)(q-2) \tan \frac{\pi}{q}} = \frac{1}{(q-1)J^2 b^q}. \quad (3.12)$$

It will turn out that we can safely compute some, but not all, of the large- βJ correlator using this expression for K . The reason is that some of the eigenfunctions have eigenvalue $K_c = 1$ in the conformal limit, leading to a divergence in the geometric series (3.7). When the time comes, in Sec. III C, we will treat those eigenfunctions in perturbation theory outside the conformal limit. For now, we proceed with Eq. (3.11).

The key property that makes it possible to diagonalize Eq. (3.11) is conformal invariance. This can be presented using the following generators of an $SL(2)$ algebra:

$$\begin{aligned} \hat{D} &= -\tau \partial_\tau - \Delta, & \hat{P} &= \partial_\tau, & \hat{K} &= \tau^2 \partial_\tau + 2\tau \Delta, \\ [\hat{D}, \hat{P}] &= P, & [\hat{D}, \hat{K}] &= -\hat{K}, & [\hat{P}, \hat{K}] &= -2\hat{D}. \end{aligned} \quad (3.13)$$

Here $\Delta = 1/q$ is the conformal dimension of the fermion. These generators commute with the kernel K_c , in the sense that up to total derivatives with respect to τ_3 and τ_4 , we have

$$\begin{aligned} &(\hat{D}_1 + \hat{D}_2)K_c(\tau_1, \tau_2; \tau_3, \tau_4) \\ &= K_c(\tau_1, \tau_2; \tau_3, \tau_4)(\hat{D}_3 + \hat{D}_4) \end{aligned} \quad (3.14)$$

and similarly for the \hat{P} and \hat{K} generators. (These are the generators appropriate for acting on the nonsymmetric kernel K_c . To get a set that commutes with the symmetric version \tilde{K}_c we should replace Δ by $1/2$.)

This symmetry is useful in two ways. First, it implies that the ladder diagrams \mathcal{F}_n are simple powers times a function of the $SL(2)$ invariant cross ratio:

$$\chi = \frac{\tau_{12}\tau_{34}}{\tau_{13}\tau_{24}}. \quad (3.15)$$

This is because the function \mathcal{F}_0 in Eq. (3.3) transforms like a conformal four-point function, and this property is preserved by acting with an $SL(2)$ -invariant operator. This will allow us to represent the kernel in the space of functions of a single cross ratio, rather than in the space of functions of two times. In other words, we can consider $K_c(\chi; \tilde{\chi})$ instead of $K_c(\tau_1, \tau_2; \tau_3, \tau_4)$. Second, it implies that the kernel commutes with the Casimir operator C_{1+2} built from the sum of the generators acting on the two times:

$$\begin{aligned} C_{1+2} &= (\hat{D}_1 + \hat{D}_2)^2 - \frac{1}{2}(\hat{K}_1 + \hat{K}_2)(\hat{P}_1 + \hat{P}_2) \\ &\quad - \frac{1}{2}(\hat{P}_1 + \hat{P}_2)(\hat{K}_1 + \hat{K}_2) \\ &= 2(\Delta^2 - \Delta) - \hat{K}_1 \hat{P}_2 - \hat{P}_1 \hat{K}_2 + 2\hat{D}_1 \hat{D}_2. \end{aligned} \quad (3.16)$$

The Casimir is a differential operator with a family of eigenfunctions given by simple powers times functions $\Psi_h(\chi)$. Because the spectrum is nondegenerate, these must be exactly the eigenfunctions of the kernel $K_c(\chi; \tilde{\chi})$ acting in the space of cross ratios. This leads to a recipe for the four-point function:

- (1) Understand the properties of \mathcal{F} and \mathcal{F}_n as functions of the cross ratio.
- (2) Find the eigenfunctions of C_{1+2} with these properties. These are particular hypergeometric functions $\Psi_h(\chi)$, related to conformal blocks of weight h .
- (3) Determine the set of h to have a complete basis of functions. This turns out to be $h = \frac{1}{2} + is$ and $h = 2, 4, 6, 8, \dots$
- (4) Compute $k_c(h)$, the eigenvalue of the kernel K_c as a function of h .
- (5) Determine the inner products $\langle \Psi_h, \mathcal{F}_0 \rangle$ and $\langle \Psi_h, \Psi_h \rangle$.
- (6) Compute the four-point function as

$$\begin{aligned} \mathcal{F}(\chi) &= \frac{1}{1 - K_c} \mathcal{F}_0 \\ &= \sum_h \Psi_h(\chi) \frac{1}{1 - k_c(h)} \frac{\langle \Psi_h, \mathcal{F}_0 \rangle}{\langle \Psi_h, \Psi_h \rangle}. \end{aligned} \quad (3.17)$$

We now go through each of these steps in detail.

1. The four-point function as a function of the cross ratio

In the conformal limit, the ladder diagrams \mathcal{F}_n will transform under $SL(2)$ like a four-point function of dimension Δ fields,

$$\mathcal{F}_n(\tau_1 \dots \tau_4) = G_c(\tau_{12})G_c(\tau_{34})\mathcal{F}_n(\chi),$$

$$\chi = \frac{\tau_{12}\tau_{34}}{\tau_{13}\tau_{24}}, \quad G_c(\tau) = \frac{b \operatorname{sgn}(\tau)}{|\tau|^{2\Delta}}. \quad (3.18)$$

Using the antisymmetry under $\tau_1 \leftrightarrow \tau_2$ and under $\tau_3 \leftrightarrow \tau_4$, the symmetry under $(\tau_1, \tau_2) \leftrightarrow (\tau_3, \tau_4)$ and an $SL(2)$ transformation, we can arrange to have $\tau_1 = 0$, $\tau_3 = 1$, $\tau_4 = \infty$ and also $\tau_2 > 0$. This restricts the cross ratio $\chi = \tau_2$ to be positive. Because of the time ordering in Eq. (3.2), the ordering of the fermions and the overall sign depends on whether χ is less than or greater than one:

$$\mathcal{F}_n(\chi) \sim \begin{cases} +\langle \psi_j(\infty)\psi_j(1)\psi_i(\chi)\psi_i(0) \rangle & 0 < \chi < 1 \\ -\langle \psi_j(\infty)\psi_i(\chi)\psi_j(1)\psi_i(0) \rangle & 1 < \chi < \infty. \end{cases} \quad (3.19)$$

When $\chi < 1$ we have an ijj configuration, and when $\chi > 1$ we have ijj ; see Fig. 10.

In the region $\chi > 1$, the correlation function has an extra discrete symmetry. This is easiest to see if we place the points on the circle using the somewhat nonstandard map

$$\frac{\tau - 2}{\tau} = \tan \frac{\theta}{2}. \quad (3.20)$$

The three operators at 0, 1 and ∞ get sent to the points $-\pi$, $-\frac{\pi}{2}$ and $\frac{\pi}{2}$ as shown in Fig. 5. The final operator at $\tau_2 = \chi$ ends up at some coordinate θ . The obvious symmetry under $\theta \rightarrow -\theta$ translates to $\chi \rightarrow \frac{\chi}{\chi-1}$. This means that in the region $\chi > 1$, we must have $\mathcal{F}(\chi) = \mathcal{F}(\frac{\chi}{\chi-1})$. Notice that this transformation maps the interval $1 < \chi < 2$ to the range $2 < \chi < \infty$, with a fixed point at $\chi = 2$. The conclusion is that the full $\mathcal{F}(\chi)$ is determined once we know it in the region $0 < \chi < 2$, and also that \mathcal{F} must have a vanishing derivative at the point $\chi = 2$.

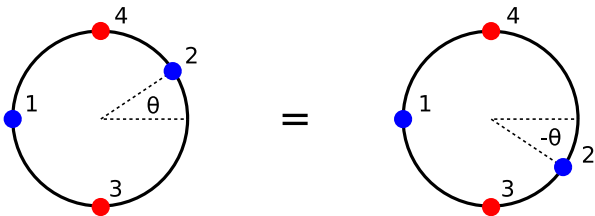


FIG. 5. The symmetry of the $\chi > 1$ correlator under $\chi \rightarrow \frac{\chi}{\chi-1}$ is manifest as $\theta \rightarrow -\theta$ after mapping to the circle.

An obvious advantage of the cross ratio is that the ladder kernel becomes a function of fewer variables. One can substitute the form (3.18) into the original expression for the kernel (3.5) and then do one of the τ integrals. The result is an equation of the form

$$\mathcal{F}_{n+1}(\chi) = \int_0^2 \frac{d\tilde{\chi}}{\tilde{\chi}^2} K_c(\chi; \tilde{\chi}) \mathcal{F}_n(\tilde{\chi}) \quad (3.21)$$

where $K_c(\chi; \tilde{\chi})$ is a symmetric kernel that is given in terms of hypergeometric functions in Appendix B.

2. Eigenfunctions of the Casimir

We now search for a complete set of eigenfunctions of the Casimir C_{1+2} with the properties just described. First we need to understand how C_{1+2} acts on functions of the cross ratio. One can check directly from Eq. (3.16) that

$$C_{1+2} \frac{1}{|\tau_{12}|^{2\Delta}} f(\chi) = \frac{1}{|\tau_{12}|^{2\Delta}} \mathcal{C}f(\chi),$$

$$\mathcal{C} \equiv \chi^2(1-\chi)\partial_\chi^2 - \chi^2\partial_\chi. \quad (3.22)$$

Writing the eigenvalue as $h(h-1)$, the equation we would like to solve is $\mathcal{C}f = h(h-1)f$. The general solution is a linear combination of

$$\chi^h {}_2F_1(h, h, 2h, \chi), \quad \chi^{1-h} {}_2F_1(1-h, 1-h, 2-2h, \chi). \quad (3.23)$$

We need to select from this set a complete basis for the space of functions with $f'(2) = 0$. These functions should also be normalizable with respect to the inner product from Eq. (3.21) that makes K symmetric,

$$\langle g, f \rangle = \int_0^2 \frac{d\chi}{\chi^2} g^*(\chi) f(\chi). \quad (3.24)$$

This is the same inner product that makes \mathcal{C} Hermitian, neglecting boundary terms. Since the eigenfunctions of a Hermitian operator are complete, we can determine the basis by finding the conditions that make the boundary terms vanish, and then selecting the eigenfunctions from among Eq. (3.23) that satisfy these conditions.

The Hermiticity condition is

$$0 = \langle g, \mathcal{C}f \rangle - \langle \mathcal{C}g, f \rangle$$

$$= \int_0^2 d\chi [g^*(1-\chi)f' - g'^*(1-\chi)f]'. \quad (3.25)$$

At $\chi = 2$ the boundary term vanishes due to the requirement $f'(2) = 0$. At $\chi = 0$ it vanishes provided that we impose that $f \rightarrow 0$ faster than $\chi^{1/2}$. Because the eigenfunctions (3.23) have logarithmic singularities at $\chi = 1$, there is another possible ‘‘boundary’’ contribution from this

point. In order for it to vanish, we need to impose that the logarithmic and constant terms in f agree as we approach $\chi = 1$ from the two sides. In other words, if we have $f \sim A + B \log(1 - \chi)$ for $\chi \rightarrow 1^-$, then we should have $f \sim A + B \log(\chi - 1)$ for $\chi \rightarrow 1^+$. This will cancel the boundary terms provided that we define the integral by approaching one in the same way from 1^- and 1^+ .

We now look for eigenfunctions with these properties. We can start in the region $\chi > 1$ by imposing that $f'(2) = 0$. This selects a linear combination of the functions (3.23) that can be written using a special hypergeometric identity as

$$\Psi_h = \frac{\Gamma(\frac{1}{2} - \frac{h}{2})\Gamma(\frac{h}{2})}{\sqrt{\pi}} {}_2F_1\left(\frac{h}{2}, \frac{1}{2} - \frac{h}{2}, \frac{1}{2}, \frac{(2 - \chi)^2}{\chi^2}\right), \quad 1 < \chi, \quad (3.26)$$

where we have chosen a convenient normalization constant. Note that $\Psi_h = \Psi_{1-h}$ in a manifest way. In the region $\chi < 1$, we must match to a linear combination

$$\Psi_h = A \frac{\Gamma(h)^2}{\Gamma(2h)} \chi^h {}_2F_1(h, h, 2h, \chi) + B \frac{\Gamma(1-h)^2}{\Gamma(2-2h)} \chi^{1-h} {}_2F_1(1-h, 1-h, 2-2h, \chi), \quad \chi < 1, \quad (3.27)$$

by requiring that the logarithmic and constant terms at $\chi = 1$ agree with Eq. (3.26). This determines

$$A = \frac{1}{\tan \frac{\pi h}{2}} \frac{\tan \pi h}{2}, \quad B = A(1-h) = -\tan \frac{\pi h}{2} \frac{\tan \pi h}{2}. \quad (3.28)$$

The final condition to impose is that Ψ_h must vanish at least as fast as $\chi^{1/2}$ as $\chi \rightarrow 0$. There are two types of solutions.

- (1) For $h = \frac{1}{2} + is$ both terms in Eq. (3.27) are marginally allowable. These solutions are monotonic for $1 < \chi$ and oscillatory for $\chi < 1$, with infinitely many oscillations.
- (3) For $h = 2n$, $n = 1, 2, 3, \dots$ the B coefficient vanishes, so Eq. (3.27) is again allowable at small χ . These solutions are monotonic for $0 < \chi < 1$ and oscillatory for $1 < \chi$ (it crosses zero n times).

Together, these two sets form a complete basis of normalizable functions with $f'(2) = 0$. We emphasize that in both cases, Ψ_h is given by Eq. (3.26) for $1 < \chi$ and Eq. (3.27) for $\chi < 1$. For the continuum states $h = \frac{1}{2} + is$ there is an integral representation that gives the correct answer for all $\chi > 0$,

$$\Psi_h(\chi) = \frac{1}{2} \int_{-\infty}^{\infty} dy \frac{|\chi|^h}{|y|^h |\chi - y|^h |1 - y|^{1-h}}. \quad (3.29)$$

This integral does not converge for the discrete states. Finally, we note for later use that near $\chi = 1$ the function Ψ_h has the expansion

$$\Psi_h \sim -\left[\log(\chi - 1) + 2\gamma + 2\psi(h) - \pi \tan \frac{\pi h}{2}\right] (\chi > 1). \quad (3.30)$$

For $\chi < 1$ we replace $\log(\chi - 1) \rightarrow \log(1 - \chi)$.

3. The eigenvalues of the kernel $k_c(h)$

The eigenfunctions Ψ_h of the Casimir \mathcal{C} were non-degenerate. Because the Casimir commutes with the kernel K_c , these functions must also be eigenfunctions of K_c . In principle, we can compute the eigenvalues $k_c(h)$ by integrating the functions $\Psi_h(\chi)$ with $K_c(\chi; \tilde{\chi})$. However, we can get the answer in a simpler way. We start by backing off of the cross ratio formalism and thinking about the Casimir acting on two times, \mathcal{C}_{1+2} . Eigenfunctions of this operator with eigenvalue $h(h-1)$ have the form of conformal three-point functions of two fermions with a dimension h operator,

$$\frac{\text{sgn}(\tau_1 - \tau_2)}{|\tau_1 - \tau_0|^h |\tau_2 - \tau_0|^h |\tau_1 - \tau_2|^{2\Delta-h}}. \quad (3.31)$$

For any value of τ_0 and h , these are also eigenfunctions of the kernel K_c . The eigenvalue $k_c(h)$ depends only on h , since we can use $SL(2)$ to move τ_0 around. In particular, we can take it to infinity, so that the eigenvalue is [see Eq. (3.11)]

$$k_c(h) = \int d\tau d\tau' K_c(1, 0; \tau, \tau') \frac{\text{sgn}(\tau - \tau')}{|\tau - \tau'|^{2\Delta-h}} = -\frac{1}{\alpha_0} \int d\tau d\tau' \frac{\text{sgn}(1 - \tau) \text{sgn}(-\tau') \text{sgn}(\tau - \tau')}{|1 - \tau|^{2\Delta} |\tau'|^{2\Delta} |\tau - \tau'|^{2-2\Delta-h}}. \quad (3.32)$$

This integral can be evaluated by dividing up the τ and τ' integrals into regions where the sign functions are constant. A quicker way to get the answer is as follows. We use

$$\frac{\text{sgn}(\tau)}{|\tau|^a} = \int \frac{d\omega}{2\pi} e^{-i\omega\tau} c(a) |\omega|^{a-1} \text{sgn}(\omega), \quad c(a) = 2i2^{-a} \sqrt{\pi} \frac{\Gamma(1 - \frac{a}{2})}{\Gamma(\frac{1}{2} + \frac{a}{2})} \quad (3.33)$$

to write the factor in Eq. (3.32) that depends on $|\tau - \tau'|$ as a Fourier transform. Then the τ and τ' integrals factorize. We can shift the integration variables and then use Eq. (3.33)

$$-(q-1) \begin{array}{c} \longrightarrow \\ \text{---} \text{---} \text{---} \\ \longleftarrow \end{array} \text{---} \text{---} \text{---} = (q-1) \begin{array}{c} \longrightarrow \\ \text{---} \text{---} \\ \longleftarrow \end{array} \longrightarrow = -(q-1) \longrightarrow$$

FIG. 6. On the left we have the kernel acting on $G(\tau)$. This is equal to $(q-1)G * \Sigma * G$. Using the approximate Schwinger-Dyson equation (2.6), this becomes $-(q-1)G$.

again for each factor. These two factors are equal up to an overall sign. Finally we get an integral of the same form as Eq. (3.33). Thus we find that

$$k_c(h) = -\frac{1}{\alpha_0} \frac{c(2-2\Delta-h)}{c(2\Delta-h)} [c(2\Delta)]^2 (-1). \quad (3.34)$$

Using α_0 from Eq. (3.11) and using Γ function identities, one finds [3]

$$k_c(h) = -(q-1) \frac{\Gamma(\frac{3}{2}-\frac{1}{q})\Gamma(1-\frac{1}{q})}{\Gamma(\frac{1}{2}+\frac{1}{q})\Gamma(\frac{1}{q})} \frac{\Gamma(\frac{1}{q}+\frac{h}{2})}{\Gamma(\frac{3}{2}-\frac{1}{q}-\frac{h}{2})} \times \frac{\Gamma(\frac{1}{2}+\frac{1}{q}-\frac{h}{2})}{\Gamma(1-\frac{1}{q}+\frac{h}{2})}. \quad (3.35)$$

We can apply this result to the eigenfunctions $\Psi_h(\chi)$ by using the representation

$$\begin{aligned} & \frac{\text{sgn}(\tau_{12})\text{sgn}(\tau_{34})}{|\tau_{12}|^{2\Delta}|\tau_{34}|^{2\Delta}} \Psi_h(\chi) \\ &= \frac{1}{2} \int d\tau_0 \frac{\text{sgn}(\tau_{12})}{|\tau_{10}|^h |\tau_{20}|^h |\tau_{12}|^{2\Delta-h}} \\ & \times \frac{\text{sgn}(\tau_{34})}{|\tau_{30}|^{1-h} |\tau_{40}|^{1-h} |\tau_{34}|^{2\Delta-1+h}} \end{aligned} \quad (3.36)$$

which holds for $h = \frac{1}{2} + is$. This follows from the $SL(2)$ covariance of the right-hand side and from Eq. (3.29). The τ_1, τ_2 dependence here is a superposition of eigenfunctions of the form (3.31), so the left-hand side is an eigenfunction of K_c with eigenvalue $k_c(h)$. The eigenfunctions in the discrete case are analytic continuations of the continuum eigenfunctions, so their eigenvalues are determined by the continuation of $k_c(h)$.

The eigenvalue $k_c(h)$ is real for all of the eigenvectors $h = \frac{1}{2} + is$ and $h = 2, 4, 6, \dots$. It is positive for the discrete states, and negative for the continuum. We will find the full analytic function useful in what follows. This function satisfies $k_c(h) = k_c(1-h)$. For generic q , it has poles at $h = 1 + \frac{2}{q} + 2n$ for $n \geq 0$ and the corresponding $h \rightarrow (1-h)$ reflection. Some simple special cases are

$$k_c(h) = -\frac{3 \tan \frac{\pi(h-1/2)}{2}}{2(h-1/2)}, \quad q = 4, \quad (3.37)$$

$$k_c(h) = \frac{2}{h(h-1)}, \quad q = \infty, \quad (3.38)$$

$$k_c(h) = -1, \quad q = 2. \quad (3.39)$$

We can understand $k_c(h)$ at some special values of h using the Schwinger-Dyson equation. When $h = 0$, we are acting the kernel on a multiple of the original $G_c(\tau)$. This should give $k_c(0) = -(q-1)$, as we argue in Fig. 6. We will see below that when $h = 2$, we are acting with the kernel on a linearized reparametrization of $G_c(\tau)$. One can then use the reparametrization invariance of Eq. (2.6) to make a similar argument that $k_c(2) = 1$; see Eq. (3.71) below.

4. The inner products $\langle \Psi_h, \Psi_h \rangle$ and $\langle \Psi_h, \mathcal{F}_0 \rangle$

Next we consider the norms of the eigenfunctions Ψ_h , beginning with the continuum $h = \frac{1}{2} + is$, and taking $s, s' > 0$. We continue to use the norm for functions of χ defined in Eq. (3.24). We expect the inner product $\langle \Psi_h, \Psi_{h'} \rangle$ to be proportional to $\delta(s-s')$. A singular contribution of this type can only come from the small- χ region of the inner product integral, where we can replace the hypergeometric functions in Eq. (3.26) by one. Using \sim to denote agreement up to terms that are finite as $s \rightarrow s'$, we have

$$\begin{aligned} \langle \Psi_h, \Psi_{h'} \rangle &\sim \frac{\pi \tan \pi h}{4h-2} \int_0^\epsilon \frac{d\chi}{\chi} (\chi^{i(s-s')} + \chi^{-i(s-s')}) \\ &\sim \frac{\pi \tan \pi h}{4h-2} 2\pi \delta(s-s'). \end{aligned} \quad (3.40)$$

Based on this calculation, one might expect that the inner product has finite terms in addition to the $\delta(s-s')$. In fact, this cannot be the case, since eigenfunctions with different values of s must be orthogonal. We conclude that the rhs of Eq. (3.40) is the exact answer.

For the discrete set, $h = 2n$, we have that $\Psi_h(\chi) = 2\text{Re}[Q_{h-1}(y)]$, where $y = (2-\chi)/\chi$ and Q is the Legendre Q function. After writing the inner product as an integral over y , one can use standard integral formulas for Q to find

$$\langle \Psi_h, \Psi_{h'} \rangle = \frac{\delta_{hh'} \pi^2}{4h-2}. \quad (3.41)$$

We also need to compute the inner product of these eigenfunctions with the zero-rung ladder \mathcal{F}_0 . As a function

of the times τ_1, \dots, τ_4 , \mathcal{F}_0 is given in Eq. (3.3). Using the conformal form of $G(\tau)$ and going to a function of χ using Eq. (3.18), we have

$$\mathcal{F}_0(\chi) = \begin{cases} -\chi^{2\Delta} + \left(\frac{\chi}{1-\chi}\right)^{2\Delta} & 0 < \chi < 1 \\ -\chi^{2\Delta} - \left(\frac{\chi}{\chi-1}\right)^{2\Delta} & 1 < \chi < \infty. \end{cases} \quad (3.42)$$

We consider the inner product with the continuum states; the case with the discrete states will follow by analytic continuation in h . The inner product integral can be done inside the integral representation (3.29). Notice that the integral representation extends to a function on the entire line $-\infty < \chi < \infty$ that satisfies $\Psi(\chi) = \Psi(\frac{\chi}{\chi-1})$. For $\chi > 1$ we have that the zero-rung ladder \mathcal{F}_0 is symmetric under the same transformation, while for $\chi < 1$ it is antisymmetric. Using these properties we can write the inner product as a single integral over the whole line:

$$\langle \Psi_h, \mathcal{F}_0 \rangle = -\frac{1}{2} \int_{-\infty}^{\infty} dy d\chi \frac{\text{sgn}(\chi)}{|\chi|^{2-h-2\Delta} |\chi-y|^h |1-y|^{1-h} |y|^h}. \quad (3.43)$$

The integration region can now be divided up and all integrals can be done using the Euler beta function. It is convenient to write the answer in terms of the eigenvalue function $k_c(h)$ as

$$\langle \mathcal{F}_0, \Psi_h \rangle = \frac{\alpha_0}{2} k_c(h). \quad (3.44)$$

We can understand the appearance of $k_c(h)$ here by realizing that \mathcal{F}_0 is proportional to the action of K_c on a delta function, so it should have an expression involving an integral of $k_c(h)$ over the basis elements. We discuss this further in Appendix C.

5. The sum of all ladders

We can now write a slightly naive expression for the full sum of ladders as

$$\begin{aligned} \mathcal{F}(\chi) &= \sum_h \Psi_h(\chi) \frac{1}{1-k_c(h)} \frac{\langle \Psi_h, \mathcal{F}_0 \rangle}{\langle \Psi_h, \Psi_h \rangle} \\ &= \alpha_0 \int_0^\infty \frac{ds}{2\pi} \frac{(2h-1)}{\pi \tan(\pi h)} \frac{k_c(h)}{1-k_c(h)} \Psi_h(\chi) \\ &\quad + \alpha_0 \sum_{n=1}^{\infty} \left[\frac{(2h-1)}{\pi^2} \frac{k_c(h)}{1-k_c(h)} \Psi_h(\chi) \right]_{h=2n}. \end{aligned} \quad (3.45)$$

The problem with this formula is that the $n = 1$ term in the sum diverges, since the eigenvalue $k_c(2) = 1$. Of course, the actual four-point function is finite; what this means is that we have to treat the contribution of the $h = 2$ eigenfunctions outside the conformal limit, where the

eigenvalues will be slightly less than one. This gives an enhanced contribution that we will analyze in Sec. III C below.⁵ For now we focus on the contribution of the $h \neq 2$ eigenfunctions, for which the conformal limit can be taken smoothly. We refer to the contribution of these eigenfunctions as $\mathcal{F}_{h \neq 2}$:

$$\begin{aligned} \frac{\mathcal{F}_{h \neq 2}}{\alpha_0} &= \int_0^\infty \frac{ds}{2\pi} \frac{(2h-1)}{\pi \tan(\pi h)} \frac{k_c(h)}{1-k_c(h)} \Psi_h(\chi) \\ &\quad + \sum_{n=1}^{\infty} \left[\frac{(2h-1)}{\pi^2} \frac{k_c(h)}{1-k_c(h)} \Psi_h(\chi) \right]_{h=2n}. \end{aligned} \quad (3.46)$$

This can be put into a more convenient form by substituting

$$\frac{2}{\tan \pi h} = \frac{1}{\tan \frac{\pi h}{2}} - \frac{1}{\tan \frac{\pi(1-h)}{2}}, \quad (3.47)$$

and then combining terms by extending the region of integration to all values of s and using the antisymmetry of the rest of the integrand under $h \rightarrow 1-h$. We get

$$\begin{aligned} \frac{\mathcal{F}_{h \neq 2}(\chi)}{\alpha_0} &= \int_{-\infty}^{\infty} \frac{ds}{2\pi} \frac{(h-1/2)}{\pi \tan(\pi h/2)} \frac{k_c(h)}{1-k_c(h)} \Psi_h(\chi) \\ &\quad + \sum_{n=2}^{\infty} \text{Res} \left[\frac{(h-1/2)}{\pi \tan(\pi h/2)} \frac{k_c(h)}{1-k_c(h)} \Psi_h(\chi) \right]_{h=2n} \end{aligned} \quad (3.48)$$

where now the integral runs over all s , and we have written the discrete sum as a sum over residues of the poles of $1/\tan(\pi h/2)$.

A nice feature of this formula is that it can be understood as a single contour integral, over a contour in the complex h plane defined as

$$\frac{1}{2\pi i} \int_{\mathcal{C}} dh = \int_{-\infty}^{\infty} \frac{ds}{2\pi} + \sum_{n=1}^{\infty} \text{Res}_{h=2n}. \quad (3.49)$$

Note that Ψ_h has poles at $h = 1 + 2n$. However, these are canceled by zeros of $1/\tan(\pi h/2)$ at the same values. Therefore the product has poles only at $h = 2n$. The contribution of the explicit residues will imply that we do not end up picking up the poles at these locations either when we shift the contour to the right.

Let us see how this works in more detail. First, we consider the case $\chi > 1$. Then we can push the contour from the s axis rightward to infinity. In the process, we cancel the sum over residues, but we pick up poles at the locations where $k_c(h) = 1$ (see Fig. 7). We refer to these values as h_m , and we will say more about them in the next section:

⁵In Appendix H we discuss a model where we effectively replace $1 - k_c(h) \rightarrow 1 - gk_c(h)$, with $g < 1$, in Eq. (3.45), which removes the $h = 2$ divergence.

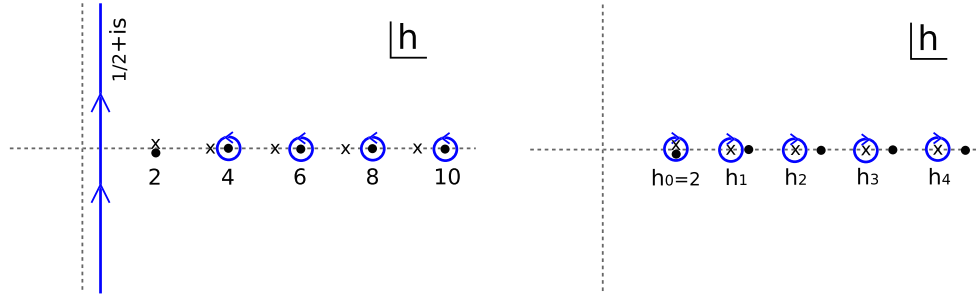


FIG. 7. The continuum piece of the contour that defines $\mathcal{F}_{h \neq 2}$ can be pushed to the right, canceling the residues of the poles of the $1/\tan(\pi h/2)$ (dots), and picking up poles from the locations where $k_c(h) = 1$ (crosses). We have a double pole at $h = 2$.

$$\mathcal{F}_{h \neq 2}(\chi) = -\alpha_0 \sum_{m=0}^{\infty} \text{Res} \left[\frac{(h-1/2)}{\pi \tan(\pi h/2)} \frac{k_c(h)}{1-k_c(h)} \Psi_h(\chi) \right]_{h=h_m}, \quad \chi > 1. \quad (3.50)$$

The case for $\chi < 1$ is more delicate, since we cannot push the ${}_2F_1(1-h, 1-h, 2-2h, \chi)$ function in $\Psi_h(\chi)$ to large positive h . So we do the following: first, we use the $h \rightarrow (1-h)$ antisymmetry of the rest of the integrand to replace the $\tan(\pi h/2)$ inside the integral by $\tan(\pi h)$. This gives an integrand that is explicitly symmetric under $h \rightarrow (1-h)$. Next, we use this symmetry to replace the B term in Eq. (3.27) by another copy of the A term. This gives

$$\begin{aligned} \frac{\mathcal{F}_{h \neq 2}(\chi)}{\alpha_0} &= \int \frac{ds}{2\pi} \frac{(h-1/2)}{\pi \tan(\pi h/2)} \frac{k_c(h)}{1-k_c(h)} \\ &\times \frac{\Gamma(h)^2}{\Gamma(2h)} \chi^h {}_2F_1(h, h, 2h, \chi) \\ &+ \sum_{n=2}^{\infty} \text{Res} \left[\frac{(h-1/2)}{\pi \tan(\pi h/2)} \frac{k_c(h)}{1-k_c(h)} \right. \\ &\left. \times \frac{\Gamma(h)^2}{\Gamma(2h)} \chi^h {}_2F_1(h, h, 2h, \chi) \right]_{h=2n}, \end{aligned} \quad (3.51)$$

where, in the residue sum, we have also used that $\Psi_h(\chi) = \frac{\Gamma(h)^2}{\Gamma(2h)} \chi^h {}_2F_1(h, h, 2h, \chi)$ for even integer h . This integrand can now be pushed to the right as before, canceling the explicit residues and picking up the poles where $k_c(h) = 1$:

$$\mathcal{F}_{h \neq 2}(\chi) = -\alpha_0 \sum_{m=0}^{\infty} \text{Res} \left[\frac{(h-1/2)}{\pi \tan(\pi h/2)} \frac{k_c(h)}{1-k_c(h)} \times \frac{\Gamma(h)^2}{\Gamma(2h)} \chi^h {}_2F_1(h, h, 2h, \chi) \right]_{h=h_m}, \quad \chi < 1. \quad (3.52)$$

6. Operators of the model

An important region of the four-point function is the OPE limit of small χ . The expansion of the four-point

function in this region gives the coefficients and dimensions of the operators appearing in the product of two fermions, $\psi_i(0)\psi_i(\chi)$. We can read these off from the expression (3.52).

The first solution to $k_c(h) = 1$ is $h_0 = 2$. Although we omitted the divergent $h = 2$ piece from the discrete sum in defining $\mathcal{F}_{h \neq 2}$, we still pick up a finite contribution from the double pole at that location when we deform the contour. Naively, this would lead to a logarithmic term that is difficult to interpret in the OPE. However, it turns out that this piece cancels against other contributions related to the $h = 2$ subspace that will be described in Sec. III C 4 below.

After $h_0 = 2$, we have an infinite set of solutions h_1, h_2, \dots that are associated to ordinary poles. The sum over these has the expected form for an operator product expansion

$$\langle 4pt \rangle = \sum_{m=1}^{\infty} c_m^2 [\chi^{h_m} {}_2F_1(h_m, h_m, 2h_m, \chi)], \quad (3.53)$$

where the h_m are the dimensions of the operators appearing, the quantity in brackets is the corresponding conformal block, and c_m^2 would be the square of the operator product coefficient. In particular, c_m^2 should be positive. From Eq. (3.52) we get

$$\begin{aligned} c_m^2 &= -\frac{\alpha_0}{N} \cdot \frac{(h_m-1/2)}{\pi \tan(\pi h_m/2)} \frac{\Gamma(h_m)^2}{\Gamma(2h_m)} \cdot \frac{1}{-k'(h_m)} \\ &\times (h_m > 2). \end{aligned} \quad (3.54)$$

In this expression, we have included the overall factor of $1/N$ that relates $\mathcal{F}(\chi)$ to the four-point function (3.2). One can check that c_m^2 is positive, because $k'(h_m)$ is negative and $\tan \pi h_m/2$ is also negative. The rest of the factors are positive.

We do not have an exact expression for the dimensions h_m , but we can parametrize the values as

$$h_m = 2\Delta + 1 + 2m + \epsilon_m, \quad (3.55)$$

where we observe that ϵ_m becomes small at large m . Asymptotically,

$$\begin{aligned} \epsilon_m &= \frac{2\Gamma(3-2\Delta)\sin(2\pi\Delta)}{\pi\Gamma(1+2\Delta)} \frac{1}{(2m)^{2-4\Delta}}, \quad m \gg 1, \\ \epsilon_m &= \frac{3}{2\pi m}, \quad \text{for } \Delta = 1/4, \\ \epsilon_m &= \frac{2\Delta}{m^2}, \quad \text{for } \Delta \rightarrow 0. \end{aligned} \quad (3.56)$$

One would like to view these as arising from two particles in *AdS* with some interaction. In general the correction to the energy is related to the scattering phase shift $\delta \sim \log S$, where S is the S matrix. This is related to the relativistically invariant amplitude by $\delta \sim \mathcal{A}/s$ where s is the center-of-mass energy, or equal to $s \sim m^2$ in this case (for large m). We see that, generically, we cannot get Eq. (3.56) from a local interaction, since those would involve powers of m^2 . For example, an interaction mediated by a particle of spin J would give $\delta \sim m^{2J-2}$, while what we have here goes like $\delta \sim 1/m$ (for $q = 4$). For the special case of $\Delta \rightarrow 0$, we have something consistent with an interaction mediated by a spin-zero field, but the interaction is going to zero as $\Delta \rightarrow 0$.

Here we have emphasized that the h_m values are the powers that appear in the OPE. By conformal invariance, these are the same powers that determine the decay of perturbations to the system after excitation by a fermion bilinear.

7. Analytic continuation to the chaos region

Another interesting region to consider is where we take the large real-time behavior of an out-of-time-order product with the ordering $\psi_i(t)\psi_j(0)\psi_i(t)\psi_j(0)$. The behavior of four-point functions in this limit is a probe of chaos. A convenient configuration is the correlator

$$\text{Tr}[y\psi_i(t)y\psi_j(0)y\psi_i(t)y\psi_j(0)], \quad y \equiv \rho(\beta)^{1/4} \quad (3.57)$$

where we have split the thermal density matrix into four factors y as in Ref. [12]. In a conformal theory, this can be obtained from the Euclidean correlator on the line, by mapping to the finite-temperature circle using Eq. (3.10) and then continuing to real time. To get the configuration (3.57), the upshot is that we should study the four-point function at a value of the cross ratio equal to

$$\chi = \frac{2}{1 - i \sinh \frac{2\pi t}{\beta}}. \quad (3.58)$$

Note that the $\chi \rightarrow \chi/(\chi - 1)$ symmetry of the correlator takes $t \rightarrow -t$ in Eq. (3.58) and it ensures the reality of Eq. (3.57). Notice that for $t = 0$ this is a value greater than one, so we should start with the formula for $\chi > 1$ and analytically continue it. For large values of t , we will end up with a small and purely imaginary cross ratio. But because

we are continuing the $\chi > 1$ expression to small χ , we do not end up with the OPE limit of small χ .

The difference between these limits arises because the continuation to small χ of the $\chi > 1$ expression for Ψ_h is not the same as the function Ψ_h evaluated directly at small χ . Indeed, for small χ , the continuation gives

$$\Psi_h^{\chi > 1}(\chi) \sim \frac{\Gamma(\frac{1}{2} - \frac{h}{2})\Gamma(h - \frac{1}{2})}{2^{1-h}\Gamma(\frac{h}{2})} (-i\chi)^{1-h} + (h \rightarrow 1 - h). \quad (3.59)$$

If the real part of h is greater than one, this will be growing for small χ . By Eq. (3.58), this translates to exponential growth as a function of t that is a diagnostic of many-body chaos.

Formally, the divergent term at $h = 2$ corresponds to a growth $\propto \chi^{-1} \propto e^{2\pi t/\beta}$ that saturates the chaos bound. We will see below that this rate of growth remains correct when we treat the enhanced $h = 2$ contribution outside the conformal limit. For now, we consider the continuation of the rest of the correlator, $\mathcal{F}_{h \neq 2}$, but we emphasize that this is a small correction to the $h = 2$ piece, in the chaos limit as well as elsewhere.

If $\mathcal{F}_{h \neq 2}$ were a finite sum of Ψ_h , we could analyze the chaos region by continuing each of the terms separately. If we try this with Eq. (3.48), or with Eq. (3.50), we will find that the residue sum does not converge after the continuation. So we have to first manipulate the expression into a form that is safer to continue. We start by defining a function $k_R(h)$ by

$$\frac{k_R(1-h)}{k_c(h)} = \frac{\cos \pi(\Delta - \frac{h}{2})}{\cos \pi(\Delta + \frac{h}{2})}. \quad (3.60)$$

This function has an interpretation in terms of the eigenvalues of the real-time ladder kernel constructed from retarded propagators (3.115). However, for our purposes we only need to know two properties. First, $k_R(1-h) = k_c(h)$ when h is an even integer, so we can replace $k_c(h) \rightarrow k_R(1-h)$ inside the residue sum of Eq. (3.48). Second, $k_R(1-h) = 1$ has only one solution with the real part of h positive, which is $h = 2$. This means that when we pull the contour that circles the $h = 4, 6, \dots$ poles back to the line $h = \frac{1}{2} + is$, as shown in Fig. 8, we will only pick up a double pole at $h = 2$ plus the integral over the line. This leads to

$$\begin{aligned} \frac{\mathcal{F}_{h \neq 2}(\chi)}{\alpha_0} &= \int \frac{ds}{2\pi} \frac{(h-1/2)}{\pi \tan(\pi h/2)} \left[\frac{k_c(h)}{1-k_c(h)} \right. \\ &\quad \left. - \frac{k_R(1-h)}{1-k_R(1-h)} \right] \Psi_h(\chi) - \text{Res} \left[\frac{(h-1/2)}{\pi \tan(\pi h/2)} \right. \\ &\quad \left. \times \frac{k_R(1-h)}{1-k_R(1-h)} \Psi_h(\chi) \right]_{h=2}. \end{aligned} \quad (3.61)$$

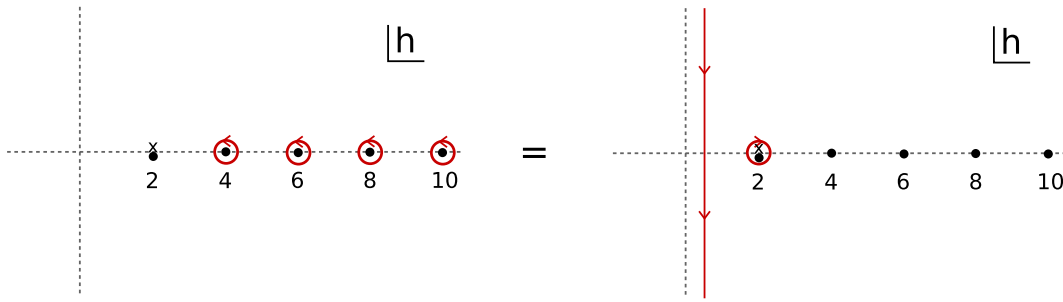


FIG. 8. To continue the sum over residues to the chaos region, we first replace the $k_c(h)$ by $k_R(1-h)$, and then pull the contour surrounding the poles back to the line $1/2 + is$, picking up the double pole at $h = 2$ but no other poles. In this form the function can safely be continued. In addition we also have the original integral along $h = 1/2 + is$ with the function k_c ; we leave this piece alone because it can already be continued.

So far this is just another legal way to write the Euclidean correlator.

Now we consider the continuation of the $\chi > 1$ expression to small χ . The integral over s does not give anything growing as χ becomes small, because we can do the continuation in such a way that the integral always remains convergent, and the integrand vanishes as $\chi \rightarrow 0$. Therefore the only growing piece in $\mathcal{F}_{h \neq 2}$ comes from the second line of Eq. (3.61). This is essentially a Regge pole. In our case it is a double pole, so we get a linear combination of $\Psi_2(\chi)$ and $\partial_h \Psi_2(\chi)|_{h=2}$. Unlike the double pole in the OPE region, this does not cancel against other contributions.

The term proportional to Ψ_2 will saturate the chaos bound, but naively the second term exceeds it, due to the extra logarithm in the small- χ behavior:

$$\partial_h \Psi_h(\chi)|_{h=2} \sim -\frac{2\pi \log \frac{1}{-i\chi}}{-i\chi} - \frac{2\pi}{-i\chi}. \quad (3.62)$$

This translates to something proportional to $t e^{2\pi t/\beta}$ at large t , which would violate the bound. Also, the term comes with a sign that is forbidden by the argument of Ref. [12]. So, by itself, $\mathcal{F}_{h \neq 2}$ would not be an allowable four-point function. However, it is consistent as a small correction to the enhanced $h = 2$ piece that we will study below. The $t e^{\frac{2\pi t}{\beta}}$ term then corresponds to a small finite-coupling shift (a decrease) in the growth exponent of the large $h = 2$ contribution.

C. Proper treatment of the $h = 2$ subspace

We saw above that the conformal limit of the kernel has eigenfunctions with eigenvalue $k_c(h) = 1$, which lead to a divergence in the four-point function. These eigenfunctions are $h = 2$ eigenfunctions of the Casimir operator C_{1+2} . In order to get a finite answer for the four-point function, we have to treat these particular eigenfunctions outside the conformal limit, by doing perturbation theory in the leading nonconformal correction to the kernel, δK . This correction arises from the leading nonconformal correction δG to the

correlators that make up the kernel. The small parameter is the inverse coupling, $1/(\beta J)$.

Since the perturbation δK breaks conformal symmetry, the line and the finite-temperature circle are inequivalent, and we have to study the problem directly on the circle. We will use an angular coordinate $\theta = 2\pi\tau/\beta$, which runs from $0 \leq \theta < 2\pi$ on the circle. (Equivalently, we can say that we work in units where $\beta = 2\pi$, and that θ is the periodic Euclidean time variable.)

It will be slightly more convenient to use the symmetric version of the kernel \tilde{K} in this section. This was defined in Eq. (3.9)

$$\begin{aligned} \tilde{K}(\theta_1, \theta_2; \theta_3, \theta_4) &= -J^2(q-1) |G(\theta_{12})|^{\frac{q-2}{2}} G(\theta_{13}) \\ &\quad \times G(\theta_{24}) |G(\theta_{34})|^{\frac{q-2}{2}}. \end{aligned} \quad (3.63)$$

We will refer to the antisymmetric eigenfunctions of this kernel as $\Psi_{h,n}^{\text{exact}}(\theta_1, \theta_2) = -\Psi_{h,n}^{\text{exact}}(\theta_2, \theta_1)$, where h is an abstract label that will become clear below, and n describes the Fourier index in the center-of-mass coordinate $e^{-in(\theta_1+\theta_2)/2}$. The kernel \tilde{K} is symmetric with respect to the standard inner product

$$\langle \Psi, \Phi \rangle \equiv \int_0^{2\pi} d\theta_1 d\theta_2 \Psi^*(\theta_1, \theta_2) \Phi(\theta_1, \theta_2). \quad (3.64)$$

To get a formula for the four-point function, we can use the fact that the zero-rung ladder \mathcal{F}_0 is proportional to the kernel acting on the antisymmetric identity matrix, $\tilde{K} \cdot I$, where

$$\begin{aligned} I(\theta_1 \dots \theta_4) &= \frac{1}{2} [\delta(\theta_{14})\delta(\theta_{23}) - \delta(\theta_{13})\delta(\theta_{24})] \\ &= -\sum_{h,n} \Psi_{h,n}^{\text{exact}}(\theta_1, \theta_2) \Psi_{h,n}^{\text{exact}*}(\theta_3, \theta_4). \end{aligned} \quad (3.65)$$

Roughly, the sum of ladders is then $\mathcal{F} = (1 - \tilde{K})^{-1} \tilde{K} \cdot I$. More precisely,

$$\begin{aligned} & [(q-1)J^2 |G(\theta_{12})|^{\frac{q-2}{2}} |G(\theta_{34})|^{\frac{q-2}{2}}] \mathcal{F}(\theta_1 \dots \theta_4) \\ &= 2 \sum_{h,n} \frac{k(h,n)}{1-k(h,n)} \Psi_{h,n}^{\text{exact}}(\theta_1, \theta_2) \Psi_{h,n}^{\text{exact}*}(\theta_3, \theta_4), \end{aligned} \quad (3.66)$$

where $k(h,n)$ is the exact eigenvalue associated to $\Psi_{h,n}^{\text{exact}}(\theta_1, \theta_2)$. For the appropriate set of eigenvectors, this formula is correct for any value of the coupling βJ .

In the conformal limit $\beta J \gg 1$ we can make contact with our previous analysis: the exact eigenfunctions $\Psi_{h,n}^{\text{exact}}$ approach eigenfunctions $\Psi_{h,n}$ of the Casimir C_{1+2} with eigenvalue $h(h-1)$. The eigenvalue $k(h,n) \rightarrow k_c(h)$ becomes a function of h only, and the sum over n in Eq. (3.66) reproduces the previous expression in terms of the functions $\Psi_h(\chi)$; see Appendix D. The sum over h includes both the continuum and discrete pieces. We can take the conformal limit smoothly for everything but $h=2$. This gives the function $\mathcal{F}_{h \neq 2}$ that we studied previously, after mapping to the circle with $\tau = \tan \frac{\theta}{2}$. We note that the cross ratio χ is given in terms of the finite-temperature coordinates as

$$\chi = \frac{\sin \frac{\theta_{12}}{2} \sin \frac{\theta_{34}}{2}}{\sin \frac{\theta_{13}}{2} \sin \frac{\theta_{24}}{2}}. \quad (3.67)$$

Before, we got an infinity in the conformal limit from the $h=2$ contribution, which is now given by a family of functions $\Psi_{2,n}$ for different Fourier index n . For these terms, we have to retain the leading nonconformal correction to the eigenvalues $k(2,n) = 1 - O(\frac{1}{\beta J})$. In the remainder of this section, we will do this in detail.

1. The $h=2$ eigenfunctions and reparametrizations

We will start by working out the $\Psi_{2,n}$ functions on the circle. In the conformal limit, we can substitute in for the propagators using Eq. (2.8) to get

$$\begin{aligned} \tilde{K}_c(\theta_1, \dots, \theta_4) &= -\alpha_0 \frac{1}{|2 \sin \frac{\theta_{12}}{2}|^{1-2\Delta} |2 \sin \frac{\theta_{13}}{2}|^{2\Delta}} \\ &\times \frac{\text{sgn}(\theta_{24})}{|2 \sin \frac{\theta_{24}}{2}|^{2\Delta}} \frac{1}{|2 \sin \frac{\theta_{34}}{2}|^{1-2\Delta}} \end{aligned} \quad (3.68)$$

with α_0 defined in Eq. (3.12). As on the line, this kernel commutes with a set of $SL(2)$ generators,

$$\begin{aligned} \hat{P} &= e^{-i\theta} [\partial_\theta - i/2], & \hat{K} &= -e^{i\theta} [\partial_\theta + i/2], \\ \hat{D} &= i\partial_\theta. \end{aligned} \quad (3.69)$$

It follows that eigenfunctions of \tilde{K}_c will be functions of two times that diagonalize the Casimir $C_{1+2} = -1/2 - \hat{K}_1 \hat{P}_2 - \hat{P}_1 \hat{K}_2 + 2\hat{D}_1 \hat{D}_2$ and the translation operator

$\hat{D}_{1+2} = \hat{D}_1 + \hat{D}_2$. One can write the Casimir as a differential operator and directly find the $h=2$ eigenfunctions.

We can get the answer another way by considering reparametrizations of the propagator. The Schwinger-Dyson equations in the conformal limit are reparametrization invariant. This means that if we consider the change in G from a linearized reparametrization $\theta \rightarrow \theta + \epsilon(\theta)$, which is

$$\delta_\epsilon G_c = [\Delta \epsilon'(\theta_1) + \Delta \epsilon'(\theta_2) + \epsilon(\theta_1) \partial_{\theta_1} + \epsilon(\theta_2) \partial_{\theta_2}] G_c, \quad (3.70)$$

then $G_c + \delta_\epsilon G_c$ will also solve the conformal Schwinger-Dyson equations (2.6). The first equation in Eq. (2.6) then implies

$$\begin{aligned} 0 &= \delta_\epsilon G_c * \Sigma_c + G_c * \delta_\epsilon \Sigma_c \rightarrow 0 \\ &= \delta_\epsilon G_c + G_c * [(q-1)J^2 G_c^{q-2} \delta_\epsilon G_c] * G_c \\ &= (1 - K_c) \delta_\epsilon G_c \end{aligned} \quad (3.71)$$

where the star denotes the following product: $(F * G)(\tau, \tau') = \int d\tau'' F(\tau, \tau'') G(\tau'', \tau')$. We conclude that $\delta_\epsilon G$ is annihilated by $(1 - K)$, so it is an eigenfunction of K with eigenvalue one. For the symmetric kernel \tilde{K} , the associated eigenfunction is $|G|^{\frac{q-2}{2}} \delta_\epsilon G$.

To get a convenient basis, we can consider $\epsilon \sim e^{-in\theta}$. Plugging the conformal correlators (2.8) into the reparametrization formula (3.70), evaluating $|G|^{\frac{q-2}{2}} \delta_\epsilon G$ and normalizing with respect to Eq. (3.64), we get

$$\Psi_{2,n} = \gamma_n \frac{e^{-iny}}{2 \sin \frac{x}{2}} f_n(x), \quad f_n = \frac{\sin \frac{nx}{2}}{\tan \frac{x}{2}} - n \cos \frac{nx}{2}, \quad (3.72)$$

$$x = \theta_1 - \theta_2, \quad y = \frac{\theta_1 + \theta_2}{2}, \quad \gamma_n^2 = \frac{3}{\pi^2 |n| (n^2 - 1)}. \quad (3.73)$$

These are eigenfunctions of \tilde{K} with eigenvalue one, and eigenfunctions of the Casimir C_{1+2} with $h=2$. For the cases $n = -1, 0, 1$, the variation $\delta_\epsilon G$ vanishes, because of the $SL(2)$ covariance of the conformal correlators. So we only have eigenfunctions for $|n| \geq 2$. For positive n , they organize into a single representation of $SL(2)$, with highest weight vector $\Psi_{2,2}$. One can repeatedly apply $P_1 + P_2$ to this function to get all of the $\Psi_{2,n}$, with $n \geq 2$. We similarly get a single lowest weight representation that describes $n \leq 2$.

In Sec. IV, we will use the reparametrization perspective to give a simple explanation of why these eigenfunctions lead to a divergence in the four-point function, and how it gets regulated. For now we proceed in the most straightforward way, correcting the infinity by finding

the shift in $k(2, n)$ that fixes the vanishing denominator in Eq. (3.66).

2. The shift in the eigenvalues

We will start by studying the correction to $k(2, n)$ at large q , where the eigenvalue problem is quite simple for all values of the coupling βJ . The simplification is because the propagators are equal to

$$G(\theta) = \frac{\text{sgn}(\theta)}{2} \left(1 + \frac{g(\theta)}{q} + \dots \right). \quad (3.74)$$

At large q we can set the side rail propagators equal to the first term. To form the rung function G^{q-2} , we exponentiate the $\frac{1}{q}$ correction as in Eq. (2.17). The eigenvalue equation $\tilde{K}\Psi = k\Psi$ is

$$-J^2 q \int d\theta_1 d\theta_2 \frac{\text{sgn}(\theta_{13})}{2} \frac{\text{sgn}(\theta_{24})}{2} \frac{e^{\frac{1}{2}[g(\theta_{12})+g(\theta_{34})]}}{2^{q-2}} \Psi(\theta_1, \theta_2) = k\Psi(\theta_3, \theta_4). \quad (3.75)$$

Because the side rail propagators are so simple, we can turn this integral equation into a differential equation by applying the differential operator $\partial_{\theta_3} \partial_{\theta_4} e^{-\frac{1}{2}g(\theta_{34})}$ to both sides and using $\partial_x \text{sgn}(x) = 2\delta(x)$. Plugging in for e^g using Eq. (2.17), parameterizing the eigenvalue as $k = 2/h(h-1)$, and making a Fourier ansatz, one finds

$$\Psi(\theta_1, \theta_2) = \frac{e^{-iny}}{\sin^{\frac{1}{2}} \tilde{x}} \psi_n(x), \quad \tilde{x} = vx + (1-v)\pi, \quad (3.76)$$

$$\left(n^2 + 4\partial_x^2 - \frac{h(h-1)v^2}{\sin^2 \frac{\tilde{x}}{2}} \right) \psi_n(x) = 0. \quad (3.77)$$

Here, v was defined in Eq. (2.18), and we are using the same notation for x, y as in Eq. (3.72). At infinite coupling, v is close to one [Eq. (2.30)]. When v is exactly equal to one, Eq. (3.77) is the equation for an eigenfunction of the Casimir C_{1+2} . However, Eq. (3.77) gives the exact eigenvectors of the large- q model for any value of the coupling.

We would like to find eigenfunctions with the right symmetry properties. As functions of the two angles θ_1, θ_2 , the four-point function has the symmetries

$$\begin{aligned} F(\theta_1, \theta_2) &= -F(\theta_2, \theta_1), \\ F(\theta_1 + 2\pi, \theta_2) &= -F(\theta_1, \theta_2), \\ F(\theta_1, \theta_2 + 2\pi) &= -F(\theta_1, \theta_2). \end{aligned} \quad (3.78)$$

We can combine the first two to obtain $F(\theta_1, \theta_2) = F(\theta_2 + 2\pi, \theta_1)$. In terms of x and y this means that

$$F(x, y) = F(2\pi - x, y + \pi). \quad (3.79)$$

The first symmetry in Eq. (3.78) can be used to restrict the range of x to be positive. Then the periodicity condition implies Eq. (3.79). To compensate for the factor of e^{-iny} in Eq. (3.76), $\psi_n(x)$ needs to be symmetric about $x = \pi$ for even n and antisymmetric for odd n . Solutions with these properties are

$$\begin{aligned} \psi_{h,n}(x) &\sim \left(\sin \frac{\tilde{x}}{2} \right)^h {}_2F_1 \left(\frac{h-\tilde{n}}{2}, \frac{h+\tilde{n}}{2}, \frac{1}{2}, \cos^2 \frac{\tilde{x}}{2} \right), \\ \tilde{n} &= \frac{n}{v} \quad (n \text{ even}), \end{aligned} \quad (3.80)$$

$$\begin{aligned} &\sim \cos \frac{\tilde{x}}{2} \left(\sin \frac{\tilde{x}}{2} \right)^h {}_2F_1 \left(\frac{1+h-\tilde{n}}{2}, \frac{1+h+\tilde{n}}{2}, \frac{3}{2}, \cos^2 \frac{\tilde{x}}{2} \right) \\ &\times (n \text{ odd}). \end{aligned} \quad (3.81)$$

The quantization condition on h comes from the boundary condition that ψ should vanish at $x = 0$, which means $\tilde{x} = \pi(1-v)$.

We are interested in the eigenfunctions that approach the $h = 2$ conformal eigenfunctions at strong coupling. For a generic value of h near two, we get a divergence as \tilde{x} goes to zero. To the first two orders in $(1-v)$, the correct condition is just that this diverging term should not be present. This means the first or second argument of the hypergeometric function should be a negative integer. The solution near two is $h_n = 2 + |\tilde{n}| - |n| = 2 + |n| \frac{1-v}{v}$. Converting to $k = 2/h(h-1)$, we get

$$k(2, n) = 1 - \frac{3|n|}{2}(1-v) + \left(\frac{7n^2}{4} - \frac{3|n|}{2} \right) (1-v)^2 + \dots \quad (3.82)$$

$$= 1 - \frac{3|n|}{\beta\mathcal{J}} + \frac{7n^2}{(\beta\mathcal{J})^2} + \dots \quad (3.83)$$

Now we move to general q . We cannot solve the eigenvalue problem exactly, but we can do first-order perturbation theory in the kernel, computing the shift in the eigenvalues of the $h = 2$ eigenfunctions by taking $\langle \Psi_{2,n}, \delta\tilde{K} \cdot \Psi_{2,n} \rangle$ where $\delta\tilde{K}$ is the leading correction to the conformal form. More specifically, we will take the leading correction in the infrared; this will be justified as long as the integrals we get for the matrix elements are convergent.

The correction to the kernel comes from substituting in the correction $G_c + \delta G$ to the conformal propagators, where δG is the leading correction in the infrared. For the large- q model, we found in Eq. (2.37) that the leading correction to the conformal answer is proportional to the function

$$f_0(\theta) \equiv 2 + \frac{\pi - |\theta|}{\tan \frac{|\theta|}{2}}. \quad (3.84)$$

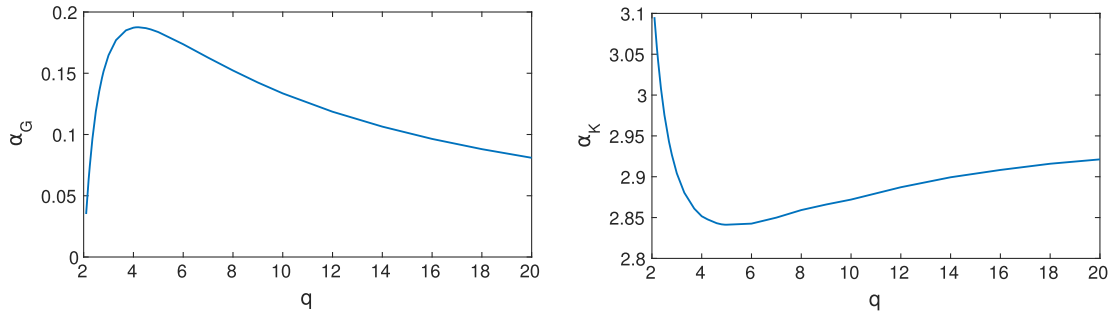


FIG. 9. The functions $\alpha_G(q)$ and $\alpha_K(q)$, computed by solving the Schwinger-Dyson equations numerically for different values of q . The first three physical values are $\alpha_G(2) = 0$, $\alpha_G(4) \approx 0.1872$, and $\alpha_G(6) \approx 0.1737$. Analytically, we know that α_G behaves as $2/q$ at large q , and like $\pi(q-2)/8$ for q near two. α_K never strays more than roughly five percent from the large- q value of three.

[Note that f_0 is not the limit $n \rightarrow 0$ of f_n defined for $n \geq 2$ in Eq. (3.72).] By solving the Schwinger-Dyson equations numerically for different values of q , we found in all cases that

$$\frac{\delta G}{G_c} = -\frac{\alpha_G}{\beta \mathcal{J}} f_0 \quad (3.85)$$

is a good approximation for large $\theta\beta\mathcal{J}$ and for a suitable constant α_G . We give a plot of $\alpha_G(q)$, from fitting against the numerical solution, in Fig. 9. One can also show directly that δG is an eigenfunction of the conformal kernel with eigenvalue one (and therefore an allowed perturbation in the infrared, by Appendix A), up to a UV divergence that should be interpreted as a local source in the Schwinger-Dyson equation. The required source is proportional to the $-i\omega$ term that we dropped in the conformal limit, but matching the numerical coefficient would require us to know how the divergence is regularized, which seems to require the exact solution; see Appendix A. Of course, in the $q = \infty$ model we have the exact solution, and one can check that the coefficient is $\alpha_G = 2/q$ at large q . In the large- q model and also in the numerics at general q , the next correction in the IR appears to be at order $(\beta\mathcal{J})^{-2}$. One expects the next correction after that to be at order $(\beta\mathcal{J})^{1-h_1}$ where h_1 is the dimension of the next irrelevant operator, i.e. the solution to $k_c(h) = 1$. When $q = 4$ we have $h_1 = 3.7735\dots$

Getting the shift in the eigenvalue from the correction δG involves some work, which we will defer to Appendix E. One approach is to compute the shift by directly evaluating the integrals in $\langle \Psi_{2,n}, \delta \tilde{K} \cdot \Psi_{2,n} \rangle$. This can be simplified by using conformal symmetry to show that the answer has to be proportional to n , and then doing the integrals at large n . We give some details on this method in Appendix E.

A quicker way to get the answer is to use the fact, shown in Appendix F, that

$$\frac{1}{q\alpha_G} \cdot \frac{\langle \Psi_{h,n}, \delta \tilde{K} \cdot \Psi_{2,n} \rangle}{1 - k_c(h)} \quad (3.86)$$

is independent of q , despite the fact that the components $q\alpha_G$, k_c , and $\delta \tilde{K}$ each depend on q . Here, $\Psi_{h,n}$ is the conformal eigenfunction with weight h . The expression (3.86) has a pole at $h = 2$, with residue proportional to the eigenvalue shift. Equating this residue with what we get in the $q = \infty$ model, and using some large- q data [$q\alpha_G = 2$, $k'_c(2) = -3/2$, and Eq. (3.83)], we find

$$k(2, n) = 1 - \frac{\alpha_K}{\beta \mathcal{J}} |n| + \dots, \quad (3.87)$$

$$\begin{aligned} \alpha_K &\equiv -qk'_c(2)\alpha_G \\ &= \left[\frac{\pi q}{\sin \frac{2\pi}{q}} + \frac{q^3(6-q) - 6q^2}{2(q-1)(q-2)} \right] \alpha_G. \end{aligned} \quad (3.88)$$

This agrees with the more direct method in Appendix E. We give a plot of the coefficient α_K in the right panel of Fig. 9. One finds that it stays reasonably close to three for all values of q .

3. The enhanced $h=2$ contribution

Because the eigenvalues of the $h=2$ eigenvectors are close to one, they give an enhanced contribution to the four-point function, of order $\beta\mathcal{J}$. This piece comes from the $h=2$ part of Eq. (3.66), where we put in the conformal results for everything except the $1 - k(h, n)$ in the denominator, which we correct using the leading shift (3.87). The result is

$$\begin{aligned} \frac{\mathcal{F}_{\text{big}}(\theta_1 \dots \theta_4)}{G(\theta_{12})G(\theta_{34})} &= \frac{6\alpha_0}{\pi^2 \alpha_K} \beta \mathcal{J} \sum_{|n| \geq 2} \frac{e^{\text{in}(y'-y)}}{n^2(n^2-1)} \\ &\quad \times \left[\frac{\sin \frac{nx}{2}}{\tan \frac{x}{2}} - n \cos \frac{nx}{2} \right] \left[\frac{\sin \frac{nx'}{2}}{\tan \frac{x'}{2}} - n \cos \frac{nx'}{2} \right], \\ x &= \theta_{12}, \quad x' = \theta_{34}, \\ y &= \frac{\theta_1 + \theta_2}{2}, \quad y' = \frac{\theta_3 + \theta_4}{2}. \end{aligned} \quad (3.89)$$

Because of the $\beta\mathcal{J}$ enhancement, this term is parametrically large compared to the $h \neq 2$ pieces we studied in the previous sections. It is not conformally invariant, in the

sense that the sum is not only a function of the cross ratio. This lack of conformal symmetry arises because the eigenvalue shift (3.87) depends on the index n that labels the $SL(2)$ descendant in the $h = 2$ representation. Concretely, we have $n^2(n^2 - 1)$ in the denominator, instead of $|n|(n^2 - 1)$ which would have given a multiple of $\Psi_2(\chi)$; see Eq. (D4).

Using the fact that the $h = 2$ eigenfunctions are linearized reparametrizations of the propagator, with reparametrization $\epsilon_n \propto e^{-in\theta}$, we can write Eq. (3.89) as

$$\mathcal{F}_{\text{big}} = \sum_n \langle \epsilon_n \epsilon_{-n} \rangle \delta_{\epsilon_n} G \delta_{\epsilon_{-n}} G, \quad (3.90)$$

$$\langle \epsilon_n \epsilon_{-n} \rangle = \left(\frac{6\alpha_0 q^2}{\alpha_K N} \right) \frac{\beta \mathcal{J}}{n^2(n^2 - 1)}.$$

This is the type of contribution one expects from a fluctuation integral over reparametrizations of the conformal saddle point, with an action given by the inverse of the ϵ propagator. We will say more about this perspective in Sec. IV below. For now, we note that one can Fourier transform (3.90) to obtain

$$\langle \epsilon(\theta) \epsilon(0) \rangle = \frac{1}{N} \frac{6(\beta \mathcal{J}) \beta^2 q^2 \alpha_0}{(2\pi)^4 \alpha_K} \left[-\frac{1}{2} (|\theta| - \pi)^2 + (|\theta| - \pi) \sin |\theta| + 1 + \frac{\pi^2}{6} + \frac{5}{2} \cos \theta \right]. \quad (3.91)$$

The sum over n in Eq. (3.89) can be done by repeatedly integrating the geometric series, or by using this propagator and Eq. (3.70). The result depends on whether the ordering of the times corresponds to an ijj or $ijij$ ordering of the fermions; see Fig. 10. In the nonalternating configuration ijj , we have the very simple expression

$$\begin{aligned} ijj \text{ order: } & \frac{\mathcal{F}_{\text{big}}(\theta_1, \theta_2, \theta_3, \theta_4)}{G(\theta_{12})G(\pi)} \\ & = \frac{6\alpha_0}{\pi^2 \alpha_K} \beta \mathcal{J} \left(\frac{\theta_{12}}{2 \tan \frac{\theta_{12}}{2}} - 1 \right) \left(\frac{\theta_{34}}{2 \tan \frac{\theta_{34}}{2}} - 1 \right). \end{aligned} \quad (3.92)$$

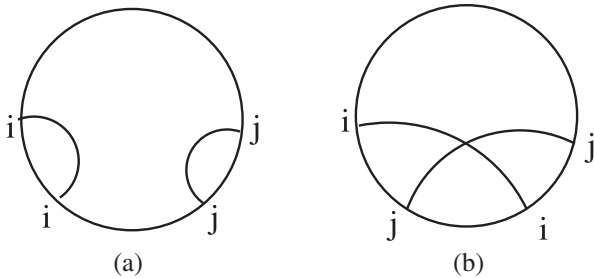


FIG. 10. Two configurations for the fermions. In (a) we have the $ijij$ configuration with $\chi < 1$ and in (b) we have the $iijj$ configuration with $\chi > 1$.

This correlator is produced by fluctuations in the total energy in the thermal ensemble. Let us be a bit more explicit. We can compute the contribution of the energy fluctuations by starting with the variation in the correlator produced by a small change in the temperature:

$$\frac{G(\tau, \beta + \delta\beta)}{G(\tau, \beta)} = 1 - \frac{2\Delta}{\beta} \left(1 - \frac{\pi\tau}{\beta \tan \frac{\pi\tau}{\beta}} \right) \delta\beta. \quad (3.93)$$

Now we use the saddle point relation $E = c/(2\beta^2)$ to get $\delta\beta = -\beta^3 \delta E/c$; see Eq. (2.34). From the fluctuations in E we therefore expect a connected piece in the four-point function that is

$$\begin{aligned} \frac{1}{N} \frac{\mathcal{F}_{\text{big}}(\tau_1, \tau_2, \tau_3, \tau_4)}{G(\tau_{12})G(\tau_{34})} & = \frac{4}{q^2} \left(1 - \frac{\pi\tau_{12}}{\beta \tan \frac{\pi\tau_{12}}{\beta}} \right) \left(1 - \frac{\pi\tau_{34}}{\beta \tan \frac{\pi\tau_{34}}{\beta}} \right) \\ & \times \frac{\beta^4}{c^2} \langle (\delta E)^2 \rangle. \end{aligned} \quad (3.94)$$

The energy two-point function can be computed from

$$\langle (\delta E)^2 \rangle = \partial_\beta^2 \log Z = \frac{c}{\beta^3}. \quad (3.95)$$

Inserting this, writing things in terms of $\theta = 2\pi\tau/\beta$, and converting c to α_K using Eq. (5.2), we find exact agreement with Eq. (3.92).

For small θ_{12} , Eq. (3.92) goes as θ_{12}^2 , suggesting the presence of a dimension-two operator, or an operator product expansion of the form $\psi(\theta_1)\psi(\theta_2) \propto (\theta_{12})^{-2\Delta+2} T(\theta_2)$. If we took also the $\theta_{34} \rightarrow 0$ limit, then we would expect to have a result proportional to $\langle T(\theta_2)T(\theta_4) \rangle$. If this was in a conformal field theory, we would have expected this to go like $(\sin \theta_{24}/2)^{-4}$. Instead we find that it is a constant. The reason is that T is essentially the Hamiltonian of the theory. As such it is conserved and its two-point function in the thermal ensemble simply measures the energy fluctuations. We can write an explicit expression for T in terms of ϵ of the form

$$T = \frac{N\alpha_S}{\mathcal{J}} \left(\epsilon''' + \frac{(2\pi)^2}{\beta^2} \epsilon' \right) + \dots \quad (3.96)$$

with α_S as in Eq. (4.5). The dots indicate possible higher-order terms in ϵ . We can then check using Eq. (3.91) that $\langle TT \rangle$ is indeed constant, and is given by Eq. (3.95)

$$\langle T(\tau_1)T(\tau_2) \rangle = \frac{c}{\beta^3} \propto \frac{N}{\beta^2(\beta \mathcal{J})}. \quad (3.97)$$

Because of the factor of $(\beta \mathcal{J})$, this becomes small in the conformal limit, seemingly in keeping with the idea that the stress tensor should vanish in a one-dimensional conformal field theory. However, the contribution to the four-point

function also involves the three-point couplings $\langle T\psi\psi\rangle$, which are the other factors in Eq. (3.94). These give two factors of $(\beta\mathcal{J})$ in the numerator, which more than compensate for the suppression of $\langle TT\rangle$.⁶

We now turn our attention to a configuration in the alternating configuration $ijij$. The result is a bit more complicated but it simplifies nicely in the case that we take one of the pairs of fermions to be diametrically opposed on the circle. For example, we can take $\theta_3 = 0$, and $\theta_4 = \pi$:

$$ijij \text{ order: } \frac{\mathcal{F}_{big}(\theta_1, \theta_2, 0, \pi)}{G(\theta_{12})G(\pi)} \\ = -\frac{6\alpha_0}{\pi^2\alpha_K}\beta\mathcal{J}\left(\frac{\theta_{12}}{2\tan\frac{\theta_{12}}{2}} - 1 - \pi\frac{\sin\frac{\theta_1}{2}\sin\frac{\theta_2}{2}}{|\sin\frac{\theta_{12}}{2}|}\right). \quad (3.98)$$

This is the configuration that is appropriate for continuing to the chaos limit. To get the function defined in Eq. (3.57), we continue to $\theta_2 = \frac{\pi}{2} - \frac{2\pi i}{\beta}t$ and $\theta_1 = \theta_2 - \pi$, finding

$$\frac{\mathcal{F}_{big}(t)}{G(\pi)G(\pi)} = \frac{6\alpha_0}{\pi^2\alpha_K}\beta\mathcal{J}\left(1 - \frac{\pi}{2}\cosh\frac{2\pi t}{\beta}\right). \quad (3.99)$$

This saturates the chaos bound.

4. Other terms from the $h=2$ subspace

Because the factor $\frac{k(2,n)}{1-k(2,n)}$ in Eq. (3.66) is large, of order $\beta\mathcal{J}$, corrections of order $(\beta\mathcal{J})^{-1}$ from the rest of the formula (3.66) will combine to give finite contributions in the conformal limit. There are several sources of these terms. First, the δG correction to the propagators on the lhs of Eq. (3.66) give a correction

$$\frac{\mathcal{F}(\theta_1\dots\theta_4)}{G(\theta_{12})G(\theta_{34})} \supset -\frac{q}{2}\left[\frac{\delta G(\theta_{12})}{G_c(\theta_{12})} + \frac{\delta G(\theta_{34})}{G_c(\theta_{34})}\right]\frac{\mathcal{F}_{big}(\theta_1\dots\theta_4)}{G_c(\theta_{12})G_c(\theta_{34})} \quad (3.100)$$

$$= \frac{3\alpha_0}{\pi^2|k'_c(2)|}[f_0(\theta_{12}) + f_0(\theta_{34})]\sum_{|n|\geq 2}\frac{e^{in(y'-y)}f_n(x)f_n(x')}{n^2(n^2-1)}. \quad (3.101)$$

Notice that this depends on q only through the factor $\alpha_0/k'_c(2)$, which is a simple explicit function of q . Next, we have a contribution from the first-order change in the $h=2$ eigenvectors, $\delta\Psi_{2,n}$. In Appendix F we show that $\delta\Psi_{2,n}$ is

⁶We emphasize that T is not a conformal operator. As the Hamiltonian of the theory, it is dimension one, but it has a time-independent two-point function that would be characteristic of a dimension-zero conformal operator. On the other hand, the OPE with two fermions vanishes as the fermions approach each other in a way that would be characteristic of a dimension-two conformal operator.

independent of q except for a coefficient of $q\alpha_G$. It is easy to check that this also leads to a term in \mathcal{F} that depends on q only through the prefactor $\alpha_0/k'_c(2)$.

Third, we have contributions from the order $(\beta\mathcal{J})^0$ term in $\frac{k(2,n)}{1-k(2,n)}$. This requires knowledge of the second-order change in the eigenvalue, which we have not computed. However, we have noticed that we get a very simple final answer if we assume

$$k(2,n) = 1 + k'_c(2)\frac{q\alpha_G|n|}{\beta\mathcal{J}} + \frac{k''_c(2)}{2}\left(\frac{q\alpha_G|n|}{\beta\mathcal{J}}\right)^2 + \dots \quad (3.102)$$

The first term is just a restating of Eq. (3.87). One can use Eq. (3.83) to check that the second term is correct in the $q = \infty$ model. By diagonalizing the kernel constructed from the numerical $G(\tau)$ (see Appendix G), we have checked that the coefficient of the second term in Eq. (3.102) is correct to within roughly percent-level multiplicative precision, for several low values of q, n . We will assume that it is actually true.

The simplification that results from Eq. (3.102) is the following. One can use Eq. (D4) to show that the contribution to \mathcal{F} from the order-one term in $\frac{k(2,n)}{1-k(2,n)}$ combines with the terms from the double pole at $h=2$ in Eqs. (3.50) and (3.52) to give, again, an expression that depends on q only through the prefactor $\alpha_0/k'_c(2)$. So we conclude that up to order $(\beta\mathcal{J})^0$, the four-point function will be given by the \mathcal{F}_{big} contribution, plus the residues of the simple poles h_1, h_2, \dots in Eqs. (3.50) or (3.52), plus terms that are universal in q up to an overall coefficient. We will compute these last terms by studying the $q = \infty$ four-point function in more detail.

D. More detail on the $q = \infty$ four-point function

In the $q = \infty$ model, we can compute the four-point function in a way that simultaneously treats all of the contributions we have been discussing so far. This is based on the fact that \mathcal{F} is a Green's function for a simple differential operator. Because the side-rail propagators in the large- q kernel are proportional to $\text{sgn}(\theta)$ [see Eq. (3.75)], we have that

$$-\frac{2}{v^2\tilde{P}^2}\partial_{\theta_1}\partial_{\theta_2}K(\theta_1\dots\theta_4) = \delta(\theta_{13})\delta(\theta_{24}), \\ \tilde{P} \equiv \frac{1}{\sin\frac{\tilde{x}}{2}}, \quad \tilde{x} = vx + (1-v)\pi. \quad (3.103)$$

In other words, the differential operator on the left-hand side is the inverse of K . Roughly, the four-point function is given by $\mathcal{F} = (K^{-1} - 1)^{-1}$. Multiplying both sides by $(K^{-1} - 1)$, we get a differential equation for \mathcal{F} with a delta function source.

To write the precise equation we get, it is convenient to use the coordinates $x = \theta_{12}$, $y = \frac{\theta_1 + \theta_2}{2}$. These overcount physical configurations of points. We can reduce this overcounting by restricting to $x \geq 0$, $x' \geq 0$ and $y \geq y'$. Then the correct equation is

$$\left[-\frac{\partial_y^2}{4} + v^2 \partial_x^2 - \frac{v^2 \tilde{P}^2}{2} \right] \mathcal{F}(x, y, x', y') \\ = \delta(y - y') \delta(x - x') + \delta(y - y' - \pi) \delta(2\pi - x - x'). \quad (3.104)$$

The second term on the rhs can be understood as the image of the first term under the symmetry $(x, y) \rightarrow (2\pi - x, y - \pi)$; see the discussion above Eq. (3.80).

We can solve this equation by separation of variables. We expand in a complete set of eigenfunctions of the operator $-\partial_x^2 + \tilde{P}^2/2$, with boundary conditions of zero at $x = 0$. These eigenfunctions are just Eqs. (3.80) and (3.81) with $h = 2$. The boundary condition implies that \tilde{n} should be an integer $n \geq 2$ plus a correction of order $(1 - v)^3$ that we will neglect. Then Eqs. (3.80) and (3.81) simplify to the functions f_n defined in Eq. (3.72), with eigenvalues $n^2/4$. These functions satisfy a completeness relation

$$\sum_{n>2} \frac{f_n(\tilde{x}) f_n(\tilde{x}')}{\pi(n^2 - 1)} = \delta(\tilde{x} - \tilde{x}'), \\ \sum_{n>2} (-1)^n \frac{f_n(\tilde{x}) f_n(\tilde{x}')}{\pi(n^2 - 1)} = \delta(2\pi - \tilde{x} - \tilde{x}'). \quad (3.105)$$

So we can write

$$\mathcal{F}(x, y, x', y') = \sum_{n>2} H_n(y - y') \frac{f_n(\tilde{x}) f_n(\tilde{x}')}{\pi(n^2 - 1)}, \quad (3.106)$$

$$\left[-\frac{1}{4} \partial_y^2 - \frac{v^2 n^2}{4} \right] H_n(y) = v[\delta(y) + (-1)^n \delta(y - \pi)]. \quad (3.107)$$

The factor of v on the right side came from $\delta(x - x') = v\delta(\tilde{x} - \tilde{x}')$ and $\delta(2\pi - x - x') = v\delta(2\pi - \tilde{x} - \tilde{x}')$. The solution for $H_n(y)$ should be continuous and 2π -periodic. The sources in Eq. (3.106) imply that we have a discontinuous derivative at $y = 0$ and $y = \pi$. The discontinuity at zero is equivalent to a discontinuity between the derivative at 0^+ and at $2\pi^-$. Solving these constraints, we find that the solution for $0 < y < 2\pi$ is

$$H_n(y) = -\frac{2}{n \sin(n\pi v)} (\cos[nv(y - \pi)] \\ + (-1)^n \cos[nv(|y - \pi| - \pi)]) \quad (3.108)$$

$$= \frac{4 \cos(ny)}{\pi n^2 (1 - v)} + \frac{4(y - \frac{\pi}{2}) \sin(ny)}{\pi n} + O(1 - v) \quad (3.109)$$

$$= \left[\frac{\beta \mathcal{J}}{2} + 1 - \left(y - \frac{\pi}{2} \right) \partial_y \right] \frac{4 \cos(ny)}{\pi n^2} + O\left(\frac{1}{\beta \mathcal{J}} \right). \quad (3.110)$$

In the second line we expanded in $1 - v$ assuming $0 < y < \pi$. (For $\pi < y < 2\pi$, we need to replace the $\pi/2$ in the second term by $3\pi/2$.) In the third line we used $\frac{1}{1-v} \approx \frac{\beta \mathcal{J}}{2} + 1$. Substituting Eq. (3.110) into Eq. (3.106) and also using $f_n(\tilde{x}) = f_n(x) + (1 - v)(\pi - x)f'_n(x) + \dots$, we get the full $q = \infty$ four-point function up to order $(\beta \mathcal{J})^0$:

$$\mathcal{F}(x, y, x', 0) = \left\{ \beta \mathcal{J} - 2 \left[-1 + \left(y - \frac{\pi}{2} \right) \partial_y \right. \right. \\ \left. \left. + (x - \pi) \partial_x + (x' - \pi) \partial_{x'} \right] \right\} \\ \times \sum_{|n| \geq 2} \frac{e^{-iny} f_n(x) f_n(x')}{\pi^2 n^2 (n^2 - 1)}. \quad (3.111)$$

One can check that the term of order $(\beta \mathcal{J})$ reproduces \mathcal{F}_{big} from Eq. (3.89) for the case $q = \infty$ ($\alpha_0 = 2$, $\alpha_K = 3$, $G = \frac{1}{2}$). Although we have not displayed it here, the next term, at order $(\beta \mathcal{J})^{-1}$ can also be computed from Eq. (3.108). Beyond that order, one has to use the hypergeometric functions (3.80) and (3.81) that generalize f_n for noninteger n .

An interesting feature of the function \mathcal{F}_{big} was that it was independent of y in the nonalternating configuration, which corresponds to $y > |x + x'|/2$. This persists at order one, since the new y dependence of Eq. (3.111) is proportional to a y derivative of \mathcal{F}_{big} . This is consistent with the idea that in the $q = \infty$ model the Hamiltonian is the only operator that appears in the OPE. Notice that this is rather nontrivial from the way we set up the calculation in the previous sections: in the OPE region, the y -dependent double pole contribution in $\mathcal{F}_{h \neq 2}$ must be completely canceled by some of the terms discussed in Sec. III C 4.

E. Summary of the four-point function

In the previous section, we argued that the order-one terms in \mathcal{F} coming from the double pole and the various corrections to the $h = 2$ contributions add up to a function that depends on q only through the prefactor $\alpha_0/k'_c(2)$. We can then use the $q = \infty$ result (3.111) to write the general four-point function up to order one. When $\chi < 1$, we have

$$\begin{aligned} \frac{\mathcal{F}(x, y, x', 0)}{G(x)G(x')} &= \alpha_0 \left\{ \frac{6\beta\mathcal{J}}{\alpha_K} - \frac{6}{|k'_c(2)|} \left[-1 + \left(y - \frac{\pi}{2} \right) \partial_y \right. \right. \\ &\quad \left. \left. + (x - \pi) \partial_x + (x' - \pi) \partial_{x'} \right] \right\} \\ &\quad \times \sum_{|n| \geq 2} \frac{e^{-iny} f_n(x) f_n(x')}{\pi^2 n^2 (n^2 - 1)} \\ &\quad - \alpha_0 \sum_{m=1}^{\infty} \text{Res} \left[\frac{(h-1/2)}{\pi \tan(\pi h/2)} \frac{k_c(h)}{1 - k_c(h)} \right. \\ &\quad \left. \times \frac{\Gamma(h)^2}{\Gamma(2h)} \chi^h {}_2F_1(h, h, 2h, \chi) \right]_{h=h_m}. \end{aligned} \quad (3.112)$$

For $\chi > 1$ we have the same formula except that we need to replace $\frac{\Gamma(h)^2}{\Gamma(2h)} F(h, h, 2h, \chi) \rightarrow \Psi_h(\chi)$ on the second line, as in Eq. (3.50). We defined α_0 in Eq. (3.12), k_c in Eq. (3.35), x, x', y in Eq. (3.89), and f_n in Eq. (3.72). α_K is plotted in Fig. 9. The cross ratio χ is defined for finite temperature in Eq. (3.67).

In the region $\chi < 1$, the first line is actually independent of y . It encodes the contribution to the four-point function from a conserved operator, T , essentially the Hamiltonian of the theory. This term is not conformally invariant. The second line represents a tower of other operators that do contribute in a conformally invariant way. The dimensions are determined by $k_c(h_m) = 1$.⁷

The expression (3.112) is very convenient for analyzing the OPE limit. If we are interested in deriving the expression for the chaos limit, then we can start from the version of Eq. (3.112) for $\chi > 1$. We then replace the sum over residues by small circle contour integrals around each point. Then we pull the contours out to $h = \frac{1}{2} + is$. In the process we pick up residues at $h = 2k, k \geq 1$. We have a double pole at $h = 2$ and single poles for $k > 1$. In the case of the single poles, we replace $k_c(h)$ by the retarded kernel $k_R(1 - h)$; see Eq. (3.60). Again, we now express those contributions in terms of small contour integrals around these points and shift the contour to $h = \frac{1}{2} + is$. After we do this, we pick up a residue at $h = 2$. Thus, the final contribution involves the difference between the residues of the k_c kernel and the retarded kernel

$$\begin{aligned} \alpha_0 \text{Res} \left[\frac{(h - \frac{1}{2})}{\pi \tan(\pi h/2)} \left(\frac{k_c(h)}{1 - k_c(h)} \right. \right. \\ \left. \left. - \frac{k_R(1 - h)}{1 - k_R(1 - h)} \right) \Psi_h(\chi) \right]_{h=2}. \end{aligned} \quad (3.113)$$

This expression contains terms going like $\chi^{-1} \log \chi$ and χ^{-1} . These should be added to similar terms that arise from the

⁷We should also note that if Eq. (3.102) is not true, we will have further contributions, probably including a ‘‘real’’ dimension-two operator.

terms involving derivatives in Eq. (3.112). The total $te^{\frac{2\pi t}{\beta}}$ term, which contains the correction to the Lyapunov exponent, has the form (3.128) which leads to Eq. (3.129). The logarithmic term that comes from the pole involving $1/(1 - k_c)$ cancels the one coming from the derivatives in Eq. (3.112).

F. The chaos exponent at finite coupling

1. The retarded kernel

One way to compute the correlator in the chaos limit is to take the exact Euclidean answer and continue it. This is the approach we have taken so far in this paper. If we are only interested in getting the asymptotic rate of growth, we can take a simpler approach, used by Kitaev in Ref. [8]. We will consider an out-of-time-order correlation function in real time, where the fermions are separated by a quarter of the thermal circle:

$$\begin{aligned} F(t_1, t_2) &= \text{Tr}[y\psi_i(t_1)y\psi_j(0)y\psi_i(t_2)y\psi_j(0)], \\ y &\equiv \rho(\beta)^{1/4}. \end{aligned} \quad (3.114)$$

The $1/N$ piece of F is determined by a set of ladder diagrams on a time contour that includes the thermal circle and also a pair of real-time folds for the operators $\psi(t_1)$ and $\psi(t_2)$. As t_1, t_2 become large, these folds grow. The asymptotic growth rate of the $1/N$ piece of F is determined only by the properties of the ladder diagrams on the real-time part of the contour. To analyze these ladders, we define a retarded kernel

$$K_R(t_1 \dots t_4) = J^2(q - 1)G_R(t_{13})G_R(t_{24})G_{lr}(t_{34})^{q-2}. \quad (3.115)$$

Here, G_R are the retarded propagators, which include the sum over insertions on the two sides of the fold. The function G_{lr} is a Wightman correlator with points separated by half of the thermal circle in addition to the real time separation. In the conformal limit

$$\begin{aligned} G_R(t) &= 2b \cos(\pi\Delta)\theta(t) \left[\frac{\pi}{\beta \sinh \frac{\pi t}{\beta}} \right]^{2\Delta}, \\ G_{lr}(t) &= b \left[\frac{\pi}{\beta \cosh \frac{\pi t}{\beta}} \right]^{2\Delta}. \end{aligned} \quad (3.116)$$

The sum of ladder diagrams in F satisfies the usual integral equation which states that adding an extra rung to each diagram and also introducing a new zero-rung diagram leaves the sum unchanged. At large time t_1, t_2 , the zero-rung diagram is numerically small, because the propagators decay exponentially in time. This means that at large time, the sum of ladders must satisfy a homogeneous equation that states that adding one rung to each ladder will not

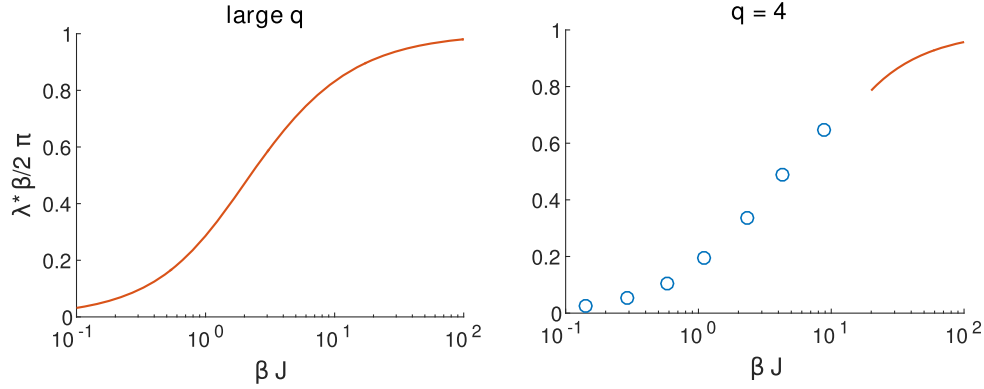


FIG. 11. Left: The exact λ_L in the large- q model. Right: λ_L for $q = 4$. The red curve shows the formula (3.129) in a region of reasonable validity. The circles are exact values, obtained by numerically solving real-time Schwinger-Dyson equations and then diagonalizing the retarded kernel. Note that the x axis is $\beta\mathcal{J}$, not βJ .

change the sum [8,33]. So F must be an eigenfunction of K_R with eigenvalue one:

$$F(t_1, t_2) = \int dt_3 dt_4 K_R(t_1 \dots t_4) F(t_3, t_4). \quad (3.117)$$

To solve this, we make a growth ansatz

$$F(t_1, t_2) = e^{\lambda_L(t_1+t_2)/2} f(t_{12}) \quad (3.118)$$

and then determine the values of λ_L such that we can find an f that gives an eigenfunction of K_R with eigenvalue one, solving Eq. (3.117). In the conformal limit, one can show by direct integration that we have eigenfunctions and eigenvalues

$$\frac{e^{-h\frac{\pi}{\beta}(t_1+t_2)}}{[\cosh\frac{\pi}{\beta}t_{12}]^{2\Delta-h}}, \quad k_R(h) = \frac{\Gamma(3-\frac{2}{q})\Gamma(\frac{2}{q}-h)}{\Gamma(1+\frac{2}{q})\Gamma(2-\frac{2}{q}-h)}. \quad (3.119)$$

This agrees with the definition of $k_R(h)$, given previously in Eq. (3.60). As we noted there, the only solution to $k_R(h) = 1$ is $h = -1$, which gives $\lambda_L = \frac{2\pi}{\beta}$. One might have expected to also find subleading growth rates in the conformal limit, corresponding to different families of eigenfunctions. Such eigenfunctions exist, but one can check that the next largest allowed value of λ_L is zero. This explains why every growing term in the chaos limit was growing at this rate, including various terms that were subleading to the enhanced contribution \mathcal{F}_{big} .

2. Large q

In the large- q model we can use this retarded kernel to find the growth exponent λ_L at all values of the coupling. From Eq. (2.13) and the definition of G_R in Eq. (2.12), together with the analytic continuation to real times $\tau \rightarrow \beta/2 + it$ of Eq. (2.17), we find that

$$G_R(t) = \theta(t), \quad qJ^2 G_{lr}(t)^{q-2} = \frac{2\pi^2 v^2}{\beta^2 \cosh^2(\frac{\pi v}{\beta} t)} \quad (3.120)$$

where v was defined in Eq. (2.18). v goes from zero at weak coupling to one at strong coupling. Substituting Eq. (3.120) into the formula for the retarded kernel, and then taking derivatives $\partial_{t_1} \partial_{t_2}$ of Eq. (3.117) with the ansatz (3.118), we get

$$\left[\frac{\lambda_L^2}{4} - \partial_x^2 \right] f(x) = \frac{2\pi^2 v^2}{\beta^2 \cosh^2(\frac{\pi v}{\beta} x)} f(x). \quad (3.121)$$

After rescaling the x variable, the equation becomes

$$-\left(\frac{\lambda_L \beta}{2\pi v} \right)^2 \tilde{f}(\tilde{x}) = \left[-\partial_{\tilde{x}}^2 - \frac{2}{\cosh^2 \tilde{x}} \right] \tilde{f}(\tilde{x}), \quad \tilde{x} = \frac{\pi v}{\beta} x, \quad \tilde{f}(\tilde{x}) = f(x). \quad (3.122)$$

This is a Schrodinger problem for a particle in the $-2/\cosh^2 \tilde{x}$ potential. There is a single bound state $\tilde{f} \propto 1/\cosh \tilde{x}$. The energy of this state is minus one, which gives the exact growth exponent

$$\lambda_L = \frac{2\pi}{\beta} v. \quad (3.123)$$

At weak coupling we have $\lambda_L \approx 2\mathcal{J}$, and at strong coupling we have $\lambda_L \approx \frac{2\pi}{\beta} [1 - 2/(\beta\mathcal{J})]$. We give a plot of λ_L in Fig. 11.

3. General q

For general q , we do not have an exact expression for λ_L at finite coupling. However, we can relate the first $(\beta J)^{-1}$ correction to the parameter α_G , and we can compute the function at small and moderate βJ numerically. First we discuss the $(\beta J)^{-1}$ correction. One way to compute this is to

do first-order perturbation theory in the retarded kernel. The leading nonconformal correction to K_R comes from plugging Eq. (3.85) into the definitions $G_R(t) = [G(it + \epsilon) - G(it - \epsilon)]\theta(t)$ and $G_{lr}(t) = G(it + \beta/2)$ to get the corrected propagators

$$\begin{aligned}\frac{\delta G_R}{G_R} &= -\frac{\alpha_G}{\beta\mathcal{J}} \left(2 - \frac{\pi \tan \frac{\pi}{q} + \frac{2\pi t}{\beta}}{\tanh \frac{\pi t}{\beta}} \right), \\ \frac{\delta G_{lr}}{G_{lr}} &= -\frac{\alpha_G}{\beta\mathcal{J}} \left(2 - \frac{2\pi t}{\beta} \tanh \frac{\pi t}{\beta} \right).\end{aligned}\quad (3.124)$$

Rather than taking this direct approach, we will use the results derived earlier in this section to get the answer by a different method. From Eq. (3.99), the leading term in the chaos limit behaves like

$$\frac{\mathcal{F}(t)}{G(\pi)G(\pi)} \approx -\frac{3\alpha_0\beta\mathcal{J}}{2\pi\alpha_K} e^{\frac{2\pi}{\beta}t}. \quad (3.125)$$

If we correct the growth exponent to $\lambda_L = \frac{2\pi}{\beta} + \delta\lambda_L$, and expand to linear order in $\delta\lambda_L$, we expect a term linear in t times the growing exponential:

$$\frac{\mathcal{F}_{\text{expect}}(t)}{G(\pi)G(\pi)} = -(t\delta\lambda_L) \cdot \frac{3\alpha_0\beta\mathcal{J}}{2\pi\alpha_K} e^{\frac{2\pi}{\beta}t}. \quad (3.126)$$

We expect $\delta\lambda_L$ to be of order $(\beta\mathcal{J})^{-1}$, so this term is of order one at large coupling. We found a term exactly of this type when we analyzed the double pole in the chaos limit of the $\mathcal{F}_{h \neq 2}$ function. The contribution that contains the log is

$$\frac{\mathcal{F}_{\text{have}}(t)}{G(\pi)G(\pi)} = -\frac{3\alpha_0}{k'_R(-1)\pi^2} \partial_h \Psi_h(\chi)|_{h=2} \quad (3.127)$$

$$\approx \frac{3\alpha_0}{2\pi k'_R(-1)} \frac{2\pi}{\beta} t e^{\frac{2\pi}{\beta}t} \quad (3.128)$$

where we took the large- t limit in the second line, using Eqs. (3.58) and (3.62). Comparing with Eq. (3.126), and rewriting α_K in terms of α_G using Eq. (3.88), we find

$$\lambda_L = \frac{2\pi}{\beta} \left(1 - \frac{-k'(2)}{k'_R(-1)} \frac{q\alpha_G}{\beta\mathcal{J}} + \dots \right). \quad (3.129)$$

We have checked that this agrees with the direct method described above.

The correction is always negative. It is consistent with the large- q exact result. Evaluating the derivatives and plugging in the numerical value for α_G , we have that when $q = 4$

$$\frac{-k'(2)}{k'_R(-1)} \frac{q\alpha_G}{\beta\mathcal{J}} \approx \frac{4.28}{\beta\mathcal{J}} \approx \frac{6.05}{\beta\mathcal{J}}, \quad (q = 4). \quad (3.130)$$

When q approaches two, the correction diverges, like

$$\frac{-k'(2)}{k'_R(-1)} \frac{q\alpha_G}{\beta\mathcal{J}} = \frac{6\pi}{(\pi^2 - 6)(q - 2)\beta\mathcal{J}}, \quad (q \rightarrow 2). \quad (3.131)$$

This divergence seems to be consistent with the fact that the $q = 2$ the model is free, so the chaos exponent must vanish for any value of $\beta\mathcal{J}$.

Another approach to computing λ_L is to numerically solve the real-time Schwinger-Dyson equations to find G_R and G_{lr} , and then use a binary search to find the largest value of λ_L such that there exists an eigenfunction $f(t_{12})$ that satisfies Eq. (3.117). This works well for small and moderate $\beta\mathcal{J}$. In Fig. 11 we plot some data points for $q = 4$ computed this way. They appear to match smoothly to the large $(\beta\mathcal{J})$ result (3.129). We will give a few more details about this approach in Appendix G.

IV. THE EFFECTIVE THEORY OF REPARAMETRIZATIONS

In this section we will discuss the effective action of the model. This gives a second perspective on the computation of the four-point function that makes some features clearer, such as the physical interpretation of the enhanced $h = 2$ contribution. It also allows us to connect the specific heat term in the free energy to the ladder kernel.

The effective action of the model is derived by starting with the original fermion path integral and doing the Gaussian integral over the disorder. This gives a bilocal action for the fermions. One can integrate out the fermions after introducing a field $\tilde{G}(\tau_1, \tau_2)$ and a Lagrange multiplier field $\tilde{\Sigma}$ that sets \tilde{G} equal to $\frac{1}{N} \sum_j \psi_j(\tau_1) \psi_j(\tau_2)$. We are left with the nonlocal action [3]

$$\begin{aligned}S/N &= -\frac{1}{2} \log \det(\partial_t - \tilde{\Sigma}) + \frac{1}{2} \int d\tau_1 d\tau_2 \left[\tilde{\Sigma}(\tau_1, \tau_2) \tilde{G}(\tau_1, \tau_2) \right. \\ &\quad \left. - \frac{J^2}{q} \tilde{G}(\tau_1, \tau_2)^q \right] \quad (4.1)\end{aligned}$$

for $\tilde{G}, \tilde{\Sigma}$. This is an exact rewriting of the theory. Because of the Lagrange multiplier constraint, we can compute the four-point function of fermions (3.2) in the $\tilde{G}, \tilde{\Sigma}$ variables as

$$\begin{aligned}&\frac{1}{N^2} \sum_{ij} \langle \psi_i(\tau_1) \psi_i(\tau_2) \psi_j(\tau_3) \psi_j(\tau_4) \rangle \\ &= \int d\tilde{\Sigma} d\tilde{G} e^{-S} \tilde{G}(\tau_1, \tau_2) \tilde{G}(\tau_3, \tau_4).\end{aligned}\quad (4.2)$$

The action has a saddle point at the solutions G, Σ of the Schwinger-Dyson equations (2.5). [Note that $\tilde{G}, \tilde{\Sigma}$ denote

the integration variables in Eq. (4.2), while G , Σ are the classical solutions to the action (4.1).] Evaluating the integrand at this saddle point gives the disconnected part of the four-point function. We can also consider fluctuations. It is convenient to define the fluctuations g , σ so that we have $\tilde{G} = G + |G|^{\frac{2-q}{2}}g$ and $\tilde{\Sigma} = \Sigma + |G|^{\frac{q-2}{2}}\sigma$. Notice that the measure is invariant $d\tilde{G}d\tilde{\Sigma} = dg d\sigma$. Expanding the action to second order in g , σ and using the saddle point equation $G = (\partial_\tau - \Sigma)^{-1}$ to simplify, we find

$$\begin{aligned} \frac{S}{N} = & -\frac{1}{4J^2(q-1)} \int d\tau_1 \dots d\tau_4 \sigma(\tau_1, \tau_2) \tilde{K}(\tau_1 \dots \tau_4) \sigma(\tau_3, \tau_4) \\ & + \frac{1}{2} \int d\tau_1 d\tau_2 \left[g(\tau_1, \tau_2) \sigma(\tau_1, \tau_2) \right. \\ & \left. - \frac{1}{2} J^2 (q-1) g(\tau_1, \tau_2)^2 \right]. \end{aligned} \quad (4.3)$$

Here, \tilde{K} is the symmetric ladder kernel defined in Eq. (3.9). We can integrate out σ , getting an action just for g . It is convenient to write this in matrix notation, as

$$\frac{S}{N} = \frac{J^2(q-1)}{4} g \cdot (\tilde{K}^{-1} - 1) g \quad (4.4)$$

where 1 is the identity matrix. We can use this to get the $1/N$ term in the four-point function (4.2), by replacing both factors of \tilde{G} in the integrand by $|G|^{\frac{2-q}{2}}g$ and then doing the Gaussian integral with an appropriately chosen contour. This immediately gives the expression (3.66) that we previously derived from the Feynman diagrams.

The expressions written so far are valid at any energy. When we go to low energies and we use the conformal expressions, G_c , Σ_c in order to evaluate the kernel \tilde{K} , then we find that the action is zero when evaluated on fluctuations that are reparametrizations of the conformal correlator, as in Eq. (3.70). This is because these fluctuations are eigenfunctions of the kernel with eigenvalue one [Eq. (3.71)]. More conceptually, it is because the action (4.1) is reparametrization invariant [under Eq. (2.7)] if we drop the ∂_t term inside the determinant. Notice that even though the action is reparametrization invariant, the solution G_c is only invariant under the $SL(2, R)$ subgroup. Thus we can view reparametrization invariance as an emergent symmetry of the infrared theory which is spontaneously broken by the conformal solution G_c . The zero modes in the action can be viewed as Nambu-Goldstone modes for the spontaneous breaking of the full conformal symmetry down to $SL(2, R)$. Note that we could consider an alternative model which does not have a reparametrization invariance, then we do not get any enhanced contribution in the IR; see Appendix H.

We can now include the leading nonconformal correction to the action (4.4), which is determined by the first-order shift in the $h = 2$ eigenvalues of the kernel (3.87).

This will provide a nonzero action for these reparametrization modes. To compute this, we consider a small reparametrization $\tau \rightarrow \tau + \epsilon(\tau)$, and evaluate the action on $\delta_\epsilon G_c$. It is convenient to work in frequency space for ϵ , and to use that reparametrizations $\delta_\epsilon G_c$ are proportional to the $h = 2$ eigenfunctions of the kernel. We get an action proportional to $n^2(n-1)$, where n labels the Matsubara frequency. This factor arises from the product of the $|n|$ in the eigenvalue shift and the $|n|(n-1)$ in the normalization of the $h = 2$ eigenfunctions. Transforming back to position space, we have

$$\begin{aligned} \frac{S}{N} = & \frac{\alpha_S}{\mathcal{J}} \int_0^\beta d\tau \frac{1}{2} \left[(\epsilon'')^2 - \left(\frac{2\pi}{\beta} \right)^2 (\epsilon')^2 \right], \\ \alpha_S \equiv & \frac{\alpha_K}{6q^2\alpha_0} = \frac{q|k'_c(2)|\alpha_G}{6q^2\alpha_0}. \end{aligned} \quad (4.5)$$

This action for ϵ is local, even though the original action is nonlocal. This is reasonable because the breaking of reparametrization invariance is a UV effect. In fact, the action that we get could have been guessed by standard effective field theory reasoning: it is simply the expression of lowest order in derivatives that vanishes for global $SL(2)$ transformations. It must vanish in that case because the correlator is $SL(2)$ invariant, $\delta_{SL(2)}G_c = 0$ is zero. Notice that these $SL(2)$ reparametrizations should not be thought of as zero modes; they simply are not part of the functional integral over G .

Therefore the emergent conformal symmetry is both spontaneously broken by the infrared solution G_c as well as explicitly broken, which gives a small action (4.5). It is small in the sense that it formally vanishes as $\mathcal{J} \rightarrow \infty$. On the other hand, notice that it is large in the sense that it is of order N . To get a reasonable theory we need to include the effects of this breaking. This pattern of symmetry breaking is reminiscent of the pions in QCD; the chiral symmetry is both spontaneously and explicitly broken (by the quark mass terms). Thus Eq. (4.5) turns the reparametrization modes into pseudo-Nambu-Goldstone bosons.

The enhanced contribution \mathcal{F}_{big} from Eq. (3.89) can now be understood in a simple way. It is the result of the part of the functional integral (4.2) that consists of summing over reparametrizations of the circle weighted by the action (4.5). This leads directly to Eq. (3.90).

We would like to generalize the action (4.5) to finite reparametrizations $\tau \rightarrow f(\tau)$. It is convenient to start with the zero-temperature case where both f and τ are coordinates on the line. f is a coordinate on the ‘‘straight’’ line where the IR correlator is a pure power, and τ is a coordinate on the reparametrized line. Near any point (we take the origin), one can write

$$f(\tau) = f(0) + f'(0) \left(\tau + \frac{1}{2} \frac{f''(0)}{f'(0)} \tau^2 + \dots \right). \quad (4.6)$$

For small τ we have a small reparametrization with $\epsilon' = 0$ and $\epsilon'' = f''/f'$, followed by a scaling and translation. The scaling and translation have no effect on the correlator on the zero-temperature line, so we can generalize

$$\frac{1}{2} \int d\tau (\epsilon'')^2 \rightarrow \frac{1}{2} \int d\tau \left(\frac{f''}{f'} \right)^2 \quad (4.7)$$

which up to a total derivative implies that the action can be written as

$$S = -N \frac{\alpha_S}{\mathcal{J}} \int d\tau \{f, \tau\},$$

$$\{f, \tau\} \equiv \frac{f'''}{f'} - \frac{3}{2} \left(\frac{f''}{f'} \right)^2. \quad (4.8)$$

In the second step we introduced the Schwarzian derivative $\{f, \tau\}$ and used integration by parts. Note that the Schwarzian derivative is invariant under $SL(2)$ symmetry $f \rightarrow \frac{af+b}{cf+d}$. This is an exact symmetry since the zero-temperature G_c is exactly invariant under this transformation.

To get the action for reparametrizations of the circle, we consider the transformation

$$f(\tau) = \tan\left(\frac{\pi\tau}{\beta}\right) \quad (4.9)$$

which maps the circle to the line. Already for this transformation we get an interesting result. Inserting Eq. (4.9) into the Schwarzian action (4.8) we get a finite-temperature correction to the free energy

$$-\beta F \supset \frac{N\alpha_S}{\mathcal{J}} \int_0^\beta d\tau \left\{ \tan\frac{\pi\tau}{\beta}, \tau \right\} = 2\pi^2 \alpha_S \frac{N}{\beta \mathcal{J}}. \quad (4.10)$$

At large q , we have $\alpha_S = \frac{1}{4q^2}$ ($\alpha_K = 3$ and $\alpha_0 = 2$), and this agrees with the term found previously in Eq. (2.31). For $q = 2$ we get $\alpha_S = \frac{1}{24\pi}$ ($\alpha_0 = \pi^2$, $\alpha_K = \pi$), and again we agree with Eq. (2.33). In Fig. 12 we give a plot of α_S and indicate a numerical check of this formula. Note that while this action nicely explains the near extremal entropy, it says nothing about the zero-temperature entropy.

If we are interested in further reparametrizations of the circle, $\tau \rightarrow g(\tau)$, we can use the composition law for the Schwarzian derivative $\{f(g(\tau)), \tau\} = (g')^2 \{f, g\} + \{g, \tau\}$ to obtain

$$\frac{S}{N} = -\frac{\alpha_S}{\mathcal{J}} \int d\tau \left\{ \tan\frac{\pi g(\tau)}{\beta}, \tau \right\}$$

$$= \frac{\alpha_S}{2\mathcal{J}} \int d\tau \left[\left(\frac{g''}{g'} \right)^2 - \left(\frac{2\pi}{\beta} \right)^2 (g')^2 \right]. \quad (4.11)$$

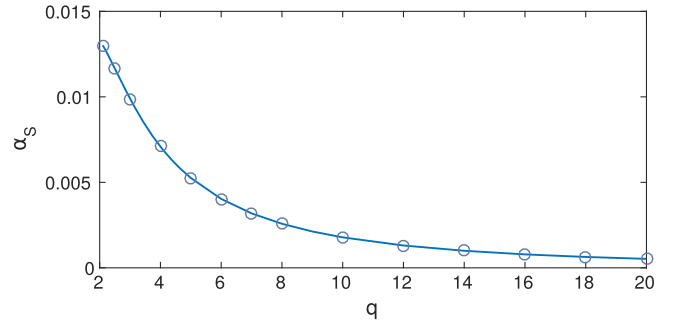


FIG. 12. The coefficient of the Schwarzian action α_S is plotted. The blue curve is the value given by the previously computed α_G . The circles are values inferred from Eq. (5.2) and the numerical evaluation of the specific heat c . The agreement is a check that the Schwarzian action is correct nonlinearly, not just for small reparametrizations.

Writing $g(\tau) = \tau + \epsilon(\tau)$ and expanding in ϵ we get both of the quadratic terms in Eq. (4.5).

V. THE DENSITY OF STATES AND THE FREE ENERGY

The large- N free energy is determined by evaluating the $\tilde{G}, \tilde{\Sigma}$ action (4.1) on the saddle point values G, Σ . In a low-temperature expansion, we have

$$\log Z = -\beta E_0 + S_0 + \frac{c}{2\beta} + \dots, \quad (5.1)$$

where the ground-state energy, entropy and specific heat are all proportional to N . The ground-state energy will not be important for our discussion. The zero-temperature entropy is given for general q by Eq. (2.32). The specific heat is determined by Eq. (4.10) as

$$\frac{c}{2} = 2\pi^2 \alpha_S \frac{N}{\mathcal{J}}. \quad (5.2)$$

For the case $q = 4$ we have $c \approx 0.396N/J$.

All of the terms in Eq. (5.1) are proportional to N . There is an important order-one correction to this free energy which we can compute from the determinant of the quadratic action (4.3). The log determinant of this action gives a term⁸

$$-\beta F \supset -\frac{1}{2} \sum_{h,n} \log[1 - k(h, n)]. \quad (5.3)$$

⁸This contribution to the free energy was first pointed out by J. Polchinski and A. Streicher, using Feynman diagrams. They also noted that the sum over near-zero modes would lead to a log term [27].

We get an interesting $\log \beta J$ term from the $h = 2$ modes, which have eigenvalues close to one. Substituting in the corrected eigenvalues (3.87), we get

$$-\beta F \supset - \sum_{n=2}^{\infty} \log \frac{n}{\beta J} + \text{const} \rightarrow \# \beta J - \frac{3}{2} \log \beta J + \text{const}. \quad (5.4)$$

This sum is divergent, but the divergence will presumably be cut off at $n \sim \beta J$, where one expects higher-order effects to make the eigenvalue $k(2, n)$ small. This will lead to a term proportional to βJ with an unknown coefficient; this is a correction to the ground-state energy. The special feature of the $h = 2$ sum is that we also get the finite log piece indicated on the right. This can be extracted by zeta function regularization or the Euler-MacLaurin formula. The logarithm means that the partition function is proportional to $\beta^{-3/2}$ at large β .

We can also get this factor of $\beta^{-3/2}$ from the action (4.5) as follows. We also do the functional integral over $\epsilon(\tau)$. However, we need to recall that we are *not* integrating over $SL(2, R)$ transformations. Thus, we need to divide the integral by the volume of $SL(2, R)$, since we should view $SL(2, R)$ as a gauge symmetry. This will result in the insertion of factors of the form $\delta(\epsilon(0))\delta(\epsilon'(0))\delta(\epsilon''(0))$ in the functional integral. When we rescale ϵ to get rid of the coefficient of the quadratic action in Eq. (4.5), we will find a factor of $(\beta \mathcal{J})^{-3/2}$ from the three delta functions.

The integral over all the nonzero modes with $h \neq 2$ will produce a $\beta \mathcal{J}$ divergence that corrects the ground-state energy, plus a β -independent factor which can be absorbed as a $1/N$ correction to S_0 in Eq. (5.1).

With this information, we can now compute the density of states by doing an inverse Laplace transform to the partition function. It is convenient to subtract the ground-state energy, so that from now on E indicates the energy above the ground state. The integral is

$$\begin{aligned} \rho(E) &= \frac{1}{2\pi i} \int_{\gamma+i\mathbb{R}} d\beta Z(\beta) e^{\beta E} \\ &\propto e^{S_0} \int \frac{d\beta}{(\beta J)^{\frac{3}{2}}} e^{\beta E + c/2\beta} \\ &\approx \sqrt{\frac{2\pi}{cJ^3}} e^{S_0 + \sqrt{2cE}}. \end{aligned} \quad (5.5)$$

In the final step we approximated the integral as a saddle point, valid for $cE \gg 1$. It is interesting that the determinant from the saddle point integral cancels the factor $\beta^{-3/2}$ from the one-loop free energy, so $\rho(E)$ approaches a constant at low energy, in this approximation. We can also compute the integral for small cE , where it becomes $\approx 4\sqrt{\pi E/J^3} e^{S_0}$. The \sqrt{E} vanishing is interesting, because it agrees with the behavior that one gets for the spectrum of a random

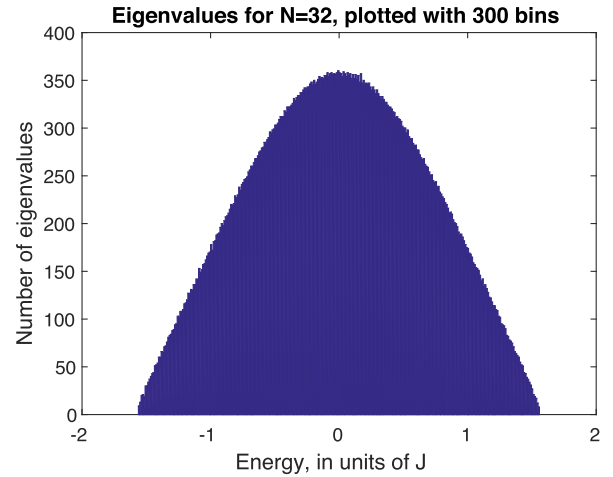


FIG. 13. The spectrum for a single realization of the $q = 4$ model with $N = 32$ fermions.

Hamiltonian. However, we cannot trust the computation for such small values of E ; at the crossover point $cE \sim 1$, the saddle point in the β integral is at $\beta \sim c \sim N/J$. At such low temperatures, the Schwarzian action discussed in the previous section stops being semiclassical, and our analysis would need to be improved.⁹

A somewhat complementary approach to the spectrum is to exactly diagonalize the Hamiltonian (2.1) for small values of N . The Majorana fermion operators ψ_i are just matrices that satisfy $\{\psi_i, \psi_j\} = \delta_{ij}$. In other words, they are Dirac gamma matrices. To represent the model with N fermions, we need a Hilbert space of dimension $2^{N/2}$. We were able to study up to $N = 32$ without any special techniques. We give a plot of the binned spectrum for $N = 32$ in Fig. 13.

One obvious feature of the plot is that there is no scale-invariant divergence $\rho(E) \propto 1/E$ or $\delta(E)$ at low energy. Instead, the density goes smoothly to zero. A naive reading of the plot suggests that the spectrum vanishes as E^p with p near one. The zero-temperature entropy does not reflect any actual degeneracy, only a large density of states near the ground state. From this perspective, a completely random Hamiltonian on a system of N qubits also has a zero-temperature entropy, $S_0 = N \log 2$, from the density $\rho(E) \propto \sqrt{E(E-2)} 2^N$. This gives a low-temperature free energy $\log Z = N \log 2 - (3/2) \log \beta$.

⁹As a side remark, note that, as we discussed in Ref. [26], the effective action (4.5) also appears for near extremal black holes. Therefore in such cases the computation of Eq. (5.5) will be valid. In that case, the fact that the density is constant at low energies is consistent with the fact that Bogomol'nyi-Prasad-Sommerfield (BPS) black holes can have a large degeneracy at exactly zero energy. For non-BPS black holes we could have further corrections that might remove the large degeneracy at exactly zero energy.

In fact, from Fig. 13, the density of states in SYK does not look too different from the random matrix semicircle. It is important to note, though, that if we increase N the density in the central region will be growing much faster than near the edges. Near the center, we expect the density characteristic of the infinite-temperature entropy, $\rho \sim 2^{N/2} \approx e^{0.35N}$, while near the edges we expect $e^{S_0 N} \approx e^{0.23N}$. By diagonalizing the Hamiltonian for different values of N between 24 and 32, and counting the number of levels within bands of width $0.3J$, we found the best fit $e^{0.33N}$ near the center and $e^{0.24N}$ near the edge, in reasonable agreement with large- N expectations. Note that the Hamiltonian, while containing of order N^4 random elements is not as random as a general random matrix in Hilbert space, which would contain 2^N random elements.

VI. TOWARDS A BULK INTERPRETATION

A natural starting point for a bulk interpretation is the action (4.1). Due to the large factor of N , this looks like a classical system for the fields $\tilde{\Sigma}$ and \tilde{G} . One of them can be easily eliminated, so we really have one field which is a function of two variables. Thus we seem to have a field theory defined on a two-dimensional space. It is natural to think of the average of the two times as a time and the difference as a new dimension. The solution to the Schwinger-Dyson equations gives us a classical background for this system, and then we have fluctuations governed by a quadratic action of the form (4.4). The computation of the four-point function of the fermions can be viewed as the computation of the propagator for this bilocal field and it involved inverting the operator $(1/\tilde{K} - 1)$ [Eq. (4.4)].

In the large- βJ limit, we have seen that there is a dominant mode associated to the emergence of a conformal symmetry which is both spontaneously and explicitly broken. A conformal symmetry is easily obtained if we consider AdS₂ gravity. When we regularize the space and we introduce some boundary conditions we get a boundary mode that is the same as the one parametrized by the function $f(\tau)$ discussed above. The AdS₂ metric preserves explicitly an $SL(2, R)$ group. This metric is spontaneously breaking the rest of the reparametrizations. The boundary mode is the corresponding Goldstone boson and it implies that pure AdS₂ gravity is not well defined, if we want to have any nontrivial excitation [7,34,35]. However, when AdS₂ arises from a higher-dimensional theory, there is always a coupling to a dilaton which is not constant on AdS₂. This explicitly breaks the conformal symmetry and it gives rise to an action for the modes parametrized by $f(\tau)$. The details of this will be discussed in a separate publication [26] and the discussion is very closely related to the analysis in Ref. [7]. In summary, both the mode parametrized by $f(\tau)$ and its action are reproduced by any near AdS₂ (or N AdS₂) geometry. This feature is insensitive to the precise details about the type of matter we can have in

AdS₂. It results purely from the emergence of the conformal symmetry and its slight breaking.

In order to elucidate the kind of matter we have in the dual of SYK we need to look at the other propagating modes contained in the field $G(\tau_1, \tau_2)$. Fortunately, for all the other modes we can use the $SL(2, R)$ symmetry to describe them. The propagating modes can be read off from the OPE expansion of the fermion four-point function. Their conformal dimensions are the solutions to $k_c(h_m) = 1$ and were discussed in Sec. III B 6. We get an infinite tower of dimensions which asymptotes to Eqs. (3.55)–(3.56) at large values of m . This asymptotic form of the dimensions has a structure that looks like a two-particle state in AdS₂. However, it is important to note that the shift in dimensions is of order one, and not order $1/N$. Therefore, we cannot view these states as a two-particle state of fermions in the bulk with weak, gravitational strength, interactions. This tower of particles is reminiscent of a string theory with a string scale of order the AdS radius. In fact, it also looks similar to what we would get in an $O(N)$ model, where we get a state for each spin and the number of single string states does not exhibit an exponential growth with energy (Hagedorn behavior). Here all members of the tower are getting an order-one shift in their dimensions.¹⁰ In two dimensions we do not have a clear notion of spin, but if we define spin by the contribution to the correlator in the chaos region, then they have spins $S > 2$ ($S = 2$ is for the $h = 2$ states related to the reparametrizations).

A. Comments on kinematic space

In this subsection we expand a bit on the comment on the relation between the two times of G and the two variables of a bulk field. Recently, this was further explored in Ref. [18].

In general we can define

$$t = \frac{\tau_1 + \tau_2}{2}, \quad \sigma = \frac{\tau_1 - \tau_2}{2}. \quad (6.1)$$

At this point this is just a simple relabeling of the times. Written in this way, we see that some of the terms in the action (4.1) become local in the t, σ space. But the Pfaffian term is still nonlocal.

Furthermore, in the IR region, the Casimir operator acting on the two times τ_1, τ_2 has the form

$$\begin{aligned} C_{12}\Phi &= -(\tau_1 - \tau_2)^2 \partial_{\tau_1} \partial_{\tau_2} \Phi \\ &= \sigma^2 (-\partial_t^2 + \partial_\sigma^2) \Phi = \nabla^2 \Phi \end{aligned} \quad (6.2)$$

¹⁰In the free $O(N)$ models we get such a tower with dimensions given exactly by the sum of dimensions of the two elementary free field components $\psi \partial^{2n+1} \psi$. In the case of the Gross-Neveu model in $2 + 1$ dimensions, the interaction that gives the lowest member gets an anomalous dimension. Namely ψ^2 has a shift from $\Delta_{\text{free}} = 2 \rightarrow \Delta = 1$.

where $\Phi(t_1, t_2) = \frac{\hat{\delta}G}{G_c}$ where $\hat{\delta}G$ is a small fluctuation around the classical solution of the action (4.1), which in the IR is given by the conformal answer G_c [Eq. (2.8)]. We see that this looks like the Laplacian in AdS_2 , in coordinates $ds^2 = \frac{-dt^2 + d\sigma^2}{\sigma^2}$, and in units where the AdS radius is set to one. This space was defined in a purely kinematic way by using general properties of the conformal group. It was called kinematic space in Refs. [28,29]. Note that even the quadratic action (4.4) for Φ is highly nonlocal. It involves $1/k_c(h) - 1$ which is a complicated function of the Casimir, $C = h(h-1) = \nabla^2$; see Eq. (3.35). We should think of this Φ as describing many degrees of freedom since there are many solutions of $1/k_c(h) - 1 = 0$, describing the tower of states in Sec. III B 6.

It is amusing to note that the expression for the energy given in Eq. (2.26) looks like an Arnowitt-Deser-Misner-like expression for the energy in terms of a property of the solution at the boundary of the geometry, namely $\tau_1 = \tau_2$ or $\sigma = 0$.

In the Euclidean theory we expect the bulk to be H_2 . However, the kinematic space defined as above, through the Casimir operator, continues to be a Lorentzian signature space. This is a general feature of the Casimir operator acting on bilocal fields as has been used recently in Ref. [29]. We can view the space as dS_2 , or AdS_2 with time periodically identified, depending on the overall sign we choose for this metric. More explicitly, in the Euclidean finite-temperature theory, we have the times τ_1 and τ_2 which are periodic variables. When we define the sum and the difference we get (for $\beta = 2\pi$)

$$\tau = \frac{\tau_1 + \tau_2}{2}, \quad \sigma = \frac{\tau_1 - \tau_2}{2}, \quad C = \sin^2\sigma(-\partial_\tau^2 + \partial_\sigma^2) \quad (6.3)$$

which looks like the wave equation on global dS_2 , or AdS_2 with time periodically identified. In fact, the funny set of eigenfunctions that we needed to sum over in e.g. Eq. (3.45) has a simple interpretation in AdS_2 or dS_2 . They are the set of normalizable solutions of this wave equation. We had a further antisymmetry restriction on the wave functions, which amounts to antisymmetry under an antipodal transformation in this dS_2 or AdS_2 space. It would be interesting to see if some variation of this model has a de Sitter interpretation. Finally, this relation to kinematic space suggests that the usual bulk of AdS/CFT requires a further inverse x-ray or Radon transform. We make a few more comments on this in Appendix I.

B. The fermions

So far, we have avoided the ‘‘elephant in the room,’’ which are the N boundary fermions. One can question whether these should correspond to N bulk fermions or not.

Before trying to answer this question, let us recall the special case of $q = 2$. In that case the N boundary fermions give rise to just one ‘‘bulk’’ fermion as follows. After we diagonalize the random mass matrix by an orthogonal transformation we find that $\phi_i = \sum_m r_{im} \psi_m$, where ψ_m is a fermion with a definite mass (or frequency).¹¹ In the large- N limit, the distribution of masses is nearly continuous and we can view it as an extra dimension. So, in this case we see that the different boundary fermions ψ_i give rise to different parts of the bulk fermion field ψ . This should be the case, since a bulk fermion has many independent creation and annihilation operators.

Before we continue, let us also make another general comment. One can imagine getting rid of the fundamental fermions by viewing the couplings j_{ijkl} as dynamical with very slow dynamics so that they are effectively constant [19]. At the order we are working, this gives the same equations.¹² Once we make the couplings j_{ijkl} dynamical, we can gauge the $O(N)$ symmetry. Naively this seems to remove the fermions from the spectrum so that we do not need to discuss them further. However, we continue to have a related operator of the form

$$O(\tau, \tau') = \psi_i(\tau) [P e^{i \int_\tau^{\tau'} A_j}]_i^j \psi_j(\tau'). \quad (6.4)$$

The one-point functions of this operator $\langle O(\tau, \tau') \rangle \sim NG(\tau, \tau')$ continue to display an $SL(2, R)$ -invariant form with dimensions Δ .

We can now wonder what the interpretation of such an operator in the bulk is. This question was studied in detail for the related case of a matrix model in the nonsinglet sector in Ref. [37]. In that case, the corresponding state was a folded closed string coming from the boundary into the bulk. In our case we can imagine a similar explanation in terms of an open string that comes in from the boundary.

Then we can view the propagating states as strings oscillating in AdS_2 ; see Fig. 14. This is just a picture, since we are not displaying the precise string theory background.

We can now go back to the ungauged model. At the level that we treated it so far, it has a global $O(N)$ symmetry. And it is tempting to think that whether or not we gauge the symmetry is some operation purely at the boundary. Therefore even for the $O(N)$ model we expect to see that the fermion contains a string going into the bulk. In that case, the index i remains at the boundary of the bulk, and we can view it as a Chan-Paton index at the boundary. But in the bulk we would have just a single string, and no uncontracted indices. An alternative point of view,

¹¹For positive m we have a complex creation operator and for negative m the corresponding annihilation operator.

¹²Except that there is an additional contribution to the free energy from the j fields, of the form $N^q \log \beta$ from the j fields. We thank S. H. Shenker for this comment. This model is structurally reminiscent of the $2 + 1$ -dimensional $O(N)$ theories with fundamental bosons and fermions studied in Ref. [36].

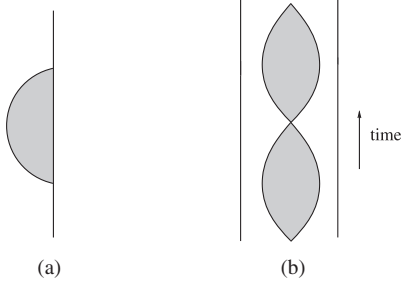


FIG. 14. (a) A particle with a string going to the boundary. (b) A pair of particles in the bulk with a string connecting them. They are oscillating in global AdS₂. We can view the string as fundamental or as a color electric flux of an $O(N)$ gauge field.

motivated by the global $SO(N)$ symmetry, would be to put $O(N)$ gauge fields in the bulk and charged fermion fields in the interior. However, in this case large- N counting would give us a coupling $g_{SO(N)} \sim 1$, which, together with the factor N , gives us a strong coupling. The fermions would be joined by a color electric flux, which looks conceptually similar to the strings discussed above. In fact we would get something like the 't Hooft model [38], but in AdS₂.

Further work would be needed to check whether this is the right interpretation.

When the couplings are random but fixed, it would be interesting to understand the corresponding bulk dual. Since the corrections to the leading answer would come at higher orders in the $1/N$ expansion (at order $1/N^{q-1}$), it seems natural to suspect that they would be associated to effects that are sensitive to quantum corrections.

C. Scrambling for near-extremal black holes and their stringy corrections

One of the original reasons for interest in the SYK model was the fact that it has the maximal chaos exponent $\lambda_L = 2\pi/\beta$. This is a necessary condition to have a theory dual to gravity, and it was thought that it might also be sufficient. A piece of evidence for this idea was that stringy corrections decrease λ_L by an amount proportional to ℓ_s^2/L^2 [11]

$$\lambda_L = \frac{2\pi}{\beta} \left(1 - \frac{\ell_s^2}{L^2} + \dots \right) \quad (6.5)$$

where L is a curvature scale at the horizon, so it seems that theories with maximal λ_L should not have large strings. However, the operator dimensions h_n that we found in the OPE suggest that the bulk theory dual to SYK has a tower of light fields roughly similar to a string spectrum with $\ell_s \sim R_{\text{AdS}}$. This seems to be a counterexample to the idea that maximal chaos implies a gravity dual. This motivates us to examine in more detail the form of the scale L that was appearing in Eq. (6.5).

Let us briefly review the shock-wave calculation that gives the chaos limit of the four-point function. We have an out-of-time-ordered four-point function with two pairs of operators. One pair is at time zero, and the other is at time t . The growing part of the correlator is given by the phase shift of the bulk field associated to the $t = 0$ pair as it crosses a shock sourced by the other pair. The general form of the shock wave plus static black hole metric is

$$ds^2 = -a(uv)dudv + b(uv)dx^i dx^i + h(x)\delta(u)du^2 \quad (6.6)$$

where we have added $D - 2$ extra flat dimensions. Einstein's equations give

$$\frac{1}{2} \left[-\frac{\partial_i^2}{b} - \left(\frac{\partial_u \partial_v b}{ab} \right) (D - 2) \right] h(x)\delta(u) = 8\pi G_N T_{uu}, \quad (6.7)$$

$$\frac{1}{2} \left[-\nabla^2 + \frac{\phi''(0)}{\phi(0)} \right] h(x)\delta(u) = 8\pi G_N T_{uu} \quad (6.8)$$

where $\phi \propto b^{\frac{D-2}{2}}$ is the ‘‘dilaton,’’ or the coefficient of the two-dimensional curvature in the action $\int \phi R^{(2)}$ after dimensional reduction on the extra flat coordinates. And ϕ'' is the second derivative with respect to proper distance from the horizon, evaluated at the horizon. Now we integrate this over the transverse space and also over u in a neighborhood of the horizon. We get

$$\frac{1}{2} \frac{\phi''}{\phi} Ah = 8\pi G_N P_u \quad (6.9)$$

where A is the area of the horizon, and h is the zero mode of the shock-wave profile. P_u is the momentum of the quantum associated to the pair of operators at time t , which is $P_u \sim (\Delta/R_{\text{AdS}}) e^{\frac{2\pi}{\beta}t}$. Dividing both sides by $2G_N$ gives

$$\frac{\phi''}{\phi} Sh = 4\pi P_u \quad (6.10)$$

where S is the entropy of the black hole. The phase shift for the other field crossing this shock is

$$\delta \sim \frac{\Delta}{R_{\text{AdS}}} h \sim \left[\frac{\Delta^2}{R_{\text{AdS}}^2} \frac{\phi}{\phi''} \right] \frac{1}{S} e^{\frac{2\pi}{\beta}t}. \quad (6.11)$$

We should regard the quantity in brackets as being the $\beta\mathcal{J}$ enhancement. In fact, for near extremal black holes, we have that the profile of the dilaton at the horizon has the form $\phi = \phi_0 + \gamma \cosh \frac{\rho}{R_{\text{AdS}_2}}$, where ϕ_0 gives the extremal entropy and γ the near extremal entropy, with $\gamma \ll \phi_0$. So we can write

$$R_{\text{AdS}}^2 \frac{\phi''}{\phi} = \frac{S - S_0}{S_0} \rightarrow \propto \frac{1}{q^2 \beta \mathcal{J}} \quad (6.12)$$

where on the left side we have a gravity expression and on the right-hand side we write the quotient of entropies that we have in the SYK model. Here we have simply reproduced the leading part of the answer from a gravity computation. We will connect it more clearly to the reparametrizations in Ref. [26]. The prefactor enhancement of the butterfly effect for near extremal black holes was noticed previously in Refs. [39,40].

Now we consider stringy corrections to the chaos exponent, following Ref. [11]. We read these off from Eq. (6.8). We reintroduce the extra dimensions, substitute

$$k^2 \rightarrow k^2 + \frac{\phi''}{\phi} \quad (6.13)$$

in the Regge behavior of the flat-space string amplitude $s^{2-\ell_s^2 k^2/2}$, and then take k to zero. This gives an effective spin which is

$$j = 2 - \frac{\ell_s^2 \phi''}{2\phi} = 2 - \frac{\ell_s^2}{2R_{\text{AdS}}^2} \frac{(S - S_0)}{S}. \quad (6.14)$$

So even if the string length is large, there is another parameter suppressing the correction to

$$\begin{aligned} \lambda_L &= \frac{2\pi}{\beta} (j - 1) \\ &= \frac{2\pi}{\beta} \left(1 - \frac{\ell_s^2}{2R_{\text{AdS}}^2} \frac{S - S_0}{S} + \dots \right). \end{aligned} \quad (6.15)$$

Note that using the expression for the ratios of entropies in Eq. (6.12) we get an estimate for the SYK model of a correction of order $\frac{1}{q^2 \beta \mathcal{J}}$ (provided $\ell_s \sim R_{\text{AdS}}$). This is indeed what we found in Eq. (3.129) up to q -dependent factors.

It is a little surprising that the change in the Regge spin can be small, despite the presence of light strings. The right interpretation seems to be that the gravity contribution gets a $\beta \mathcal{J}$ (or near-extremal) enhancement, but the higher stringy exchanges do not. So gravity dominates and we have a spin near two.

VII. BRIEF CONCLUSIONS

The SYK model is an interesting quantum-mechanical model displaying a spontaneously and explicitly broken reparametrization symmetry. These features dominate the low-energy properties of the model and are expected to be universal for any large- N system with emergent reparametrization symmetry. One motivation to study this model is that near-extremal black holes also display this pattern of symmetry breaking [26]. We also expect that this will be

relevant to other condensed matter physics models. This symmetry breaking pattern gives rise to several features of the low-energy dynamics. First, it gives rise to a specific heat that is linear in the temperature. It also gives rise to a large contribution to the four-point function, which saturates the chaos bound in the out-of-time-ordered configuration. All these features are expected to be universal features of systems with emergent reparametrization symmetry or $NCFT_1$ s.

We also studied several features that are special to this particular model, such as the spectrum of dimensions of fermion bilinear operators. These suggest that the dual description should contain a single Regge trajectory with low-tension strings in nearly AdS_2 space. We also gave a detailed description of the nonenhanced parts of the four-point function. Several questions remain about the proper holographic interpretation of this particular model.

ACKNOWLEDGMENTS

We thank D. Anninos, A. Kitaev, J. Polchinski, S. Shenker and Z. Yang for discussions. J. M. is supported in part by U.S. Department of Energy Grant No. de-sc0009988. D. S. is supported by the Simons Foundation Grant No. 385600.

APPENDIX A: THE SCHWINGER-DYSON EQUATIONS AND THE KERNEL

We consider the Schwinger-Dyson equations (2.5). We treat the $i\omega$ term as a perturbation. In fact for an arbitrary perturbation we can write the equations as

$$G * \Sigma + G * s = -1 = -\delta(\tau_1 - \tau_2), \quad \Sigma = J^2 G^{q-1} \quad (A1)$$

where the $*$ stands for $G * \Sigma = \int d\tau G(\tau_1, \tau) \Sigma(\tau, \tau_2)$ and G is the full solution with the source. The source induced by the $-i\omega$ term in Eq. (2.5) is $s = -\delta'(\tau - \tau_2)$. We can now write $G = G_c + \delta G$, where δG is the perturbation to the conformal solution induced by the presence of the source.

Expanding the equations to first order, using the second equation to express $\delta \Sigma$ in terms of δG , and convolving with G on the right, we obtain

$$\delta G - (q-1)J^2 G_c * G_c^{q-2} \delta G * G_c = G_c * s * G_c \quad (A2)$$

which can also be written as

$$[(1 - K_c) \delta G](\tau_1, \tau_2) = - \int d\tau \partial_\tau G_c(\tau_1 - \tau) G_c(\tau - \tau_2) \quad (A3)$$

where we have used the homogeneous equation $G_c * \Sigma_c = -\delta(\tau - \tau')$.

For simplicity, we will discuss the solution of these equations on the line, rather than the finite-temperature circle. Then the right-hand side has the form $\frac{\text{sgn}(\tau_{12})}{|\tau_{12}|^{4\Delta}}$. This is a function like Eq. (3.31) with $\tau_0 \rightarrow \infty$ and $h \rightarrow -2\Delta$. Therefore it seems that we could solve for δG by inverting $1 - K_c$. However, $k_c(-2\Delta) = \infty$ [see Eq. (3.35)], which would lead to $\delta G = 0$, so we cannot solve the equation this way. However, we could also consider adding terms δG that obey $(1 - K_c)\delta G = 0$. A formal solution would be an $h = -1$ mode which gives the correction $\delta G \propto G_c \frac{1}{|J\tau|}$ [see again Eq. (3.31) with $\tau_0 \rightarrow \infty$]. This is formally annihilated by $1 - K_c$, but crucially, it is not actually annihilated because of a UV divergence. This divergence arises from the region where the two times in the integral $K_c \delta G$ are very close to each other. In this region $\delta G \propto \frac{\text{sgn}(\tau)}{|J\tau|^{1+2/q}}$ and

$$[K_c \cdot \delta G](\tau_1, \tau_2)_{\text{divergent}} \propto J^2 \int d\tau_3 d\tau_4 G_c(\tau_{13}) G_c(\tau_{24}) \frac{\text{sgn}(\tau_{34})}{|J\tau_{34}|^{3-2/q}}. \quad (\text{A4})$$

This divergence would be regulated in the full theory, at scale $\tau_{34} \sim \frac{1}{J}$. This will have the effect of replacing

$$\frac{\text{sgn}(\tau_{34})}{|J\tau_{34}|^{3-2/q}} \rightarrow \frac{\#}{J^2} \delta'(\tau_{34}) \quad (\text{A5})$$

where we used that the antisymmetry of the function implies the need to look at the first derivative of the rest. In other words, all we are using about the left-hand side is that it is a sharply peaked antisymmetric function of $(J\tau_{34})$. The factors of J on the right-hand side come from the range of τ_{34} that is contributing to the integral. This then leads to an expression with the same form as the right-hand side of Eq. (A3), including the correct J dependence. However, the numerical coefficient will depend on the details of how the divergence is regulated in the full theory. In other words, to compute the full coefficient, we need to know the whole flow, in order to know how the coincident point divergence of the conformal case is regulated.

Another point of this appendix is to show that the same kernel that appears in the four-point function also appears

when we want to compute the corrections around the IR solution.

APPENDIX B: THE KERNEL AS A FUNCTION OF CROSS RATIOS

The kernel gives the $(n + 1)$ -ladder diagram in terms of the n -ladder diagram as

$$\begin{aligned} & \frac{\text{sgn}(\tau_{12})\text{sgn}(\tau_{34})}{|\tau_{12}|^{2\Delta}|\tau_{34}|^{2\Delta}} \mathcal{F}_{n+1}(\chi) \\ &= -\frac{1}{\alpha_0} \int d\tau_a d\tau_b \frac{\text{sgn}(\tau_{1a})\text{sgn}(\tau_{2b})}{|\tau_{2b}|^{2\Delta}|\tau_{1a}|^{2\Delta}|\tau_{ab}|^{2-4\Delta}} \\ & \quad \cdot \frac{\text{sgn}(\tau_{ab})\text{sgn}(\tau_{34})}{|\tau_{ab}|^{2\Delta}|\tau_{34}|^{2\Delta}} \mathcal{F}_n(\tilde{\chi}), \\ & \chi = \frac{\tau_{12}\tau_{34}}{\tau_{13}\tau_{24}}, \quad \tilde{\chi} = \frac{\tau_{ab}\tau_{34}}{\tau_{a3}\tau_{b4}}. \end{aligned} \quad (\text{B1})$$

We would like to use conformal symmetry to turn this into a one-dimensional integral equation. We can take $\tau_1 = 0$, $\tau_3 = 1$, $\tau_4 = \infty$, so that $\tilde{\chi} = \frac{\tau_{ab}}{\tau_a - 1}$ and $\chi = \tau_2$, and then replace the τ_b integration variable by $\tilde{\chi}$. The measure is $d\tau_a d\tau_b = d\tau_a d\tilde{\chi} (1 - \tau_a)$. One finds

$$\mathcal{F}_{n+1}(\chi) = \frac{1}{\alpha_0} \int_{-\infty}^{\infty} \frac{d\tilde{\chi}}{|\tilde{\chi}|^2} \left(\frac{|\chi||\tilde{\chi}|}{|\chi - \tilde{\chi}|} \right)^{2\Delta} \text{sgn}(\chi\tilde{\chi}) m(\chi, \tilde{\chi}) \mathcal{F}_n(\tilde{\chi}), \quad (\text{B2})$$

$$m(\chi, \tilde{\chi}) = \text{sgn}(\chi - \tilde{\chi}) \int_{-\infty}^{\infty} d\tau \frac{\text{sgn}(\tau)\text{sgn}(1 - \tau)\text{sgn}\left(1 - \frac{1 - \tilde{\chi}}{\chi - \tilde{\chi}}\tau\right)}{|\tau|^{2\Delta} |1 - \tau|^{1-2\Delta} \left|1 - \frac{1 - \tilde{\chi}}{\chi - \tilde{\chi}}\tau\right|^{2\Delta}}. \quad (\text{B3})$$

The integral over τ can be done by dividing up the region of integration and using

$$\begin{aligned} & \int_0^1 \frac{d\tau}{(1 - x\tau)^a \tau^b (1 - \tau)^c} \\ &= \frac{\Gamma(1 - b)\Gamma(1 - c)}{\Gamma(2 - b - c)} {}_2F_1(a, 1 - b, 2 - b - c, x). \end{aligned} \quad (\text{B4})$$

The answer is

$$\begin{aligned} m(\chi, \tilde{\chi}) &\equiv \begin{cases} \frac{2\pi}{\sin 2\pi\Delta} F(1 - 2\Delta, 2\Delta, 1, z) - B_{2\Delta}\left(\frac{1}{1-z}\right) - B_{1-2\Delta}\left(\frac{1}{1-z}\right) & z \leq 0, \\ -\frac{2\pi}{z^{2\Delta} \sin 2\pi\Delta} F(2\Delta, 2\Delta, 1, \frac{z-1}{z}) + \frac{2\pi}{\sin 2\pi\Delta} F(2\Delta, 1 - 2\Delta, 1, z) & 0 \leq z \leq 1, \\ -\frac{2\pi}{\sin 2\pi\Delta} F(2\Delta, 1 - 2\Delta, 1, 1 - z) + B_{2\Delta}(z^{-1}) + B_{1-2\Delta}(z^{-1}) & 1 \leq z, \end{cases} \\ z &\equiv \frac{1 - \min(\chi, \tilde{\chi})}{|\chi - \tilde{\chi}|}, \quad B_h(x) = \frac{\Gamma(h)^2}{\Gamma(2h)} x^h {}_2F_1(h, h, 2h, x). \end{aligned} \quad (\text{B5})$$

We are interested in applying this integral kernel to functions $\mathcal{F}(\chi)$ with the symmetry of the four-point function. This means that we should have $\mathcal{F}(\chi) = \mathcal{F}(\chi/(\chi-1))$. This transformation maps the interval between zero and two into the complement on the real line, so we can restrict our attention to $f(\chi)$ with $0 \leq \chi \leq 2$. Using the invariance and changing integration variables in Eq. (B2), we get a closed equation in this interval:

$$\begin{aligned} \mathcal{F}_{n+1}(\chi) = & \frac{1}{\alpha_0} \int_0^2 \frac{d\tilde{\chi}}{\tilde{\chi}^2} \mathcal{F}_n(\tilde{\chi}) \left[\frac{\chi^{2\Delta} \tilde{\chi}^{2\Delta}}{|\chi - \tilde{\chi}|^{2\Delta}} m(\chi, \tilde{\chi}) \right. \\ & \left. + \text{sgn}(\tilde{\chi} - 1) \frac{\chi^{2\Delta} \tilde{\chi}^{2\Delta}}{|\chi + \tilde{\chi} - \chi\tilde{\chi}|^{2\Delta}} m\left(\chi, \frac{\tilde{\chi}}{\tilde{\chi} - 1}\right) \right]. \end{aligned} \quad (\text{B6})$$

The expression in brackets times $1/\alpha_0$ is the kernel $K_c(\chi, \tilde{\chi})$ described in Eq. (3.21).

APPENDIX C: REPRESENTING \mathcal{F}_0 IN TERMS OF Ψ_h

Using contour manipulations very similar to the one we used to derive Eqs. (3.50) and (3.52), it is possible to write a formula for \mathcal{F}_0 as a sum over residues. There are two differences: first, we do not have a divergent term at $h = 2$, so we do not need to subtract it. Second, since we have $k_c(h)$ in the integrand instead of $k_c(h)/[1 - k_c(h)]$, we are interested in the poles of $k_c(h)$, which occur at values $h = \frac{2}{q} + 1 + 2n$. We get the following formulas for \mathcal{F}_0 . When $\chi > 1$,

$$\mathcal{F}_0(\chi) = -\alpha_0 \sum_{n=0}^{\infty} \text{Res} \left[\frac{(h-1/2)}{\pi \tan(\pi h/2)} k_c(h) \Psi_h(\chi) \right]_{h=\frac{2}{q}+1+2n}, \quad \chi > 1 \quad (\text{C1})$$

and when $\chi < 1$ we have

$$\mathcal{F}_0(\chi) = -\alpha_0 \sum_{n=0}^{\infty} \text{Res} \left[\frac{(h-1/2)}{\pi \tan(\pi h/2)} k_c(h) \frac{\Gamma(h)^2}{\Gamma(2h)} \chi^h {}_2F_1(h, h, 2h, \chi) \right]_{h=\frac{2}{q}+1+2n}, \quad \chi < 1. \quad (\text{C2})$$

These expressions (C1) and (C2) can be checked by numerically evaluating the residue sums and comparing to Eq. (3.42).

APPENDIX D: WRITING $\Psi_h(\chi)$ IN TERMS OF $\Psi_{h,n}(\theta_1, \theta_2)$

By solving the Casimir differential equation, one finds that the antisymmetric eigenfunctions of C_{1+2} with weight $\Delta = 1/2$ and symmetry under $(x, y) \rightarrow (2\pi - x, y + \pi)$ are

$$\Psi_{h,n}(\theta_1, \theta_2) = \gamma_{h,n} \frac{e^{-iny}}{2 \sin \frac{x}{2}} \psi_{h,n}(|x|), \quad x = \theta_{12}, \quad y = \frac{\theta_1 + \theta_2}{2} \quad (\text{D1})$$

where the functions $\psi_{h,n}$ are the ones appearing in Eqs. (3.80) and (3.81), but with $v = 1$ so that $\tilde{n} = n$. The norms of the continuum eigenfunctions $h = 1/2 + is$ can be determined by assuming that $\langle \Psi_{h,n}, \Psi_{h',n} \rangle = 2\pi \delta(s - s')$, where the inner product is defined in Eq. (3.64), and analyzing the integral near $x = 0$ and $x = 2\pi$, as in Eq. (3.40). One finds an expression involving a product of gamma functions. With these normalizations, we have that

$$\begin{aligned} \frac{2h-1}{\pi \tan(\pi h)} \frac{\Psi_h(\chi)}{\left(2 \sin \frac{\theta_{12}}{2}\right) \left(2 \sin \frac{\theta_{34}}{2}\right)} = & 2 \sum_n \Psi_{h,n}^*(\theta_1, \theta_2) \Psi_{h,n}(\theta_3, \theta_4), \\ \chi = & \frac{\sin \frac{\theta_{12}}{2} \sin \frac{\theta_{34}}{2}}{\sin \frac{\theta_{13}}{2} \sin \frac{\theta_{24}}{2}} \end{aligned} \quad (\text{D2})$$

which shows that the continuum part of the formulas (3.45) and (3.66) agree. When we go to the discrete case where h is an even integer, the continuum normalization $\gamma_{h,n}^2$ diverges for $|n| \geq h$, and the factor of $1/\tan(\pi h)$ in Eq. (D2) also diverges. The coefficient of this divergence gives the relation

$$\frac{2h-1}{\pi^2} \frac{\Psi_h(\chi)}{\left(2 \sin \frac{\theta_{12}}{2}\right) \left(2 \sin \frac{\theta_{34}}{2}\right)} = 2 \sum_{|n| \geq h} \Psi_{h,n}^*(\theta_1, \theta_2) \Psi_{h,n}(\theta_3, \theta_4) \quad (\text{D3})$$

where the $\Psi_{h,n}$ are now defined with discrete norms so that $\langle \Psi_{h,n}, \Psi_{h',n'} \rangle = \delta_{hh'} \delta_{nn'}$. This establishes the equivalence of the discrete parts of Eq. (3.45) and (3.66). A special case that we use in the main text of the paper is

$$\Psi_2(\chi) = 2 \sum_{|n| \geq 2} \frac{e^{in(y-y')} f_n(x) f_n(x')}{|n|(n^2 - 1)} \quad (\text{D4})$$

where $x = \theta_{12}$, $y = \frac{\theta_1 + \theta_2}{2}$, $x' = \theta_{34}$, $y' = \frac{\theta_3 + \theta_4}{2}$ and χ is defined as in Eq. (D2). The functions f_n were defined in Eq. (3.72).

APPENDIX E: DIRECT APPROACH TO THE SHIFT IN EIGENVALUE

In this appendix we sketch a second derivation of Eq. (3.88), which consists of substituting $G + \delta G$ in for the propagators in the kernel, with δG given in Eq. (3.85), and then analyzing the integrals to compute

$\langle \Psi_{2,n}, \delta \tilde{K} \cdot \Psi_{2,n} \rangle$. When we correct the propagator, we get corrections to \tilde{K} of two types. One type is a correction to the rung propagators; see Fig. 4. In that case, we can use the fact that $\Psi_{2,n}$ is an eigenfunction of the unperturbed kernel to do two of the integrals. This gives an expression that is independent of q , up to an overall multiple $(q-2)\alpha_G$. Comparing to the $q = \infty$ case, one finds that in general

$$\delta_{\text{rung}} k(2, n) = -\frac{(q-2)\alpha_G 3|n|}{\beta \mathcal{J} 2}. \quad (\text{E1})$$

The corrections to the rail propagators are not as simple. The change in the kernel is

$$\delta_{\text{rail}} \tilde{K} = -J^2(q-1) |G(\theta_{12})|^{\frac{q-2}{2}} \delta G(\theta_{13}) \times G(\theta_{24}) |G(\theta_{34})|^{\frac{q-2}{2}} + (13 \leftrightarrow 24). \quad (\text{E2})$$

Our first goal is to show that $\langle \Psi_{2,n}, \delta_{\text{rail}} \tilde{K} \cdot \Psi_{2,n} \rangle$ is proportional to $|n|$. We can do this using conformal symmetry. It will be useful to represent the function f_0 appearing in Eq. (3.85) as an integral

$$f_0 = \int_{-\pi}^{\pi} d\theta_0 \frac{\left| \sin \frac{\theta_{10}}{2} \sin \frac{\theta_{20}}{2} \right|}{\left| \sin \frac{\theta_{12}}{2} \right|}. \quad (\text{E3})$$

This implies that δG has the form of an integrated conformal three-point function of two fermions with an operator of dimension minus one. Another useful identity is based on

$$\frac{1}{8} \frac{\sin^2 \frac{\theta_{12}}{2}}{\sin^2 \frac{\theta_{10}}{2} \sin^2 \frac{\theta_{20}}{2}} = \sum_{n=2}^{\infty} e^{in\theta_0} e^{-iny} f_n(x), \quad \text{for } |e^{i\theta_0}| < 1, \quad (\text{E4})$$

which implies that $\Psi_{2,n}$ is proportional to an integrated conformal three-point function of two fermions with a dimension-two operator:

$$\Psi_{2,n}(\theta_1, \theta_2) = \frac{\gamma_n}{4\pi} \int_0^{2\pi} d\theta_0 e^{-in\theta_0} \frac{2 \sin \frac{\theta_{12}}{2}}{(2 \sin \frac{\theta_{10}}{2})^2 (2 \sin \frac{\theta_{20}}{2})^2}, \quad \gamma_n^2 = \frac{3}{\pi^2 |n|(n^2-1)}. \quad (\text{E5})$$

Here the integral is defined by giving θ_0 a small imaginary part $i\epsilon \text{sgn}(n)$.

The shift $\langle \Psi_{2,n}, \delta_{\text{rail}} \tilde{K} \cdot \Psi_{2,n} \rangle$ is an integral over four times $\theta_1, \dots, \theta_4$ of a product of propagators and eigenfunctions. The idea is to represent the eigenfunctions $\Psi_{2,n}$ and the change in the propagator δG using the integral formulas (E5) and (E3). This adds three new integration variables,

$\theta_a, \theta_b, \theta_c$. The complete expression is proportional to the integral over all seven θ variables of

$$\gamma_n^2 e^{in(\theta_a - \theta_b)} \left| \frac{\sin \frac{\theta_{12}}{2} \sin \frac{\theta_{34}}{2}}{\sin \frac{\theta_{13}}{2} \sin \frac{\theta_{24}}{2}} \right|^{2\Delta} \frac{\text{sgn}(\theta_{12}\theta_{34}\theta_{13}\theta_{24})}{\sin^2 \frac{\theta_{1a}}{2} \sin^2 \frac{\theta_{2a}}{2} \sin^2 \frac{\theta_{3b}}{2} \sin^2 \frac{\theta_{4b}}{2}} \times \left| \frac{\sin \frac{\theta_{1c}}{2} \sin \frac{\theta_{3c}}{2}}{\sin \frac{\theta_{13}}{2}} \right| \quad (\text{E6})$$

plus a similar term with $(13 \leftrightarrow 24)$. First we consider holding $\theta_a, \theta_b, \theta_c$ fixed and doing the integral over $\theta_1, \dots, \theta_4$. The θ_a and θ_b variables are the integration parameters in the representation (E5) of $\Psi_{2,n}$. They should be understood as having small imaginary parts of opposite sign. With this prescription, the integral over $\theta_1 \dots \theta_4$ is convergent, and has analytic dependence on θ_a and θ_b . [The naive divergence of the integral $\theta_{13} = 0$ is not present because of the $\text{sgn}(\theta_{13})$ factor.] Now, the important point is that the integral is $SL(2)$ covariant, with external weights $h = 2$ for the θ_a, θ_b variables and weight $h = -1$ for the θ_c variable. So the answer must be proportional to

$$\gamma_n^2 e^{in(\theta_a - \theta_b)} \frac{\sin \frac{\theta_{ac}}{2} \sin \frac{\theta_{bc}}{2}}{\sin^5 \frac{\theta_{ab}}{2}}. \quad (\text{E7})$$

We cannot have absolute value signs or sgn functions in this expression, because it must have analytic dependence on θ_a, θ_b . Finally, we integrate over the last three variables. The integral over θ_c turns the numerator into $\cos \theta_{ab}/2$. In the integral over θ_a , the opposite $i\epsilon$ prescriptions for θ_a, θ_b imply that we pick up the residue of the fifth-order pole at $\theta_a = \theta_b$. This is proportional to $n^2(n^2-1)$. Combining with the factor γ_n^2 defined in Eq. (3.72) we conclude that $\langle \Psi_{2,n}, \delta_{\text{rail}} \tilde{K} \cdot \Psi_{2,n} \rangle$ is indeed proportional to $|n|$.

To determine the coefficient of proportionality, one can compute the ratio of the rung and rail corrections by analyzing the integrals at large n . More precisely, we take n large and β large, with $\Omega = 2\pi n/\beta$ held fixed. In this limit it is better to use a proper time coordinate on the circle, τ , rather than the angle $\theta = 2\pi\tau/\beta$. The $h = 2$ eigenfunctions (3.72) are proportional to

$$\Psi(\tau_1, \tau_2) \propto \frac{e^{i\Omega(\tau_1 + \tau_2)/2}}{\tau_{12}} f(\Omega\tau_{12}/2), \quad f(\rho) = \cos \rho - \frac{\sin \rho}{\rho}. \quad (\text{E8})$$

For large n , all integrals will be dominated by the UV, where the propagator and correction are

$$G_c = b \frac{\text{sgn}\tau}{|\tau|^{2\Delta}}, \quad \frac{\delta G}{G_c} \propto \frac{1}{|\tau|}. \quad (\text{E9})$$

The frequency Ω scales out, so we can choose the value $\Omega = 2$. Then the rung and rail contributions to the eigenvalue are proportional to the integrals

$$I_{\text{rail}} = \int d\tau_2 d\tau_3 d\tau_4 e^{i\tau_2 - i\tau_3 - i\tau_4} f(\tau_2) \frac{\text{sgn}(\tau_2) \text{sgn}(\tau_{34})}{|\tau_2|^{2-2\Delta} |\tau_{34}|^{2-2\Delta}} \times \frac{\text{sgn}(\tau_3) \text{sgn}(\tau_{24})}{|\tau_3|^{1+2\Delta} |\tau_{24}|^{2\Delta}} f(\tau_{34}), \quad (\text{E10})$$

$$I_{\text{rung}} = \frac{q-2}{2} \int d\tau_2 d\tau_3 d\tau_4 e^{i\tau_2 - i\tau_3 - i\tau_4} f(\tau_2) \frac{\text{sgn}(\tau_2)}{|\tau_2|^{3-2\Delta}} \times \frac{\text{sgn}(\tau_{34}) \text{sgn}(\tau_3) \text{sgn}(\tau_{24})}{|\tau_{34}|^{2-2\Delta} |\tau_3|^{2\Delta} |\tau_{24}|^{2\Delta}} f(\tau_{34}) \quad (\text{E11})$$

where the proportionality constant is the same in both cases. Since we know the normalized rung contribution, we can get the full answer by computing the ratio of the above integrals and using Eq. (E1):

$$\delta k(2, n) = \left(1 + \frac{I_{\text{rail}}}{I_{\text{rung}}}\right) \delta_{\text{rung}} k(2, n). \quad (\text{E12})$$

The rung integral is easy to evaluate using the fact that we started with eigenvectors of the original kernel. The rail integral takes more work (it is convenient to represent some of the factors in the integrand as Fourier transforms) but the integrals can be done, and one eventually finds agreement with Eq. (3.88).

APPENDIX F: THE FIRST-ORDER CHANGE IN $h = 2$ EIGENVECTORS

In this appendix we show that the first-order shift in the $h = 2$ eigenvectors $\Psi_{2,n}^{\text{exact}} = \Psi_{2,n} + \delta\Psi_{2,n} + \dots$ is independent of q up to an overall multiple:

$$\delta\Psi_{2,n} = \frac{q\alpha_G}{2} \delta\Psi_{2,n}^{q=\infty}. \quad (\text{F1})$$

Morally, the reason is the following. The $h = 2$ eigenvectors are given by reparametrizations of G_c , and the first-order corrections are related to reparametrizations of δG , which itself is universal in q up to a coefficient. However, we will not need this interpretation. To give the actual argument, we start by considering the reparametrization $\delta_\epsilon I$, where

$$I(\tau_1, \tau_2) = \int d\tau_a d\tau_b G(\tau_1, \tau_a) \Sigma(\tau_a, \tau_b) G(\tau_2, \tau_b). \quad (\text{F2})$$

Here, reparametrizations are defined to act as in Eq. (3.70), and we consider the function I to have weight $\Delta = 1/q$. With this definition, I is reparametrization covariant, in the sense that the reparametrization of the answer for the integral is the same as the reparametrization of the various

parts that go inside the integral. Writing this statement out for linearized reparametrizations and using the exact Schwinger-Dyson equations

$$\int dt_a G(t_1, t_a) \Sigma(t_a, t_2) = -\delta(t_{12}) + \partial_{t_2} G(t_1, t_2), \quad (\text{F3})$$

we find

$$(1-K) \cdot \delta_\epsilon G = \frac{1}{q} H_\epsilon, \quad H_\epsilon(\tau_1, \tau_2) \equiv \int d\tau'(\tau) G(\tau_1, \tau) \partial_\tau G(\tau_2, \tau) - (1 \leftrightarrow 2). \quad (\text{F4})$$

This is true for any value of the coupling, provided that K and G are the exact kernel and propagator. Using $\tilde{K} = |G|^{\frac{q-2}{2}} K |G|^{-\frac{q-2}{2}}$, and taking a matrix element with one of the conformal eigenvectors $\Psi_{h,n}$, we get [the inner product is as in Eq. (3.64)]

$$\langle \Psi_{h,n}, (1 - \tilde{K}) \cdot |G|^{\frac{q-2}{2}} \delta_\epsilon G \rangle = \frac{1}{q} \langle \Psi_{h,n}, |G|^{\frac{q-2}{2}} H_\epsilon \rangle. \quad (\text{F5})$$

Naively, the leading piece of the lhs of Eq. (F5) is at order $(\beta J)^{-1}$, where we use the conformal answers for everything. However, this gives zero because $|G_c|^{\frac{q-2}{2}} \delta_\epsilon G_c$ is an eigenvector of \tilde{K}_c with eigenvalue one. In fact, the leading IR terms are at order $(\beta J)^{-2}$. We get these by substituting either δG or δK into the left side. The rhs has no terms at this order, so these contributions must cancel:

$$\langle \Psi_{h,n}, (1 - \tilde{K}_c) \cdot \delta_\epsilon (|G_c|^{\frac{q-2}{2}} \delta G) \rangle - \langle \Psi_{h,n}, \delta \tilde{K} \cdot |G_c|^{\frac{q-2}{2}} \delta_\epsilon G_c \rangle = 0. \quad (\text{F6})$$

The integral defining the lhs of Eq. (F6) has a UV divergence; we define the integral by taking only the cutoff-independent $(\beta J)^{-2}$ piece and discarding the power divergence. In the exact theory, UV divergences in this expression and on both sides of Eq. (F5) will be regulated to terms at order $(\beta J)^{-h}$ and $(\beta J)^{-h-1}$. Depending on h these might dominate over the IR term we are interested in, but as long as $h \neq 2$ they can be separated.

Let us examine Eq. (F6) in more detail. We can act with the kernel to the left, giving $(1 - k_c(h))$. Now, $|G_c|^{\frac{q-2}{2}} \delta_\epsilon G_c$ is proportional to $(1/q)$ times an $h = 2$ conformal eigenvector, and the quantity being reparametrized on the lhs is independent of q , up to a multiple α_G . So we conclude that

$$\frac{1}{q\alpha_G} \frac{\langle \Psi_{h,n}, \delta \tilde{K} \cdot \Psi_{2,n} \rangle}{1 - k_c(h)} \quad (\text{F7})$$

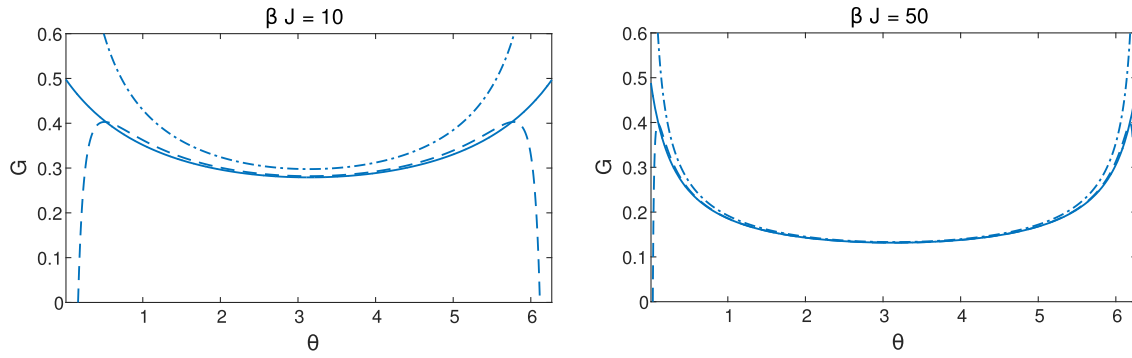


FIG. 15. The exact $G(\theta)$ in the $q = 4$ model is shown in solid lines, for $\beta J = 10$ (left) and $\beta J = 50$ (right). We also plot the conformal answer G_c in dash-dotted lines, and the conformal answer plus the first correction $G_c f_0$ in dashed lines.

is independent of q . Apart from the prefactor, this expression is the first-order perturbation theory formula for the matrix element of $\langle \Psi_{h,n}, \delta \Psi_{2,n} \rangle$, so we conclude Eq. (F1). Although we did not need explicit formulas for the corrected eigenvectors in this paper, one can get them by expanding and normalizing Eqs. (3.80) and (3.81).

APPENDIX G: NUMERICAL SOLUTION OF THE SCHWINGER-DYSON EQUATIONS

In this appendix, we discuss the numerical solution of the Schwinger-Dyson equations at finite βJ . The Euclidean solutions give us the coefficient α_G (and thus also α_K, α_S). One can also use these solutions to directly compute the large- N free energy. The real-time solutions were used to compute the blue circles in Fig. 11.

We will begin by discussing the Euclidean equations, at finite temperature:

$$\begin{aligned} G(\omega_n)^{-1} &= -i\omega_n - \Sigma(\omega_n), \\ \Sigma(\tau) &= J^2 G(\tau)^{q-1}. \end{aligned} \quad (\text{G1})$$

Here $\omega_n = 2\pi(n + 1/2)/\beta$ is a Matsubara frequency. One can solve these equations just by iterating them, starting with the free correlator and using a numerical Fourier transform to switch between frequency ω_n and time $\theta = 2\pi\tau/\beta$. In order to get the iteration to converge, one should take a weighted update¹³

$$G_j(\omega_n) = (1-x)G_{j-1}(\omega_n) + x \frac{1}{-i\omega_n - \Sigma_{j-1}(\omega_n)} \quad (\text{G2})$$

where the weighting x is a parameter. One can set it by beginning with $x = 0.5$ and then monitoring the difference $\int |G_j - G_{j-1}|^2$ between successive steps. If this begins to increase, one divides x by a half and continues the iteration. Some exact solutions are shown for different values of βJ in Fig. 15.

For large values of βJ , the difference between the exact and conformal correlators is fit very well by

$$G \approx G_c - \frac{\alpha_G}{\beta \mathcal{J}} G_c f_0 \quad (\text{G3})$$

where f_0 was defined in Eq. (3.84) and α_G is a fitting parameter. More precisely, this holds as long as $\tau \mathcal{J}$ is large. We determine α_G from the numerical solutions by fitting for the coefficient in the region $\pi/2 \leq \theta \leq \pi$. In the numerics we have a finite frequency cutoff and finite J , but we take both large and look for convergence. For small $q < 3$ to get accurate results we have to extrapolate in both variables, first in the cutoff and then in J .

The function $\alpha_G(q)$ was plotted in Fig. 9. Some explicit values are $\alpha_G(2) = 0$, $\alpha_G(4) \approx 0.1872$, $\alpha_G(6) \approx 0.1737$, $\alpha_G(8) \approx 0.1522$, and $\alpha_G(10) \approx 0.1336$. A Padé approximant that stays within approximately one percent of the numerical answer is

$$\alpha_G(q) \approx \frac{2(q-2)}{16/\pi + 6.18(q-2) + (q-2)^2}. \quad (\text{G4})$$

With the solution to the Schwinger-Dyson equations, we can also compute the free energy using Eq. (2.25). In terms of the correlators and the self-energy at Matsubara frequencies, we have

$$\begin{aligned} \frac{\log Z}{N} &= \frac{1}{2} \log 2 + \frac{1}{2} \sum_{n=-\infty}^{\infty} \log \left[1 + \frac{\Sigma(\omega_n)}{i\omega_n} \right] \\ &\quad - \frac{\beta}{2} \int_0^\beta \left[\Sigma(\tau) G(\tau) - \frac{J^2}{q} G(\tau)^q \right]. \end{aligned} \quad (\text{G5})$$

To get this expression from Eq. (2.25), we have used the free answer $\log Z = \frac{N}{2} \log 2$ in the case $J = 0$ to set the constant. The effect was to replace

$$\sum_n \log(-i\omega_n) \rightarrow \log 2. \quad (\text{G6})$$

¹³We are grateful to A. Kitaev for suggesting this.

The answer we expect for the free energy is an expansion in powers of $1/(\beta J)$:

$$\frac{\log Z}{N} = a_1 \beta J + a_2 + \frac{a_3}{\beta J} + \dots \quad (\text{G7})$$

where $-a_1 J$ is the ground-state energy density, a_2 is the zero-temperature entropy density, and $2a_3$ is the specific heat density. We can remove the ground-state energy by considering

$$\frac{\log Z - J \partial_J \log Z}{N} = a_2 + 2 \frac{a_3}{\beta J} + \dots \quad (\text{G8})$$

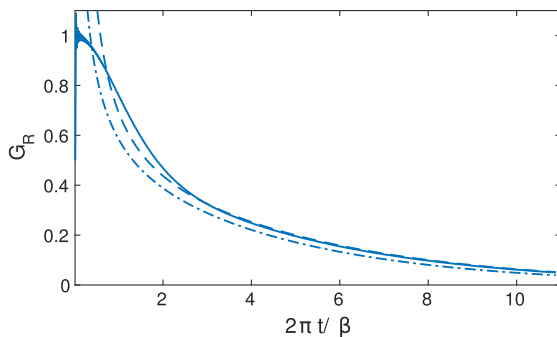
The derivative term can be evaluated using Eq. (2.26). Evaluating the sum of these terms on the numerical solution to the Schwinger-Dyson equations for moderately large βJ , we find very good agreement with the $S_0(q)$ given in Eq. (2.32). The agreement is good enough that we can subtract S_0 and study the remainder for different values of βJ in order to compute a_3 . This was used to compute the circles in Fig. 12.

We can also continue the equations (G1) to get the retarded and Wightman correlators in real time, following Ref. [13]. For this it is important to use the spectral function $\rho(\omega)$. Here, ω with no subscript is a real-time frequency, which takes continuous values. We are using conventions where the spectral function can be defined as the real part of the Fourier transform of the retarded propagator:

$$\begin{aligned} \rho(\omega) &\equiv 2\text{Re}G_R(\omega) = G^>(\omega)(1 + e^{-\beta\omega}), \\ G^>(t) &\equiv \langle \psi(t)\psi(0) \rangle = G(it + \epsilon). \end{aligned} \quad (\text{G9})$$

The Matsubara propagator $G(\omega_n)$ can be written in terms of ρ as

$$G(\omega_n) = \int \frac{d\omega'}{2\pi} \frac{\rho(\omega')}{-i\omega_n + \omega'}. \quad (\text{G10})$$



In this form, one can easily continue to complex frequency. The continuation to real-time frequency is essentially the retarded propagator: $G_R(\omega) = -iG(-i\omega + \epsilon)$. To get the real-time Schwinger-Dyson equation we also have to understand how to continue $\Sigma(\omega_n)$. Writing the second equation (G1) in frequency space and using Eq. (G9) we have

$$\begin{aligned} \Sigma(\omega_n) &= J^2 \int_0^\beta e^{i\omega_n \tau} G(\tau)^{q-1}, \\ G(\tau) &= \int \frac{d\omega}{2\pi} e^{-i\omega \tau} \frac{\rho(\omega)}{1 + e^{-\beta\omega}}. \end{aligned} \quad (\text{G11})$$

After doing the τ integral we get an equation that can be continued to complex frequency,

$$\Sigma(\omega_n) = J^2 \int \left[\prod_{j=1}^{q-1} \frac{d\omega_j}{2\pi} \frac{\rho(\omega_j)}{1 + e^{-\beta\omega_j}} \right] \frac{1 + e^{-\beta \sum_j \omega_j}}{-i\omega_n + \sum_j \omega_j}. \quad (\text{G12})$$

Now we have a closed set of equations for ρ that can be iterated. First, we compute the retarded propagator from the continuation of the first equation in Eq. (G1):

$$G_R(\omega)^{-1} = [-iG(-i\omega + \epsilon)]^{-1} = -i\omega + \epsilon - i\Sigma(-i\omega + \epsilon). \quad (\text{G13})$$

Next, we compute the spectral function by taking twice the real part. Finally, we substitute ρ into Eq. (G12) to get the new self-energy. An appropriately weighted iteration of this procedure converges. In implementing these equations numerically, we have to put both an IR cutoff and a UV cutoff on the frequencies. This makes the problem more challenging than the Euclidean problem, but we still get good agreement with the conformal answer and the leading correction. See Fig. 16 for a plot.

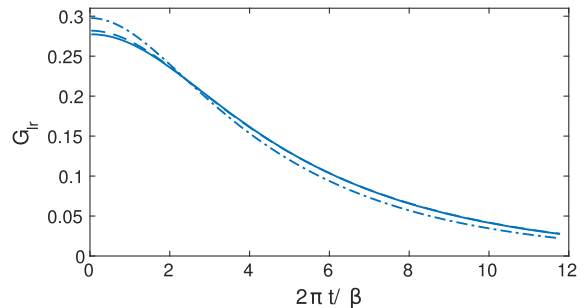


FIG. 16. The retarded propagator G_R (left) and the half-circle Wightman correlator G_{I_r} (right) are plotted in the $q = 4$ model with $\beta J = 10$. The solid curve is the numerical answer, the dash-dotted curve is the conformal answer, and the dashed curve is the conformal answer plus the leading correction (3.124). The behavior of the numerical G_R near $t = 0$ is somewhat contaminated by finite-cutoff wiggles.

The only place we used these real-time solutions in the main text was to compute the circles in Fig. 11. To evaluate these we solve the above equations to get G_R and G_{l_r} , which can also be written in terms of ρ . We then assume an ansatz (3.118). This turns Eq. (3.117) into a one-dimensional integral equation for $f(t_{12})$. This can be discretized and represented as a matrix equation. λ_L is determined by the condition that this matrix should have an eigenvalue equal to one. We find this by doing a binary search.

APPENDIX H: A MODEL WITHOUT THE REPARAMETRIZATION SYMMETRY

It is natural to ask whether there is a model where instead of $1/(1-K)$ in the expression for the four-point function (3.7) we get $1/(1-gK)$, with a $g < 1$. This would move the pole away from $h=2$ and would lead to a finite expression in the conformal limit. It is clear from our discussion in Sec. IV that this can only be true in a model without reparametrization symmetry.

A simple model with these properties arises if we assume that the couplings $j_{i_1 \dots i_q}$ are time-dependent fields with a two-point function

$$\langle j_{i_1 \dots i_n}(t) j_{i_1 \dots i_n}(0) \rangle = \frac{J^2 (q-1)!}{N^{q-1}} \times \frac{1}{|t|^{2\alpha}}. \quad (\text{H1})$$

The new factor is the last one. In the limit $\alpha \rightarrow 0$ we recover the original model (to leading orders in the $1/N$ expansion).

With this modification we can still write the Schwinger-Dyson equations as

$$\begin{aligned} \frac{1}{G(\omega)} &= -i\omega - \Sigma(\omega), \\ \Sigma(\tau) &= J^2 [G(\tau)]^{q-1} \frac{1}{|\tau|^{2\alpha}}. \end{aligned} \quad (\text{H2})$$

In the low-energy limit, we can now make a scale-invariant ansatz as before

$$G_c = \frac{b \operatorname{sgn}(\tau)}{|\tau|^{2\hat{\Delta}}}. \quad (\text{H3})$$

With this ansatz we can solve the low-energy limit of Eq. (H2) (dropping the $i\omega$ term) and we find that

$$\hat{\Delta}_\Sigma = \hat{\Delta}(q-1) + \alpha = 1 - \hat{\Delta}, \quad \hat{\Delta} = \frac{1-\alpha}{q} \quad (\text{H4})$$

where we have denoted the dimension of G_c by $\hat{\Delta}$, since it is not equal to $1/q$. The overall coefficient has exactly the same expression as before [Eq. (2.9)] in terms of $\hat{\Delta}$

$$J^2 b^q \pi = \left(\frac{1}{2} - \hat{\Delta} \right) \tan \pi \hat{\Delta}. \quad (\text{H5})$$

We can now consider the kernel that appears in the four-point function computation. It has an expression similar to the one before [Eq. (3.6)],

$$\begin{aligned} \hat{K}_c(\tau_1, \tau_2; \tau_3, \tau_4) &= -(q-1) G_c(\tau_{13}) G_c(\tau_{24}) \frac{\Sigma_c(\tau_{34})}{G_c(\tau_{34})} \\ &= -(q-1) b^q J^2 \frac{\operatorname{sgn}(\tau_{13}) \operatorname{sgn}(\tau_{24})}{|\tau_{13}|^{2\hat{\Delta}} |\tau_{24}|^{2\hat{\Delta}}} \frac{1}{|\tau_{34}|^{2-4\hat{\Delta}}} \\ &= -\frac{(q-1)}{\left(\frac{1}{\hat{\Delta}} - 1\right)} K_{c, \hat{\Delta}} \end{aligned} \quad (\text{H6})$$

where $K_{c, \hat{\Delta}}$ is the usual kernel but with $\Delta \rightarrow \hat{\Delta}$. Namely, in Eqs. (3.11)–(3.12) we replace $\Delta \rightarrow \hat{\Delta}$ and $q \rightarrow 1/\hat{\Delta}$.

The eigenvalues of the new kernel are then equal to

$$\hat{k}_c(h) = g k_{c, \hat{\Delta}}(h), \quad g \equiv \frac{(q-1)}{\left(\frac{1}{\hat{\Delta}} - 1\right)} \quad (\text{H7})$$

where $k_{\hat{\Delta}}(h)$ is the usual expression in terms of Δ [i.e. we replace $1/q \rightarrow \hat{\Delta}$ everywhere in Eq. (3.35)]. Now if $0 < \alpha < 1$, then we see that $\hat{\Delta} < 1/q$ which means that $g < 1$. This implies that now the sum that appears in the computation of the four-point function is regular and of the form

$$\frac{1}{1 - \hat{K}} = \frac{1}{1 - g K_{\hat{\Delta}}}. \quad (\text{H8})$$

Therefore now we do not have to worry about the $h=2$ contribution. For $h=2$ we find that $\hat{K} = g < 1$ and the sum is finite. In this case, the expression analogous to Eq. (3.45) is finite. Since $k'_c(h=2) < 0$, the first pole is at a value $h_p < 2$. Something similar happens with the retarded kernel, \hat{K}_R where the pole moves to a value $-1 < h_{\text{chaos}} < 0$. More explicitly, using the formula (3.60) we find

$$\hat{k}_R(1-h) = \frac{\cos \pi \left(\hat{\Delta} - \frac{h}{2} \right)}{\cos \pi \left(\hat{\Delta} + \frac{h}{2} \right)} k_{c, \hat{\Delta}}(h). \quad (\text{H9})$$

We can easily check from here that $\hat{k}_R(h=0) = q-1 > 1$ and that $\hat{k}_R(h=-1) = g < 1$. Therefore there is always a solution for $\hat{k}_R(h_{\text{chaos}}) = 1$ for $-1 < h_{\text{chaos}} < 0$, leading to the behavior $e^{(-h_{\text{chaos}}) \frac{2\pi}{\beta} t}$. This means that we have a growing contribution but it grows more slowly than the bound. Here we are assuming that when we go to the finite-temperature theory we also change the two-point function (H1) to its finite-temperature version.

As $\alpha \rightarrow 0$, it seems clear that we will get a divergence that will go like $1/\alpha$. The coefficient of this divergence

would be a function of cross ratios. This is different than the function that multiplies $\frac{1}{\beta\mathcal{J}}$ that we discussed in Sec. III C 3.

As we take the limit $\alpha \rightarrow 0$ the sum over the normalizable $h = 2$ modes, in Fourier space, involves a factor of the form $1/(1 - \hat{K}) \propto 1/(\alpha + \frac{n}{(\beta J)})$, where we also included the terms that would break the conformal symmetry when $\alpha = 0$. Then depending on whether α or $1/(\beta J)$ is larger, we go from one regime to the other.

We can then derive an effective action for reparametrizations which would reproduce the above kernel. We find that it should have the schematic form

$$\sum_n \left[\frac{1}{J\beta} n^2 (n^2 - 1) + \alpha (n^2 - 1) |n| \right] |\epsilon_n|^2 \quad (\text{H10})$$

where the last term in the action is nonlocal. It should come from the variation of the modified term in the effective action

$$\int d\theta_1 d\theta_2 \frac{J^2}{|2 \sin \frac{\theta_{12}}{2}|^{2\alpha}} G_c(\theta_{12})^q \quad (\text{H11})$$

when we make a reparametrization of G_c and then expand to quadratic order in ϵ . When α is zero, the term is reparametrization invariant, but one can check that if we expand to linear order in α it does give the second term in Eq. (H10).

We could view the two-point function of the j 's as arising from a higher-dimensional conformal field theory. If that field theory has a holographic dual, then we would be describing something that lives on an AdS_2 subspace of a higher-dimensional bulk. Such a theory would not have a purely dynamical two-dimensional gravity. This setup arises naturally in the Kondo model and its holographic duals. See Ref. [41] for a Kondo model example that inspired the SYK model studied in this paper, and Ref. [42] and references therein for holographic examples.

APPENDIX I: FURTHER COMMENTS ON KINEMATIC SPACE

In this appendix we expand a bit more on the comments in Sec. VI A, where we explored properties of the two-dimensional space characterized by two times t_1, t_2 of a bilocal field.

We can consider the finite-temperature Lorentzian theory. After defining the following coordinates the Casimir becomes (setting $\beta = 2\pi$)

$$t = \frac{t_1 + t_2}{2}, \quad \sigma \rightarrow \frac{t_1 - t_2}{2}, \quad \rightarrow C \rightarrow \sinh^2 \sigma (-\partial_t^2 + \partial_\sigma^2) \quad (\text{I1})$$

where we now have the wave equation on the outside of the Lorentzian black hole. We see that the two-point function

G_c is determining the metric of the space we should consider.

We can easily get to the interior by taking $t_1 \rightarrow t_1 + i\beta/4, t_2 \rightarrow t_2 - i\beta/4$ so that now we get

$$C \sim \cosh^2 \sigma (\partial_t^2 - \partial_\sigma^2) \quad (\text{I2})$$

which is the wave operator in the interior region. The fact that we have a complex shift in the two times by $t_1 - t_2 \rightarrow t_1 - t_2 + i\beta/2$ is related to the fact that we can easily create particles in the interior if we have access to both sides of the thermofield double, or if we perform small perturbations of the thermofield double state [43].

Finally, there is an elegant relation between bulk and boundary using embedding coordinates. Points on the boundary can be written in terms of projective coordinates $X_M = (X_{-1}, X_0, X_1)$, with $(X.X) \equiv -X_{-1}^2 - X_0^2 + X_1^2 = 0$ and $X \sim \lambda X$. If we have a pair of such points on the boundary, X_M^a and X_M^b , then we can define

$$Y^L = \frac{e^{MNL} X_M^a X_N^b}{(X^a.X^b)} \quad (\text{I3})$$

where $(X^a.X^b)$ is simply the inner product using the $SL(2)$ metric. This obeys $(Y.Y) = -1$. Of course, conceptually, this is the same as what we have discussed above, except that now we see that the formulas are $SL(2)$ covariant.

1. The kinematic space in the full model at $q = \infty$

As a final comment, we will consider the case of $q \rightarrow \infty$. This case looks simpler because the only state in the singlet spectrum is the $h = 2$ state. As we approach the $q \rightarrow \infty$ limit the other states are decoupling, but their energies are not becoming large. In this sense it is different than the very large 't Hooft coupling limit of a gauge theory, where the decoupling of the string states happens because they become heavy. An observation is that in this case we get an interesting picture in terms of the ‘‘bulk’’ coordinates defined in Eq. (6.1). In this limit the kernel is given by

$$K(t_1, t_2; t_3, t_4) = \text{sgn}(t_{13}) \text{sgn}(t_{24}) \frac{1}{(|t_{34}| + \epsilon)^2} - (3 \leftrightarrow 4),$$

$$\epsilon = \frac{1}{\mathcal{J}}. \quad (\text{I4})$$

We then find that it obeys the equation

$$\begin{aligned} & - (|t_{12}| + \epsilon)^2 \partial_{t_1} \partial_{t_2} K(t_1, t_2; t_3, t_4) \\ & = [\delta(t_1 - t_3) \delta(t_2 - t_4) - (3 \leftrightarrow 4)] \\ & = (\sigma + \epsilon)^2 (-\partial_t^2 + \partial_z^2) K(t, z; t', z') \end{aligned} \quad (\text{I5})$$

where we defined t, σ as in Eq. (6.1). After defining $z = \sigma + \epsilon$ we find that we get the wave operator in AdS_2

(parametrized by t, z) with a cutoff at $z = \epsilon$. In particular, here $z \geq \epsilon$ always and, for the spectral problem we are putting boundary conditions that set the normalizable functions to be zero at $\tilde{z} = \epsilon$. So in this case the kernel is really $K = \frac{2}{\tilde{V}_\epsilon}$ [see also Eq. (3.38)], where ∇_ϵ is the Laplacian in AdS_2 with Dirichlet boundary conditions at $z = \epsilon$. Now the quadratic term in Eq. (4.4) becomes $\frac{1}{K} - 1 = \frac{1}{2}\nabla_\epsilon^2 - 1$ and has a simple local form. This is interesting because a popular way to regularize AdS computations consists in setting a cutoff a $\tilde{z} = \epsilon$. However, it was unclear which kind of regularization of the boundary theory would give such a cutoff. Here we

see an example, where we get the same kind of regularized AdS_2 problem. In this theory we flow rather quickly from the topological theory in the UV to the IR AdS_2 -like theory. This needs to be taken with a grain of salt given that we do not know whether there is a way to think about the model as a local theory in AdS. Also the above construction seems more related to regulating the kinematic space than the actual bulk.

In the finite-temperature case we also get a dS_2 , or AdS_2 with periodic time. In this case we also need to rescale the size of the circles relative to their naive values; see Eq. (3.77).

-
- [1] J. L. Karczmarek, J. M. Maldacena, and A. Strominger, Black hole non-formation in the matrix model, *J. High Energy Phys.* **01** (2006) 039.
- [2] I. R. Klebanov, String theory in two-dimensions, in *String Theory and Quantum Gravity '91: Proceedings of the Trieste Spring School and Workshop, ICTP, Trieste, Italy, 15–26 April, 1991*, edited by J. Harvey *et al.* (World Scientific, Singapore, 1992), p. 30.
- [3] A. Kitaev, A simple model of quantum holography, <http://online.kitp.ucsb.edu/online/entangled15/kitaev/>; <http://online.kitp.ucsb.edu/online/entangled15/kitaev2/>.
- [4] S. Sachdev and J.-w. Ye, Gapless Spin Fluid Ground State in A Random, Quantum Heisenberg Magnet, *Phys. Rev. Lett.* **70**, 3339 (1993).
- [5] S. Sachdev, Holographic Metals and the Fractionalized Fermi Liquid, *Phys. Rev. Lett.* **105**, 151602 (2010).
- [6] V. de Alfaro, S. Fubini, and G. Furlan, Conformal invariance in quantum mechanics, *Nuovo Cimento Soc. Ital. Fis.* **34A**, 569 (1976).
- [7] A. Almheiri and J. Polchinski, Models of AdS_2 backreaction and holography, *J. High Energy Phys.* **11** (2015) 014.
- [8] A. Kitaev, <http://online.kitp.ucsb.edu/online/joint98/kitaev/>.
- [9] S. H. Shenker and D. Stanford, Black holes and the butterfly effect, *J. High Energy Phys.* **03** (2014) 067.
- [10] A. Kitaev, in *The Fundamental Physics Prize Symposium, 2014* (to be published).
- [11] S. H. Shenker and D. Stanford, Stringy effects in scrambling, *J. High Energy Phys.* **05** (2015) 132.
- [12] J. Maldacena, S. H. Shenker, and D. Stanford, A bound on chaos, *J. High Energy Phys.* **08** (2016) 106.
- [13] O. Parcollet and A. Georges, Non-fermi-liquid regime of a doped Mott insulator, *Phys. Rev. B* **59**, 5341 (1999).
- [14] S. Sachdev, Bekenstein-Hawking Entropy and Strange Metals, *Phys. Rev. X* **5**, 041025 (2015).
- [15] P. Hosur, X.-L. Qi, D. A. Roberts, and B. Yoshida, Chaos in quantum channels, *J. High Energy Phys.* **02** (2016) 004.
- [16] W. Fu and S. Sachdev, Numerical study of fermion and boson models with infinite-range random interactions, *Phys. Rev. B* **94**, 035135 (2016).
- [17] Y.-Z. You, A. W. W. Ludwig, and C. Xu, Sachdev-Ye-Kitaev model and thermalization on the boundary of many-body localized fermionic symmetry protected topological states, [arXiv:1602.06964](https://arxiv.org/abs/1602.06964).
- [18] A. Jevicki, K. Suzuki, and J. Yoon, Bi-local holography in the SYK model, *J. High Energy Phys.* **07** (2016) 007.
- [19] J. Polchinski and V. Rosenhaus, The spectrum in the Sachdev-Ye-Kitaev model, *J. High Energy Phys.* **04** (2016) 001.
- [20] D. Anninos, T. Anous, and F. Denef, Disordered quivers and cold horizons, [arXiv:1603.00453](https://arxiv.org/abs/1603.00453).
- [21] D. Anninos, T. Anous, P. de Lange, and G. Konstantinidis, Conformal quivers and melting molecules, *J. High Energy Phys.* **03** (2015) 066.
- [22] N. Goheer, M. Kleban, and L. Susskind, $(1+1)$ -Dimensional Compactifications of String Theory, *Phys. Rev. Lett.* **92**, 191601 (2004).
- [23] D. A. Roberts and D. Stanford, Two-Dimensional Conformal Field Theory and the Butterfly Effect, *Phys. Rev. Lett.* **115**, 131603 (2015).
- [24] S. Jackson, L. McGough, and H. Verlinde, Conformal bootstrap, universality and gravitational scattering, *Nucl. Phys.* **B901**, 382 (2015).
- [25] G. Turiaci and H. Verlinde, On CFT and quantum chaos, [arXiv:1603.03020](https://arxiv.org/abs/1603.03020).
- [26] J. Maldacena, D. Stanford, and Z. Yang, Conformal symmetry and its breaking in two dimensional nearly anti-de Sitter space, [arXiv:1606.01857](https://arxiv.org/abs/1606.01857).
- [27] J. Polchinski and A. Streicher (private communication).
- [28] B. Czech, L. Lamprou, S. McCandlish, and J. Sully, Integral geometry and holography, *J. High Energy Phys.* **10** (2015) 175.
- [29] B. Czech, L. Lamprou, S. McCandlish, B. Mosk, and J. Sully, A stereoscopic look into the bulk, *J. High Energy Phys.* **07** (2016) 129.
- [30] A. Georges, O. Parcollet, and S. Sachdev, Quantum fluctuations of a nearly critical heisenberg spin glass, *Phys. Rev. B* **63**, 134406 (2001).

- [31] N. Iizuka and J. Polchinski, A matrix model for black hole thermalization, *J. High Energy Phys.* **10** (2008) 028.
- [32] B. Michel, J. Polchinski, V. Rosenhaus, and S. J. Suh, Four-point function in the IOP matrix model, *J. High Energy Phys.* **05** (2016) 048.
- [33] D. Stanford, Many-body chaos at weak coupling, *J. High Energy Phys.* **10** (2016) 009.
- [34] T. M. Fiola, J. Preskill, A. Strominger, and S. P. Trivedi, Black hole thermodynamics and information loss in two-dimensions, *Phys. Rev. D* **50**, 3987 (1994).
- [35] J. M. Maldacena, J. Michelson, and A. Strominger, Anti-de Sitter fragmentation, *J. High Energy Phys.* **02** (1999) 011.
- [36] S. Giombi, S. Minwalla, S. Prakash, S. P. Trivedi, S. R. Wadia, and X. Yin, Chern-Simons theory with vector fermion matter, *Eur. Phys. J. C* **72**, 2112 (2012).
- [37] J. M. Maldacena, Long strings in two dimensional string theory and non-singlets in the matrix model, *J. High Energy Phys.* **09** (2005) 078; Long strings in two-dimensional string theory and non-singlets in the matrix model, *Int. J. Geom. Methods Mod. Phys.* **03**, 1 (2006).
- [38] G. 't Hooft, A two-dimensional model for mesons, *Nucl. Phys.* **B75**, 461 (1974).
- [39] S. Leichenauer, Disrupting entanglement of black holes, *Phys. Rev. D* **90**, 046009 (2014).
- [40] A. P. Reynolds and S. F. Ross, Butterflies with rotation and charge, [arXiv:1604.04099](https://arxiv.org/abs/1604.04099).
- [41] O. Parcollet, A. Georges, G. Kotliar, and A. Sengupta, Overscreened multichannel SU(N) Kondo model: Large- N solution and conformal field theory, *Phys. Rev. B* **58**, 3794 (1998).
- [42] J. Erdmenger, M. Flory, C. Hoyos, M.-N. Newrzella, A. O'Bannon, and J. Wu, Holographic impurities and Kondo effect, *Fortschr. Phys.* **64**, 322 (2016).
- [43] J. M. Maldacena, Eternal black holes in anti-de Sitter, *J. High Energy Phys.* **04** (2003) 021.